

**DEVELOPMENT OF ANALYTICAL METHODOLOGY
FOR QUANTIFICATION OF TRACE AND ULTRA-
TRACE METALLIC IMPURITIES IN NUCLEAR
MATERIALS USING ICP-MS**

By
BRIJLESH KUMAR NAGAR
CHEM01201504003

Bhabha Atomic Research Centre

A thesis submitted to the
Board of Studies in Chemical Sciences
In partial fulfillment of requirements
for the Degree of
DOCTOR OF PHILOSOPHY
of
HOMI BHABHA NATIONAL INSTITUTE



May, 2018

Homi Bhabha National Institute

Recommendations of the Viva Voce Committee

As members of the Viva Voce Committee, we certify that we have read the dissertation prepared by **Brijlesh Kumar Nagar** entitled "Development of analytical methodology for quantification of trace and ultra-trace metallic impurities in nuclear materials using ICP-MS" and recommend that it may be accepted as fulfilling the thesis requirement for the award of Degree of Doctor of Philosophy.

Chairman - Dr. Sunil Jaikumar

Date: 27.09.2018

Sunil tai Kumar

Guide / Convener - Dr. B. S. Tomar

Date:

27/9/2018

B. S. Tomar

Examiner - Prof. Ashwini K. Choudhary

Date:

27.9.2018

Ashwini K. Choudhary

Member 1- Dr. Sanjukta A. Kumar

Date:

08/10/2018

Spalt

Member 2- Dr. N. L. Misra

Date:

27.09.2018

Nand Lal Misra

Member 3- Dr. Pradeep Kumar

Date:

27/9/2018

Pradeep Kumar

Final approval and acceptance of this thesis is contingent upon the candidate's submission of the final copies of the thesis to HBNI.

We hereby certify that we have read this thesis prepared under our direction and recommend that it may be accepted as fulfilling the thesis requirement.

Date: 27-09-2018

Place: Mumbai

B. S. Tomar

Dr. B. S. Tomar

Guide

I was absent during the ph.D. viva-voce of Shri B.K. Nagar, however, I agree with the thesis content and the recommendation of viva-voce board.

Spalt
08/10/2018

STATEMENT BY AUTHOR

This dissertation has been submitted in partial fulfillment of requirements for an advanced degree at Homi Bhabha National Institute (HBNI) and is deposited in the Library to be made available to borrowers under rules of the HBNI.

Brief quotations from this dissertation are allowable without special permission, provided that accurate acknowledgement of source is made. Requests for permission for extended quotation from or reproduction of this manuscript in whole or in part may be granted by the Competent Authority of HBNI when in his or her judgment the proposed use of the material is in the interests of scholarship. In all other instances, however, permission must be obtained from the author.

Brijlesh Kumar

Brijlesh Kumar Nagar

DECLARATION

I, hereby declare that the investigation presented in the thesis has been carried out by me. The work is original and has not been submitted earlier as a whole or in part for a degree / diploma at this or any other Institution / University.

Brijlesh Kumar

Brijlesh Kumar Nagar

List of Publications arising from the thesis

Journals

1. Determination of Trace and Ultratrace Elements in Uranium-Silicide (U_3Si_2) Fuel Employing Inductively Coupled Plasma Mass Spectrometry
B.K.Nagar, Abhijit Saha, S.B.Deb, and M.K.Saxena
Atomic Spectroscopy Vol. 35(5) Sept./Oct. 187-192 (2014).
2. Development of an Analytical Method for Quantification of Trace Metallic Impurities in U-Mo Alloy Employing Time of Flight based ICP-M
B.K.Nagar, M.K.Saxena and B.S.Tomar
Atomic Spectroscopy Vol. 38(5) Sept./Oct. 117-123 (2017).
3. Microwave-assisted dissolution of highly refractory dysprosium titanate (Dy_2TiO_5) followed by chemical characterization for major and trace elements using ICP-MS, UV-visible spectroscopy and conventional methods.
Brijlesh Kumar Nagar, Khushboo Kumari, Shadhan Bijoy Deb, Manoj Kumar Saxena and Bhupendra Singh Tomar
Spectrochimica Acta : **Online 07/21/2018**
<https://doi.org/10.1515/ract-2018-2934>
4. Quantification of Trace and Ultra-trace Impurities in U-Zr Alloy by Inductively Couple Plasma Time of Flight Mass Spectrometry (ICP-TOF-MS) After Simultaneous Separation of U and Zr
B.K.Nagar, M.K.Saxena and B.S.Tomar
Atomic Spectroscopy Vol. 38(5) Sept./Oct. 185-192 (2018).

5. Quantification of trace level rare earth elements in Al matrices by ICP-MS

Brijlesh Kumar Nagar, Shadhan Bijoy Deb, Manoj Kumar Saxena and

Bhupendra Singh Tomar

Spectrochimica Acta: **In Press**

Conferences

1. Development of a systematic analytical methodology for chemical characterization of dysprosium titanate after its microwave assisted digestion

B.K. Nagar, S.B. Deb, Abhijit Saha and M.K. Saxena

5th DAE-BRNS Interdisciplinary Symposium on Materials Chemistry

(ISMC-2014) held on 9-13 Dec. (2014), Page no. 87

2. Quantitative Separation of trace amount of rare earth elements from nuclear grade alumina

B.K.Nagar, S.B.Deb, M.K.Saxena and B.S.Tomar,

DAE-BRNS Symposium SESTEC-2018, BITS Pilani, K K Birla Goa

Campus, Goa Campus, May 23-26, (2018), Page no. 5

Brijlesh Kumar

Brijlesh Kumar Nagar

DeDicated to

My grand-parents

Late Smt. Ram Raji

Late Shri Chiragan

&

My Parents

Late Smt. Rama Devi

Shri rammoorat

ACKNOWLEDGEMENTS

I express my sincere gratitude to my research guide **Prof. B. S. Tomar**, Ex. Director, RC & IG , and Head, RACD, for his constant source of inspiration throughout my thesis work. I am deeply indebted to him for his advice, guidance and encouragement at every point of my thesis work.

I also want to express my heartfelt thanks to Chairman of the Doctoral Committee, **Prof. Sunil Jaikumar**, Head, NCCCM, Haidarabad, for his valuable suggestions and continuous encouragement during the doctoral committee meetings.

I am grateful to **Shri M. K. Saxena**, Head, RACD, for his valuable insight and persistent support throughout this work.

I also want to express my gratitude to all committee members, **Prof. Sanjukta A. Kumar**, **Prof. N. L. Misra**, and **Prof. Pradeep Kumar**, for their invaluable suggestions and insightful comments provided during the doctoral committee meetings. I am thankful to them for their strong support and cooperation throughout the course of my Ph. D. program.

I also thank my co-authors their help during various experimental works.

Last but not least, I thank my wife **Smt. Kiran B. Nagar**, for her wholehearted support, care and co-operation during the entire course of my Ph.D work. I thank my son **Ishan**, and daughter **Ishanvi** who made all my time after office hours so joyful and cherishing, that I found a good opportunity to complete my Ph. D work.

CONTENTS

	Page No.
SYNOPSIS	I
LIST OF FIGURES	X
LIST OF TABLES	XIII
Chapter 1- Introduction	1-24
1.1. Nuclear Energy	1
1.2. Indian Nuclear Energy Program	2
1.3. Nuclear Fuel cycle	3
1.4. Important Nuclear Materials	5
1.4.1. Nuclear Fuels	5
1.4.1.1. Ceramic fuels	5
1.4.1.2. Metallic fuel	5
1.4.1.3. Inter-metallic fuels	7
1.4.2. Cladding materials	7
1.4.3. Control rods and burnable poisons	8
1.4.4. Moderator and Coolant	9
1.5. Chemical characterization of nuclear materials	9
1.5.1. Sample Dissolution	10
1.5.1.1. Conventional Acid Dissolution	10
1.5.1.2. Dissolution by fusion method	10
1.5.1.3. Microwave Dissolution	13
1.5.2. Assay of Trace metallic impurities	14

1.5.3.Trace non-metal assay	17
1.5.3.Bulk elements assay	19
1.5.4.Isotopic composition and Oxygen/ metal ratio determination	21
1.6. Importance of the thesis work	22
Chapter 2 -Experimental methods and Techniques	25-72
2.1. Introduction	25
2.2. Mass spectrometry	26
2.2.1. Inductively Coupled Plasma Time-of-Flight Mass Spectrometry (ICP-tof-MS)	29
2.2.1.1 Sample Introduction System	31
2.2.1.2 Sample Ionization	33
2.2.1.3 Ion Sampling/ Extraction	37
2.2.1.4 Ion Focusing	38
2.2.1.5 Mass analyzer	38
2.2.1.6 Detector	41
2.2.2 Interferences in ICPMS	42
2.2.3 Optimization and Calibration of ICP-MS	45
2.2.4 Advantage and disadvantage of ICP-MS	47
2.3. Gamma Spectroscopy	48
2.3.1 NaI (Tl)- scintillation counters	51
2.3.2 Detector Counting Efficiency and Resolution of NaI (Tl)	52
2.4. UV-Visible Spectrophotometry	53
2.4.1 Basic principle	53
2.4.2 Advantage and disadvantage of UV-Visible Spectrophotometry	57

2.5.	Microwave Dissolution	59
2.6.	Matrix separation Methodologies	60
2.6.1	Solvent Extraction	61
2.6.2	Ion Exchange chromatography	63
2.6.3	Precipitation method	66
2.7.	Gravimetric method of major matrix analysis	67
Chapter 3- Determination of trace and ultra trace impurities in uranium silicide		73-90
(U₃Si₂) nuclear fuel employing ICP-MS		
3.1.	Introduction	73
3.2	Experimental Section	77
3.2.1.	Instrumentation	77
3.2.2.	Reagents and Solutions	78
3.2.3.	Dissolution and Matrix Separation	79
3.2.4.	Choice of isotopes	80
3.2.5.	Recovery Studies using Standard Addition Technique	81
3.2.6.	Gamma spectrometry study	81
3.3.	Results and discussion	82
3.3.1.	Method validation by Standard Addition Technique	84
3.3.2.	Recovery Studies by γ -Spectrometry Employing ⁵¹ Cr and ¹⁵²⁺¹⁵⁴ Eu	87
	Tracers	
3.3.3.	Detection limits	88
3.3.4.	Analysis of the real uranium silicide samples	89
3.4	Conclusion	90
Chapter 4-Quantification of Trace Metallic Impurities in U-Mo Alloy by ICPMS		91-111

4.1.	Introduction	91
4.2.	Experimental Section	94
4.2.1.	Instrumentation	94
4.2.2.	Chemicals and Solutions	95
4.2.3.	Preparation of anion exchange column	95
4.2.4.	Preparation of Synthetic Samples	96
4.2.5.	Dissolution of U-Mo alloy	96
4.2.6.	Column studies	97
4.3	Results and discussion	97
4.3.1.	Retention Study of U and Mo	97
4.3.2.	Retention of analytes	98
4.3.3	Study of Isobaric Interferences	106
4.3.4.	Detection limit	106
4.3.5.	Analysis of Real Samples	108
4.4	Conclusion	108
Chapter 5-Quantification of trace and ultra-trace impurities in U-Zr alloy by		112-141
ICP-MS		
5.1.	Introduction	112
5.2	Experimental	116
5.2.1.	Instrumentation	116
5.2.2.	Chemicals and Solutions	117
5.2.3.	Preparation of Aqueous and Organic Medium	117
5.2.4.	Preparation of Synthetic Solutions	117
5.2.5.	Dissolution of U-Zr alloy	118

5.2.6. Separation of Matrix Elements	118
5.2.7. Aqueous Phase Analysis	118
5.3. Results and discussion	119
5.3.1. Extraction of Zr from HCl and HNO ₃ Medium in TBP	119
5.3.2. Extraction of Zr in TOPO	119
5.3.3. Effect of TBP	121
5.3.4. Non Spectroscopic Interference	123
5.3.5. Recovery of Analytes	124
5.3.6. Standard Addition Method for Validation	126
5.3.7. Study of Isobaric Interferences	132
5.3.8. Detection Limit	136
5.3.9. Validation of Separation Procedure by γ -Spectrometry Using ¹⁵²⁺¹⁵⁴ Eu Tracer	138
5.3.10. Analysis of Real Samples	138
5.4. Conclusion	138
Chapter 6- Chemical Characterization of Dysprosium Titanate (Dy₂TiO₅)	142-157
6.1. Introduction	142
6.2. Experimental	145
6.2.1. Instrumentation	145
6.2.2. Chemicals	145
6.2.3. Microwave Dissolution of Dysprosium-titanate	145
6.2.4. Synthetic Sample Preparation	146
6.2.5. Separation of Mo from Dy and Ti	146
6.2.6. Precipitation of Molybdenum	147

6.2.7. Precipitation of Dy	147
6.2.8. Measurement of Absorbance for Titanium complex	147
6.3. Result and Discussion	148
6.3.1. ICP MS measurement of Dy, Ti and Mo	148
6.3.2. Determination of molybdenum (Mo)	148
6.3.3. Determination of Dysprosium (Dy)	150
6.3.4. Determination of Titanium (Ti)	151
6.3.5. Analysis of Synthetic Dysprosium titanate samples	153
6.3.6. Analysis of real Sample	153
6.3.7. Estimation of trace impurities in MoO ₃ and Dy ₂ O ₃ by ICP-MS	154
6.4 Conclusion	157
Chapter 7 -Chemical Characterization of aluminum oxide (Al₂O₃)	158-171
7.1. Introduction	158
7.2. Experimental	161
7.2.1. Instrumentations	161
7.2.2. Reagents and Solutions	162
7.2.3. Microwave dissolution of Alumina	163
7.2.4. Dissolution of Aluminium metal	163
7.2.5. Separation of Trace elements	163
7.2.6. Gamma spectrometry study using ¹⁵²⁺¹⁵⁴ Eu as tracer	164
7.3. Result and discussion	164
7.3.1. Matrix dissolution and Separation	164
7.3.2. Recovery study of rare earth by standard addition method	164
7.3.3. Correction for spectroscopic interferences	167

7.3.4. Detection Limits	167
7.3.5. Recovery study by gamma spectrometry	168
7.3.6. Analysis of Real Samples	169
7.4. Conclusion	170
Chapter 8- Summary and future outlook	172-175
References	176-204

SYNOPSIS

Nuclear power is the fourth-largest source of electricity in India after thermal, hydroelectric and renewable sources of electricity. In 1950's Dr. Homi Jahangir Bhabha formulated the India's three stage nuclear power program. In the first stage, natural uranium fueled pressurized heavy water reactors (PHWR) is used to produce electricity while generating Pu-239 as by-product. In the second stage, fast breeder reactors (FBRs) fueled with Pu-239 is used, while the uranium-238 present in the fuel transmutes to additional plutonium-239. The third stage envisages an advanced nuclear power system involving Th-232 -U-233 fueled reactors [1].

For safe and smooth reactor operation, chemical quality control (CQC) of every nuclear material is essential. The presence of some trace metallic and non-metallic elements in the nuclear fuel can affect the optimum performance of a reactor (2, 3). These trace elements which get incorporated in nuclear fuel either from the precursors or during various fuel fabrication steps need to be quantified precisely and accurately. The available instrumental techniques for the determination of trace metallic elements in various nuclear materials are inductively coupled plasma mass spectrometry (ICP-MS) (4), inductively coupled plasma atomic emission spectrometry (ICP-AES) (5), flame atomic absorption spectroscopy (AAS) (6), ion chromatography (IC) (7) etc. Among all these techniques, ICP-MS is the most versatile multi-elemental technique with rapid analysis, high sample throughput, long linear calibration range, low detection limit, and fewer spectroscopic interferences etc.

The objective of the work carried out as a part of the present thesis is to develop methodologies for determination of trace elements in nuclear fuels beings used for

some of the advanced fuels proposed in Indian nuclear programme. A brief account of the studies is given below.

Chapter 1 gives the introduction to the subject of chemical quality control of nuclear materials with regard to trace element determination.

Chapter 2 gives the details of the experimental methodologies followed for determination of trace metallic in nuclear materials viz., U_3Si_2 , U-Mo, U-Zr, Dy_2TiO_3 , and Al_2O_3 . Depending upon the matrix, different dissolution strategies were adopted. The determination of trace metallic impurities was carried out by Time of flight ICP-MS.

Chapter 3 describes the studies carried out towards determination of trace and ultra-trace levels of elements in U_3Si_2 fuel employing ICP-MS. Reduced enrichment for research and test Reactor (RERTR) program has been initiated worldwide to replace high enriched uranium (HEU) based fuel to low enriched uranium (LEU) based fuels (8) in order to make it proliferation resistant. In order to compensate for the reduced fissile content in LEU-based fuel, fuels are being studied so as to achieve high density. Uranium-silicide (U_3Si_2) fuel dispersed in an aluminum (Al) matrix has been found to perform extremely well even at high burn-up in LEU with U densities up to $\sim 5.0 \text{ g cm}^{-3}$ (9).

In the present study the matrix element silicon (Si) was separated as its volatile fluoride (silicon tetrafluoride SiF_4) during dissolution, whereas uranium (U) was separated by conventional solvent extraction method using tri-n-butyl phosphate (TBP) in carbon tetrachloride (CCl_4). The recovery of various elements was studied by standard addition method. Thirteen elements viz. B, Cd, Co, Cr, Cu, Dy, Eu, Gd, Mg, Mn, Ni, Sm, and V were recovered quantitatively, and determined by ICP-MS.

An independent tracer technique with ^{51}Cr and $^{152+154}\text{Eu}$ tracers was also employed to determine the recovery of transition elements and rare earth elements in the developed separation method. The instrument detection limit (IDL) and the method detection limit (MDL) for the 13 analytes were found in the range of 6–700 ng L⁻¹ and 8–200 µg kg⁻¹ respectively.

Chapter 4 describes the studies on development of an analytical method for quantification of trace metallic impurities in U-Mo alloy employing time of flight based ICP-MS. Several types of metallic fuels such as inter-metallic and alloys are being studied which can provide high U density (10). Low enriched uranium alloys with 6 to 12 wt. % of Mo are under consideration in the Indian nuclear program owing to their high density. Further, alloying Mo with uranium stabilizes uranium in the γ -phase, which is preferred owing to the advantages related to better accommodation of fission products and swelling behavior. Reported studies show that maximum γ -phase stabilization can be achieved with 10% Mo in U-Mo alloy (11).

In the present study a separation method was developed for simultaneous separation of U and Mo. U and Mo can be separated by solvent extraction; however their simultaneous separation is not possible. To achieve the simultaneous separation anion exchange method was considered. U and Mo form anionic complex in HCl medium. In the presented study the anionic complexes formed, by U and Mo in 4 M HCl was retained on an anion exchange column which helped in simultaneous separation of the U and Mo matrix. Systematic study was carried out to evaluate the capacity of the column in order to optimize the sample quantity during loading. Further studies were carried out to determine the recovery of expected impurity elements with and without

the matrix during the column separation. Recovery in the matrix was also validated using standard addition method.

The recoveries of Al, As, Ce, Cr, Co, Cs, Cu, Dy, Eu, Er, Gd, Hf, Ho, La, Lu, Mg, Mn, Nd, Ni, Pb, Pr, Rb, Rh, Sc, Sm, Sr, Tb, Tm, V, W, Y, Yb and Zr, was found to be 75-100%. The method was used to analyze simulated and real samples successfully. The developed method is simple as compared to solvent extraction and precipitation method; in addition for routine sample analysis the method is relatively less laborious. Further the separation method does not generate any organic radioactive waste. The instrument detection limit (IDL) and the method detection limit (MDL) for the Thirty three analytes were found in the range of 5-200 ngL⁻¹ and 1-15 µgKg⁻¹ respectively.

Chapter 5 gives the details of the studies towards quantification of trace and ultra-trace impurities in U-Zr alloy by ICP-MS after separation of U and Zr. The metallic nuclear fuel based on U-Zr and U-Pu-Zr alloys are preferred in fast breeder reactors (FBRs) compared to conventional oxides and carbides owing to their high fissile density, high burn up, high breeding ratio, less doubling time, good fuel-clad compatibility, high thermal conductivity, and inherent passive safety. In India, fabrication and irradiation studies are being pursued in order to develop metallic fuel based fast breeder reactors (12). Metallic fuels have been used in nuclear reactors in the past (EBR I&II USA) and are also proposed for advanced nuclear reactors, such as, traveling wave reactor (TWR), fusion-fission hybrid reactor (FFHR), sodium cooled fast reactors (SFR) etc. (13). In the fast breeder reactors U-Pu-Zr fuel is used in the main core, whereas U-Zr is used as blanket material for breeding.

A methodology has been developed for determination of trace and ultra-trace metallic impurities in U-Zr alloy fuel by ICP-MS after the solvent extraction of bulk matrix. A detailed study was performed to optimize the concentration of tri-n-octyl phosphine oxide (TOPO), tri-n-butyl phosphate (TBP), nitric acid and hydrochloric acid for maximum removal of the matrix elements (U and Zr). The spectroscopic interferences due metal oxides were eliminated using mathematical correction formula.

Due to unavailability of certified reference material of U-Zr alloy, standard addition method was used to validate the methodology. It was found that out of fifty five elements (Ag, Al, As, B, Ba, Bi, Cd, Ce, Co, Cr, Cs, Cu, Dy, Er, Eu, Fe, Ga, Gd, Hf, Hg, Ho, Ir, La, Li, Lu, Mg, Mn, Mo, Nb, Nd, Ni, Pb, Pd, Pr, Pt, Rb, Re, Rh, Ru, Sb, Sc, Se, Sm, Sn, Sr, Ta, Tb, Te, Ti, Tm, V, W, Y, Yb and Zn) thirty six elements (Al, Ba, Bi, Cd, Ce, Co, Cr, Cs, Dy, Eu, Er, Ga, Gd, Ir, Ho, La, Lu, Mn, Nd, Ni, Pb, Pr, Pt, Rh, Rb, Ru, Sc, Sm, Sr, Tb, Te, Tm, V, Y, and Yb) have recovery more than 90% with %RSD <10. The matrix (U and Zr) concentration after separation was <10 $\mu\text{g ml}^{-1}$. The instrumental detection limit (IDL) and method detection limit (MDL) were found to be in the range 0.1-9.4 $\mu\text{g L}^{-1}$ and 1.0-25.0 $\mu\text{g Kg}^{-1}$ respectively.

Chapter 6 describes the studies on microwave-assisted dissolution of dysprosium-titanate (Dy_2TiO_5) followed by chemical characterization. Dysprosium titanate (Dy_2TiO_5) is being used as control rod material in VVER reactors (14). In addition to lower swelling the matrix has advantages of high melting point ($\sim 1870^\circ\text{C}$), resistance to cladding materials, ease of fabrication and produce non-radioactive final isotopes. Dysprosium titanate is fabricated by solid reaction route, using Dy_2O_3 -78.1%, TiO_2 -19.7% and Mo-1.8%. Once fabricated like other nuclear materials the chemical quality

control of the material is crucial. It is important to certify the major matrix (Dy, Ti and Mo) and the trace level impurities to ensure the desired performance of the material.

Dissolution of dysprosium titanate by conventional method is not possible; therefore, a microwave dissolution method was developed and optimized. The combination of acids and instrumental parameters were varied systematically. In presence of H₂SO₄ and HCl in 3:2 (volume), dysprosium-titanate completely dissolved in the optimized condition of microwave system.

Mo and Dy were determined by gravimetric method and Ti by spectrophotometric method. The method was validated using synthetic solution prepared from pure Dy, Ti, and Mo solutions. The Mo was precipitated using α -benzoine oxime and Dy was precipitated using oxalic acid solution. The effect of Dy and Ti on recovery of Mo was studied. It was found that recovery of Mo is affected due to presence of Dy, while it is not changed in the presence of Ti. Also, Recovery of Dy was studied in the presence of Mo, and Ti. It was found that Recovery of Dy is affected due to presence of Mo, while Ti do not affect. Since, Dy and Mo, could not be determined if present together, they were separated first before precipitation. An anion exchange column was used to separate Mo from Dy and Ti. The precipitates of Mo and Dy were converted to respective oxides on heating. The recovery of Mo, Dy and Ti were excellent following the separation procedure. The purity of oxides of Dy and Mo were checked by quantification of trace elements using ICP-MS.

Chapter 7 describes the studies on microwave assisted dissolution of Al₂O₃ followed by quantification of ultra-trace amount of rare earth elements employing inductively coupled plasma time of flight mass spectrometry (ICP-tof-MS) after pre-concentration and matrix separation. Alumina is an exceptionally important ceramic material which

has many technological applications. It has several special properties like high melting point, chemical inertness, electrical and thermal properties. α - Al_2O_3 is one of the promising insulating ceramic materials for International Thermonuclear Experimental Reactor (ITER) and commercial reactors, because of its high electrical resistance (15). Uranium aluminium alloys are used as fuel elements plates for advanced test reactor (16). The presence of impurities in the alumina changes its properties drastically. The rare earth impurities have a bearing on grain boundary strengthening in alumina (17)

Conventional dissolution method such as hot plate and alkali fusion could not dissolved alumina completely. Therefore, microwave dissolution method was used to dissolve the alumina matrix. The method was optimized for minimum acids and dissolution time. In the present work an analytical method is developed to pre-concentrate the ultra-trace amount of rare earth from the aluminum matrix. The rare earth elements are precipitated with sodium hydroxide solution whereas the aluminum in presence of excess amount of sodium hydroxide formed soluble sodium aluminates. The rare earth elements are separated using Whatmann-542 filter paper and re-dissolved in concentrated hydrochloric acid. The rare earth elements are finally taken in 1% HNO_3 for ICP-MS analysis. The method is validated using standard addition method employing ICP-MS and an independent tracer method using $^{152+154}\text{Eu}$ tracer by gamma spectrometry. It was found that recovery in both cases were more than 98% with %RSD less than 5%. The instrumental detection limits (IDLs) and method detection limits (MDLs) were found between 0.1-2.0 ng L^{-1} and 1-5 $\mu\text{g Kg}^{-1}$ respectively.

Chapter 8 summarizes the highlights of the studies carried out as part o the present thesis.

References:

1. A. Gopalakrishnan, Annual Review of Energy and the Environment, 27(2002)369
2. Aziz, S. Jan, F. Waqar, B. Mohammad, M. Hakim and W. Yawar, J. Radioanal. Nucl. Chem. 284, 117 (2010).
3. A.L.d. Souza, M.E.B. Cotrim and M.A.F. Pires, Microchem. J. 106, 194 (2013).
4. Z. Varga, R. Katona, Z. Stefánka, M. Wallenius, K. Mayer and A. Nicholl, Talanta 80, 1744 (2010).
5. G.V. Ramanaiah, Talanta 46, 533 (1998).
6. D.A. Batistoni and P.N. Smichowski, Appl. Spectrosc. 39, 222 (1985).
7. M. Betti, J. Chromatogr. A 789, 369 (1997).
8. A. Bhatnagar, P. Mukhaerjee, S.B. Chafle, S. Sengupta and V.K. Raina, RERTR 2012-34th International Meeting on Reduced Enrichment for Research and Test Reactors (October 14-17, 2012).
9. U.S. Nuclear Regulatory Commission: "Safety Evaluation Report Related to the Evaluation of Low-Enriched Uranium Silicide-Aluminum Dispersion Fuel for Use in Non-Power Reactors," U.S. Nuclear Regulatory Commission Report NUREG-1313 (July 1988).
10. V.P. Sinha, P.V. Hegde, G.J. Prasad, G.K. Dey and H.S. Kamath, J. Alloys and Compds. 506, 253 (2010).
11. E. Perez, B. Yao, D.D. Keiser Jr., and Y-H. Sohn, J. Nucl. Mater. 402, 8 (2010).
12. R. K. Sinha, Advanced Nuclear Reactor System- An Indian Perspective, Energy procedia, 7 (2011) 34-50

13. Y. Hu, M. Xu, Nucl. Power Eng. 29 (2008) 53-56
14. ORNL/TM-2001/238 Report: Development of improved burnable poisons for commercial nuclear power reactors.
15. NISTIR 5030, N.J.Simon, Cryogenic properties of inorganic insulation materials for ITER magnets: A Review
16. F. Thummler, H. E. Lilienthal and S.Nazare. Powder Metallurgy 12(23), (1969) 1-22
17. J. P. Buban, K.Matsunaga, J.Chen, N.Shibata, W.Y.Ching, T.Yamamoto, Y.Ilkuhara, Grain boundary strengthening in alumina by rare earth impurities, Science 311 (2006) 212-215

LIST OF FIGURES

Fig. 1.1	Indian three stage nuclear program	3
Fig.1.2	Typical schematic diagram of nuclear fuel cycle	4
Fig. 2.1	Basic diagram of mass spectrometry: generation of ions, separation of these ions by their mass-to-charge ratio in the mass separator and detection of ions in the ion detector.	29
Fig. 2.2	Block diagram of orthogonal accelerated time-of-flight mass spectrometer s (GBC 8000R Model)	30
Fig. 2.3	Concentric glass pneumatic (Meinhard) nebuliser	31
Fig. 2.4	Cyclonic spray chamber	33
Fig. 2.5	A Typical picture of Plasma Torch	34
Fig. 2.6	Temperature profile of Plasma	35
Fig 2.7	Orthogonal Accelerated time of flight mass analyzer	40
Fig.2.8	Electron multipliers : (a) Discrete- dynodes electron multiplier and (b) continuous-dynodes electron multiplier	41
Fig.2.9	A typical mass spectrum (50 ppb multi-element standard solution).	42
Fig.2.10	A systematic block diagram of optimization and calibration of ICPMS	45
Fig.2.11	Block diagram of basic gamma spectrometry system	48
Fig.2.12	A typical gamma-ray spectrum	50
Fig.2.13	Electronic transitions: (a) Possible electronic transitions (b) Transitions in UV-Visible region	54
Fig.2.14	A schematic diagram of a UV-visible spectrophotometer	55

Fig.2.15	Calibration plot for absorption spectra of titanium (in 2.5N H ₂ SO ₄ and 3% H ₂ O ₂)	57
Fig 2.16	Sample dissolution by: (a) Conduction and convection heating and (b) microwave heating	59
Fig. 2.17	Microwave rotor and high pressure vessel	60
Fig. 2.18	The distribution of a solute between aqueous and organic phase	61
Fig. 2.19	Steps in a ion exchange column chromatography	65
Fig. 2.20	Strong base resin in the form of tertiary ammonium chloride	66
Fig.2.21	A systematic diagram for precipitation gravimetry	68
Fig.3.1	Core configuration of new nuclear research facility [8]	76
Fig.3.2	photographs of dissolution apparatus in fume hood	79
Fig.4.1	Schematic cross sectional view of U-Mo fuel	92
Fig.4.2	A photograph of anion exchange column	96
Fig.4.3	Systematic diagram for the analysis of U-Mo alloy	109
Fig.5.1	Formation of fissionable ²³⁹ Pu from ²³⁸ U	112
Fig.5.2	Block diagram of sodium cooled FBRs	113
Fig.5.3	Percentage extraction of zirconium: (a) with 30% TBP and 0.1M TOPO at different concentration of HNO ₃ and HCl and (b) with different concentration of TOPO at 4M HNO ₃ , 4M HCl and 4M HNO ₃ -4M HCl mixture	121
Fig.5.4	Percentage extraction of U (a) and Zr (b) as a function of metal ion concentration in presence of varying amount of U	123
Fig.5.5	Variation in sensitivity with matrix concentration Experimentally determined MO ⁺ /M ⁺ ratios and Zr ⁺⁺ /Zr ⁺ ratio by	124

Fig.5.6	ICPMS at optimized conditions	135
Fig. 5.7	Systematic diagram for analysis of U-Zr alloy	139
Fig. 6.1	Flow-sheet of separation and estimation of Dy, Ti and Mo in Dy ₂ TiO ₅	154

LIST OF TABLE

Table 1.1	Properties of FBR nuclear fuels	6
Table 1.2	List of fusion mixture (flux) commonly used for dissolution of refractory	12
Table 1.3	Specifications of metallic impurities in nuclear fuels (in $\mu\text{g g}^{-1}$)	15
Table 1.4	Specification of non metals in nuclear fuels(in $\mu\text{g g}^{-1}$)	18
Table 1.5	Reagent and product formula used for assay of some important bulk elements [75]	20
Table 2.1	Some background ions observed from mineral acid solvents	43
Table 2.2	Optimized operating conditions of ICP-MS	46
Table 3.1	Salient Features of the NRF at Trombay [180]	75
Table 3.2	Optimized operating conditions of ICP-MS	78
Table 3.3	List of isotopes monitored during mass spectrometric analysis	80
Table 3.4	Results of Recovery Studies using ICPMS (Sample Amount: ~ 1.0 g, Vol. = 25 mL, and N = 10)	84
Table 3.5	Results of Recovery Studies by γ -Spectrometry (N=10, 60 s Counting)	88
Table 3.6	Instrumental detection limit (IDL) and method detection limit (MDL) of All the Analytes (N=5)	88
Table 3.7	Results of Analysis of Three Real U_3Si_2 Fuel for Metals by ICP-MS	89
Table 4.1	Optimized operating conditions of ICP-MS	94
Table 4.2	Retention studies of 52 elements (each having 200 ppb) in the	98

absence of matrix

Table 4.3	Recovery of trace elements in synthetic U-Mo Sample (Sample Amount =0.1g, Volume=25mL, N=10)	99
Table 4.4	Instrument detection limit (IDL) and Method detection limit (MDL) of all the analytes (N=10)	107
Table 4.5	Trace element concentrations in the U-Mo Samples of different lots (in $\mu\text{g/g}$)	109
Table 5.1	Retention Studies of 55 Elements (each at 100 ppb) in the Absence of the Matrix	125
Table 5.2	Recovery of Trace Elements in Synthetic U-Zr Sample (Sample Amount =0.1 g, Volume=25 mL, N=10)	126
Table: 5.3	Spectroscopic interference of the analytes due to isobaric, doubly charged and oxide species.	133
Table 5.4	Instrument Detection Limit (IDL) and Method Detection Limit (MDL) (N=10)	136
Table 5.5	Result of Recovery Studies by γ -Spectrometry (N=10, 60 s Counting)	138
Table 5.6	Trace Element Concentration in the U-Zr Samples of different Lots (in $\mu\text{g g}^{-1}$)	140
Table 6.1	Microwave operating conditions	146
Table 6.2	Determination of major elements by ICP-MS in the synthetic samples	148
Table 6.3	Recovery of molybdenum in pure molybdenum solution (N=3)	149
Table 6.4	Effect of Dy in the precipitation of Mo (N=3).	150

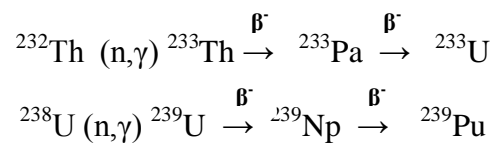
Table 6.5	Recovery of Mo in presence of Ti (N=3).	150
Table 6.6	Recovery of Dy in presence of Mo (N=3).	151
Table 6.7	Recovery of Dy in presence of Ti (N=3).	151
Table 6.8	Recovery of Ti in presence of Mo (N=3).	152
Table 6.9	Recovery of Ti in presence of Dy (N=3).	152
Table 6.10	Estimation of Mo, Dy and Ti by developed method in synthetic samples (N=3)	153
Table 6.11	Analysis of real dysprosium titanate samples of different lots	154
Table 6.12	Estimation of trace impurities in the real samples by ICP-MS	155
Table 7.1	Optimized operating conditions of ICP-MS	162
Table 7.2	Microwave operating conditions	163
Table 7.3	Recovery of rare earth elements in high purity aluminium metal after matrix separation (Sample Wt.= 1.0 g, Vol.=10 mL, N=10)	165
Table 7.4	Instrumental detection limits(IDLs) and method detection limits (MDLs)	168
Table 7.5	Result of recovery studies by γ -spectrometry (N=10, 60 s Counting)	169
Table 7.6	The impurities in real sample of alumina and aluminium metals	170

Chapter 1

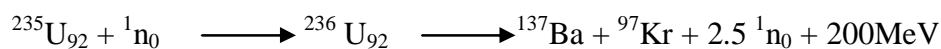
Introduction

1.1 Nuclear Energy

Nuclear energy is a clean, safe, reliable and competitive energy source. It is the only source of energy that can replace a significant part of the fossil fuels (coal, oil and gas) which pollute the atmosphere and contribute to the greenhouse effect. Nuclear energy is produced by nuclear fission in a nuclear reactor. The nuclear fuel materials have fissile isotopes, such as ^{235}U , ^{233}U and ^{239}Pu [1, 2]. In fission process two or three neutrons are produced and they help the self-sustaining chain reaction which releases energy with a controlled rate in a nuclear reactor. ^{235}U and ^{239}Pu are the commonly used fissile isotopes in nuclear reactors. Among the uranium isotopes ^{235}U is a naturally available fissile material whereas it's another fissile isotope, ^{233}U is not available in nature and obtained by the neutron irradiation of thorium (Th) in a nuclear reactor. ^{232}Th and ^{238}U being fertile isotopes [3-6] get converted into fissile isotopes, namely ^{233}U & ^{239}Pu respectively by following nuclear reactions:



Fission of ^{235}U by neutron can be described as:



Some of the released neutrons cause fission of another ^{235}U nucleus, thus sustaining the fission chain reaction. One gram of uranium yields about as much energy as a ton of coal or oil. Nuclear waste is correspondingly about a million times smaller than fossil fuel waste, and it is totally confined.

1.2 Indian Nuclear Energy Program

Nuclear power is the fourth-largest source of electricity in India after thermal, hydroelectric and renewable sources of electricity. In comparison to other fossil fuels, nuclear power requires less quantities of fuel. No other source of energy can produce such an amount of power from a very small quantity of material [7, 8]. Moreover it is also a green source of energy. To utilize the large abundant of thorium in India, Dr. Homi J. Bhabha envisaged a three-stage Indian nuclear power program in 1954 [9-11].

Stage 1: In the first stage natural uranium is used in pressurized heavy water reactors (PHWR) to produce electricity and ^{239}Pu . PHWR uses natural uranium as fuel and heavy water as moderator and coolant. Plutonium produced is separated from the spent fuel in reprocessing plants.

Stage 2: The second stage deals with the fast reactor technology. In the second stage the plutonium obtained from the first stage is mixed with uranium (as a mixed-oxide (MOX) or as metallic fuel) and used in the Fast Breeder Reactors. The fast breeder reactors utilize fission of plutonium for power and breed more plutonium from the ^{238}U . Thorium is proposed to be used in the reactor to produce ^{233}U .

Stage 3: The third stage of Indian nuclear program envisages utilization of thorium in place of uranium for power generation. Advanced heavy water reactors (AHWR) will be

used in this stage. Power will be generated from the ^{232}Th - ^{233}U fuel aided by plutonium. Currently this stage is still in the research stage [12]. Effort are on towards developing an advance heavy water reactor that will use both Th - ^{233}U and Th - Pu mixed oxide as fuel.

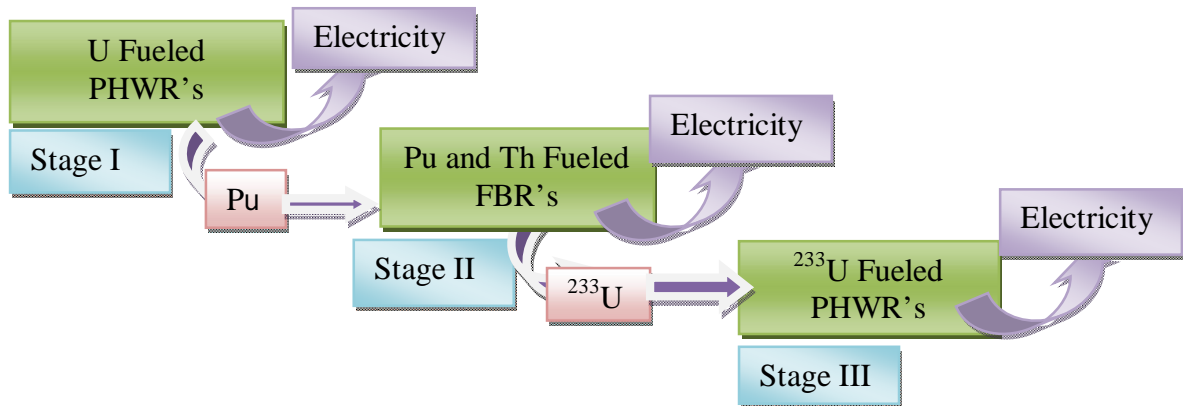


Fig. 1.1: Indian three stage nuclear program

1.3 Nuclear Fuel cycle

The nuclear fuel cycle includes a series of stages through which nuclear fuel progresses. A lot of man power and technology input is required to develop such indigenous projects starting from mining and milling of ores, fuel and structural materials fabrication and processing, chemical and physical quality control and quality assurance, spent fuel reprocessing, radioactive waste management, including designing, manufacturing, construction of infrastructure and instruments. If spent fuel is not reprocessed, the fuel cycle is referred to as an open fuel cycle (or a once-through fuel cycle); if the spent fuel is reprocessed, it is referred to as a closed fuel cycle [13, 14]. India is following closed fuel cycle [15] and following are the various processes.

- (i) Uranium extraction from uranium ore, and conversion to yellowcake

- (ii) Conversion of yellow cake to UO_2
- (iii) Fuel fabrication
- (iv) Fission and activation of the fuel in reactors
- (v) Interim storage of spent nuclear fuel
- (vi) Reprocessing of spent nuclear fuel.
- (vii) Nuclear Waste management

A schematic diagram of the processes involved in a nuclear fuel cycle program is given in Figure 1.2.

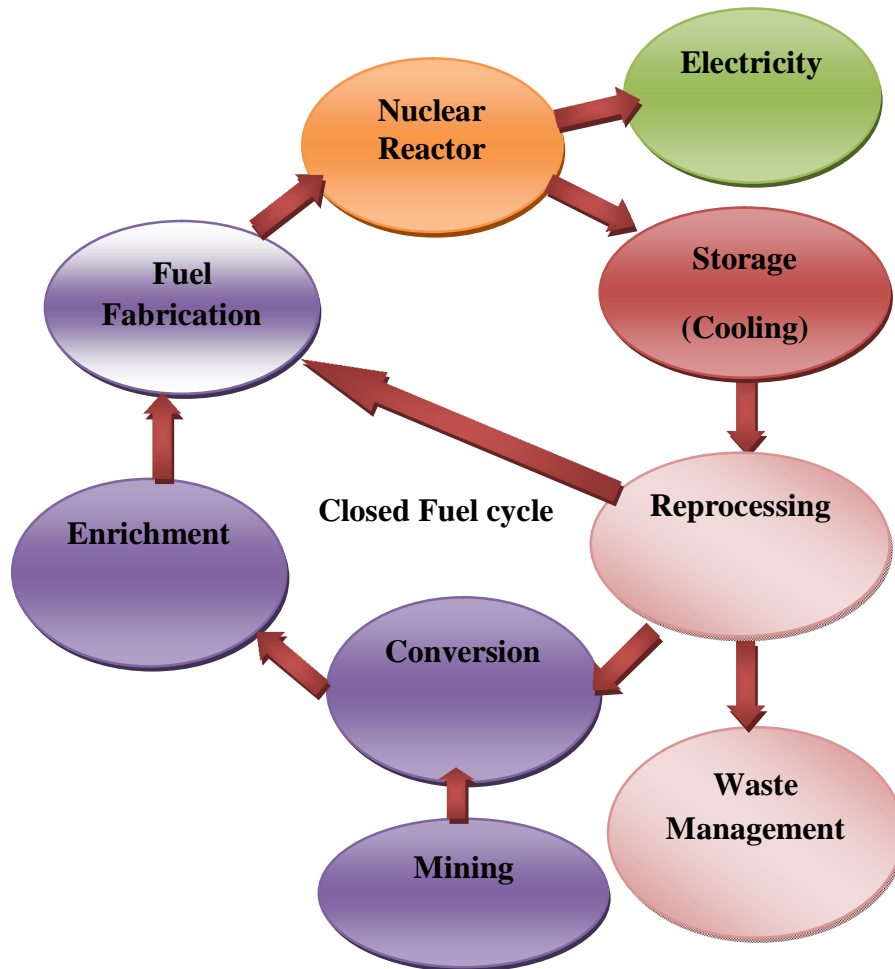


Fig.1.2 Typical schematic diagram of nuclear fuel cycle

1.4 Important Nuclear Materials

1.4.1 Nuclear Fuels

Nuclear fuels are the materials which generate large amount of heat during nuclear fission reaction. Types of nuclear fuels used in research and power reactors are different. Nuclear fuel decides the various parameters in a nuclear reactor and could be classified depending upon its nature as:

1.4.1.1 Ceramic fuels

These fuels are further categorized as oxides or non-oxides. Natural UO_2 is used as nuclear fuel in pressurized heavy water reactors (PHWRs), while pressurized water reactors (PWRs) and boiling water reactors (BWRs) use enriched UO_2 . The oxide fuels are chemically stable and compatible with water. They also show high radiation resistance. Mixed oxide (MOX) of U and Pu is the preferred choice as fuels for the fast breeder reactors (FBRs). The proposed advanced heavy water reactors (AHWR) designed for Th utilization will be using mixed oxide fuels of U, Pu and Th. The non-oxide ceramic nuclear fuels are the mixed carbide and nitride of U and Pu. These fuels have certain advantages such as better thermal conductivity, denser fissile content and better breeding ratio over the oxide fuels. The Fast breeder test reactor (FBTR) at Kalpakkam, India, utilises the mixed carbides of U and Pu, $(\text{U,Pu})\text{C}$, as fuel (16). However, due to their pyrophoric nature, their handling and fabrication need enhanced safety requirements.

1.4.1.2 Metallic fuel

Metallic fuel was the first to be selected for the experimental fast reactors in the USA and the UK, in the 1950s, owing to ease of its fabrication, high thermal conductivity and high fissile and fertile atom densities. They are capable of providing high breeding ratio.

Hence, they are considered to be suitable for fast reactors [17-20]. The EBR-I in the USA used unalloyed uranium, U-Zr and Pu-Al and the Enrico Fermi reactor was fuelled with U-Mo alloy [21]. Table 1.1 summaries properties for FBR nuclear fuels [22].

Table 1.1: Properties of FBR nuclear fuels

Properties	(U _{0.8} Pu _{0.2})O ₂	U-19Pu-10 Zr	U-15Pu (with Zr liner on clad)
Heavy metal density (g/cc)	9.78	14.30	18.80
Melting point (°K)	3083	1400	1353
Thermal conductivity (W/m °K)			
1000K	2.6	25	-
2000K	2.4		
Crystal structure	Flourite	bcc (γ)	Orthorhombic (α)
Breeding ratio	1.09	1.36	1.56
Doubling time (y)	40	9.4	7
Swelling	Moderate	High	High
Handling	Easy	Inert atmosphere	Inert atmosphere
Compatibility:			
Clad	Average	Eutectics formation	Eutectic formation issue
Coolant	Average	Good	Good
Dissolution & Reprocessing amenability	Established	Pyro-reprocessing	Pyro-reprocessing
Fabrication/irradiation experience	Large Good	Limited	No reported experience

1.4.1.3 Intermetallic fuels

Uranium intermetallic fuels such as uranium aluminides (UAl_3) and uranium silicides (U_3Si_2) are mainly used in research and test reactors for neutron production [23, 24]. As compared to ceramic fuels, intermetallic fuels can achieve higher densities thereby requiring lower fuel inventories. The fuel for Apsara research reactor at Bhabha Atomic Research Centre was U-Al based intermetallic fuel which is replaced by U-Si based intermetallic fuel in the new research reactor coming up at Trombay.

1.4.2 Cladding materials

The fission of U atoms produces fission products, which emit neutrons, β and γ rays. These particles can be lethal to humans, so the use of fuel cladding keeps the radioactive materials isolated from the coolant/moderator, which surrounds the cladding at the same time transmit the heat to coolant. The material for fuel cladding is selected after other design aspects of the reactor's core, such as, the nuclear fuel, the moderator and coolant materials have already been decided. Therefore, there are multiple design constraints for the selection of the fuel cladding material. These constraints include the neutron absorption cross section, maximum service temperature, creep resistance, mechanical strength, neutron radiation resistance, thermal expansion, thermal conductivity and chemical compatibility with fuel, fission products and coolant [25-29]. The cladding material should be transparent to neutrons, meaning that the material should have low present a neutron absorption cross-section to minimize neutron losses (such as Mg, Be, Si, Al, and Zr).

1.4.3 Control rods and burnable poisons

Control rods are used to control the fission reaction. These materials have elements with high neutron absorption cross section, such as, B, Cd, Gd, Dy etc. Boron carbide (B₄C) is a widely used neutron absorber because of its high B content, high chemical inertness and high refractory nature. The neutronic absorption of B₄C is due to ¹⁰B, which undergoes following capture reaction:



The cross section of this reaction varies from 3850 barns for thermal neutron to few barns for fast neutron and allows the use of boron carbide with natural isotopic content (19.8% ¹⁰B) or enriched upto 90% depending upon the type of reactor [30].

Gadolinium has a very high thermal neutron capture cross section. The reaction product has a very low capture cross-section. The element is therefore, used as a “burnable” poison in the nuclear reactors to control the reactivity of fresh reactor fuel assembly. In a specific reactor requirement gadolinium is used in the form of gadolinium aluminate [31]. Dysprosium titanate (Dy₂TiO₅) is used to control the fission reaction in VVERs reactors [32]. Many pressurized water reactors (PWRs) operate with silver-indium-cadmium (Ag-In-Cd) as control rods [33].

1.4.4 Moderator and Coolant

Moderator is used to slowdown the neutrons generated during nuclear fission reaction. Light water (H₂O), heavy water (D₂O), graphite and beryllium are used as neutron

moderator in different nuclear reactors [34-36]. Coolant is a medium which transfers heat from the reactor core to turbine system. Light water is very good coolant for BWRs, while in PHWR's heavy water is used as coolant. Fast reactor used liquid sodium as coolant.

1.5 Chemical characterization of nuclear materials

Chemical characterization of materials is the first and the most important step in chemical quality control (CQC) exercise, which involves determination of major, minor and trace elements with good accuracy and precision. Chemical quality control provides a means to ensure the quality of the fabricated material as per the required chemical specifications. In the case of nuclear reactor materials, the finished products should meet the stringent chemical specifications for major to trace constituents, since they affect the material properties as well as performance under prevailing operating conditions. Besides major and minor constituents, knowledge of concentrations of trace elements like H, N, C, S, B, Cl, F, Cd, Co, and rare earth elements (REEs) is essential to establish the suitability of the materials. The presence of trace metallic and non-metallic impurities in the nuclear fuel can affect the optimum performance of a reactor [37, 38]. The materials of interest are mainly nuclear fuels (U_3Si_2 , U-Zr, U-Mo, U-Zr-Pu etc) and structural materials (Dy_2TiO_5 , Al_2O_3 , Gd_2ZrO_5 , Zircoloy, stainless steel etc.) of existing as well as upcoming Indian research and power reactors. Depending on the content of element of interest in the matrix, IUPAC Gold book [39] describe the major, minor, trace and ultra trace element as :

Major: >1 wt% ($>10000 \mu\text{g g}^{-1}$)

Minor: <1 wt% and >0.01wt% (<10000 $\mu\text{g g}^{-1}$ and >100 $\mu\text{g g}^{-1}$)

Trace: <0.01wt% and >0.0001wt% (<100 $\mu\text{g g}^{-1}$ and >1 $\mu\text{g g}^{-1}$)

Ultra trace: <0.0001 wt%. (<1 $\mu\text{g g}^{-1}$)

The available methods for the determination of trace metallic elements in various nuclear materials are inductively coupled plasma mass spectrometry (ICP-MS) [40-43], inductively coupled plasma atomic emission spectrometry (ICP-AES) [44,45], flame atomic absorption spectroscopy (FAAS) [46,47], ion chromatography (IC) [48,49], etc.

Analytical methodology for characterization involves the following steps:

1.5.1 Sample dissolution

1.5.2 Trace metal determination

1.5.3 Trace non-metal determination

1.5.4 Major content determination

1.5.5 Isotopic composition and Oxygen/ metal ratio determination

1.5.1 Sample Dissolution

Most analytical measurements are performed on solutions (usually aqueous) of the analyte. While some samples dissolve readily in water or aqueous solutions of the common acids or bases, others require powerful reagents and rigorous treatment. In general, there are three methods of decomposing solid samples to obtain aqueous solution of analytes. These are: (1) heating with aqueous strong acids (or occasionally bases) in open vessels; (2) fusion in molten salt; (3) microwave heating with acids. These methods differ in the temperatures and the strengths of the reagents used.

1.5.1.1 Conventional Acid Dissolution

The most common reagents for open-vessel decomposition of inorganic analytical samples are the mineral acids. Much less frequently, ammonia and aqueous solutions of the alkali metal hydroxides are used. Ordinarily, a suspension of the sample in the acid is heated by flame or a hot plate until the dissolution is judged to be complete by the absence of a solid phase.

1.5.1.2 Dissolution by fusion method

The different types of refractory materials are encountered during CQC and for each type, several different dissolution techniques are feasible. Methods in current use include acid dissolution in pressure vessels and fusion techniques using a variety of flux mixtures [50,51]. For routine work fusion methods are preferred because they are usually rapid compared to acid dissolution, and a number of samples may be analyzed simultaneously. For routine analysis of bulk elements, this dissolution method is appropriate. But, for trace analysis, this method is not appropriate, especially when ICP-MS or ICP-AES is used due to large total dissolved solid present in the dissolved samples. In Table 1.2 some common fusion mixtures for typical dissolution of some refractory materials have been listed [52-54].

Table 1.2: List of fusion mixture (flux) commonly used for dissolution of refractory materials

Flux (m.p. °C)	Fusion Temperature (°C)	Type of Crucible	Type of Sample Decomposed
Na ₂ S ₂ O ₇ (403 °C) or K ₂ S ₂ O ₇ (419°C)	Up to red heat	Pt, quartz porcelain	For insoluble oxides and oxide-containing samples, particularly those of Al, Be, Ta, Ti, Zr, Pu, and the rare earths.
NaOH (321) or KOH (404)	450-600	Ni, glassy carbon	For silicates, oxides, phosphates, and fluorides
Na ₂ CO ₃ (853) or K ₂ CO ₃ (903)	900-1000	Ni, Pt (for short periods)	For silicate and silica-containing samples (clays, minerals, rocks, glasses), refractory oxides, quartz and insoluble phosphates and silicates.
Na ₂ O ₂	600	Ni, Pt	For sulfides; acid-insoluble alloys of Fe, Ni, Cr, Mo, W, and Li; Pt alloys; Cr, Sn, and Zn minerals
H ₃ BO ₃	250	Pt	For analysis of sand, aluminum silicates, titanite, natural aluminum oxide (corundum), and enamels
Na ₂ B ₄ O ₇ (878)	1000-1200	Pt	For Al ₂ O ₃ ; ZrO ₂ and zirconium ores, minerals of the rare earths, Ti, Nb, and

			Ta, aluminum-containing materials; iron ores and slags.
Li ₂ B ₄ O ₇ (920) o r LiBO ₂ (845)	1000-1100	Pt, graphite	For almost anything except metals and sulfides. The tetraborate salt is especially good for basic oxides and some resistant silicates. The metaborate is better suited for dissolving acidic oxides such as silica and TiO ₂ and nearly all minerals.
NH ₄ HF ₂ (125) NaF (992) KF (857) or KHF (239)	900	Pt	For the removal of silicon, the destruction of silicates and rare earth minerals, and the analysis of oxides of Nb, Ta, Ti, and Zr.

1.5.1.3 Microwave Dissolution

The use of microwave ovens for the decomposition of both inorganic and organic samples was first proposed in the mid-1970s and by now has become an important method for sample preparation [55-58]. Microwave digestions can be carried out in either closed or open vessels, but closed vessels are more popular owing to the higher pressures and higher temperatures that can be achieved. One of the main advantages of microwave decompositions compared with conventional methods using a flame or hot plate (regardless of whether an open or a closed container is used) is speed. Typically, microwave decompositions of even difficult samples can be accomplished in ten to twenty minutes. In contrast, the same results require several hours when carried out by

heating over a flame or hot plate. The difference is due to the different mechanism by which energy is transferred to the molecules of the solution in the two methods. Finally closed-vessel microwave decompositions are often easy to automate, thus reducing operator time required to prepare samples for analysis. The details of microwave will be discussed in the chapter 2 (instrumentation and method).

1.5.2 Assay of Trace metallic impurities

Among the trace impurities present in nuclear fuel, the trace metallic elements need to be determined because they may have adverse affect on the neutron economy as well as the physical properties of these materials. Thus, from the point of view of metallurgy and neutrons economy, it is necessary to know the levels of these impurities and verify the technical specifications. The compounds of uranium used in nuclear reactors have strict limits for impurities such as Boron (B), Cadmium (Cd) and some rare-earths e.g. Samarium (Sm), Europium (Eu), Gadolinium (Gd), Dysprosium (Dy), etc., [59]. These elements have large neutron absorption cross-sections and hence are very significant in thermal reactors for assessing neutron economy as well as for certifying the total impurities as a part of the chemical quality assurance of fuels. Sodium, magnesium and aluminium, if present in uranium oxide fuel in amounts higher than the specified levels, may reduce the relative amount of fissile materials and form appreciable amounts of uranates of these elements with uranium in lower and higher oxidation states in reactor operating and transient conditions, respectively Formation of these uranates in appreciable quantity may cause expansion of fuel volume leading to rupture of fuel cladding. Also in minor accidents involving crack of cladding, uranates with higher

valency of uranium may be formed which may lead to fuel expansion due to their low density and propagate further cracking of the clad. Hence quantifying these elements helps in deciding whether the prepared material can be taken for intended use. Zinc is another metal whose quantification is important. It has very low melting point and if present in larger amounts will cause liquid metal embrittlement thereby altering the fuel structure. Refractory elements like tungsten, molybdenum and tantalum, if present in large amounts, may cause creep resistance resulting in clad damage. Elements like iron, chromium, nickel are monitored to check for the process pick-up and condition of process equipment. Presence of iron and nickel in high concentration leads to problem in sintering of the fuel, which is required to increase the fuel density for higher power production. In particular, the trace metallic impurities affect the integrity of the fuel material and the neutron economy significantly [60]. Table 1.2 gives the specifications of some of the metallic trace elements in thermal and fast reactor fuels [61, 62].

Table 1.3 Specifications of metallic impurities in nuclear fuels (in $\mu\text{g g}^{-1}$)

Elements	Thermal Reactors		Fast Reactors (Ceramic Grade)			ThO ₂
	Natural	Enriched	UO ₂	PuO ₂	(U,Pu)O ₂	
Ag	1	25	1	10	20	-
Al	50	400	500	250	500	50
B	0.3	1	10	10	20	0.3
Be	-	-	20	20	20	1
Ca	50	250	100	500	250	200
Cd	0.2	1	20	20	20	0.2

Ce	-	-	-	-	-	4
Co	-	75	10	20	20	1
Cr	25	400	200	200	250	25
Cu	20	400	10	50	100	50
Dy	0.15	-	-	-	-	0.2
Eu	-	-	-	-	-	0.08
Fe	100	400	400	350	500	100
Gd	0.1	1	0.1	1	-	0.2
Mg	50	200	25	100	25	50
Mn	10	200	-	-	-	10
Mo	4	400	-	-	-	20
Na	-	400	-	-	100	-
Ni	30	400	400	300	500	30
Pb	-	400	-	-	-	20
Si	60	200	-	-	-	60
Sm	-	-	-	-	-	0.4
Sn		400				1
V	-	400	-	-	100	5
W	-	100		200	200	-
Zn	-	400		200	100	-

Apart from nuclear fuel, various other materials such as moderator, coolant, structural materials need to conform to stringent specifications with respect to presence of trace and ultra trace metallic impurities in similar way.

1.5.3 Trace non-metal assay

The trace non-metallic impurities also affect the integrity of the fuel and structural materials. Some of the non-metals are present in gaseous form in reactor operating conditions. Apart from neutron economy, presence of gaseous impurities may cause swelling of the fuel which may result in rupturing of cladding. Fluorine and chlorine get incorporated into the nuclear fuel during the mining and reprocessing processes. These two elements, being very corrosive, cause local depassivation of the oxide film on the internal surface of the clad tube leading to detrimental effect in the operating reactor environment. The effect of these halides is more prominent in the presence of moisture as they form their respective acids, on reacting with moisture, which leads to corrosion of the clad [63, 64]. In nuclear fuels, non-metallics (H, C, N, O, Cl, F, S, P etc.) present at both trace and major level play an important role in their performance. Hydrogen in the fuel, if present above 1 ppm can cause embrittlement in the clad. Sulphur causes problem during the sintering of pellets while chlorine and fluorine cause local depassivation and corrosion of the clad, if present above the specified limits. During fabrication of fuel pellets, sintering is carried out in inert hydrogen atmosphere. If sulphur is present above certain specified limits in fuel pellets, it results in the formation of corresponding actinide oxo sulphides and H_2S during sintering and this causes shattering of the pellets especially, ThO_2 pellets in powder form [65]. Presence of carbon in excess amounts than the

specified limits will cause carburization of structural materials by reacting with zirconium alloys in thermal reactors and stainless steel in fast breeder reactors, thereby making them fragile [66]. The hydrogen content of the sintered and dried nuclear fuel is an important quality feature. Higher hydrogen contents may lead to damage of the Zircaloy clad tube. Moisture content above the specified limits also causes corrosion of clad, modifies the O/M ratio of the fuel and releases hydrogen which can cause pressure build-up. In nuclear fuels, nitrogen gets incorporated as trace impurity during the dissolution and purification steps. Nitric acid is invariably added during all these steps. The main problem with nitrogen is formation of ^{14}C by the $^{14}\text{N} (n, p) ^{14}\text{C}$ reaction and its release as CO, which leads to carburization and influences the operation of reprocessing process for spent nuclear fuel [67, 68]. Nitrogen also reacts with clad materials to form oxynitrides and these nitrides lead ultimately to poor corrosion resistance. Table 1.3 gives the specification of non-metallic impurities for various nuclear fuel materials [60,69].

Table 1.4 Specification of non metals in nuclear fuels(in $\mu\text{g g}^{-1}$)

Elements	Natural UO₂	Enriched UO₂	Ceramic grade PuO₂	ThO₂
C	200	100	200	100
H	1	-	-	1
N	-	100	200	75
F	10	25	25	10
Cl	-	15	50	25
S	-	-	300	50

1.5.4 Bulk elements assay

The assay of bulk elements such as U, Pu, Zr and Th in the nuclear fuels, Zr in zircoloy, Gd and Al in gadolinium aluminate, Dy and Ti in dysprosium titanate etc. decide the life of fuel/nuclear materials inside the reactors. Therefore, accurate and precise quantification of major (bulk) elements is essential prior to their application in a reactor. Classical or traditional assay of bulk elements are mainly done by gravimetric and, titrametric methods. Traditional gravimetric determinations have been concerned with the transformation of the element, ion or radical to be determined into a pure stable compound which is suitable for direct weighing or for conversion into another chemical form that can be readily quantified. The mass of the element, ion or radical in the original substance can then be readily calculated from a knowledge of the formula of the compound and the relative atomic masses of the constituent elements [70-74].

Gravimetric analysis is a macroscopic method usually involving relatively large samples compared with many other quantitative analytical procedures. It is possible to achieve a very high level of accuracy, and even under normal laboratory conditions, it should be possible to obtain repeatability of results within 0.3-0.5%. The details of precipitation of few element important to nuclear industry are given in Table 1.4 with reagent and product formula.

Titrimetry, in which volume serves as the analytical signal, made its first appearance as an analytical method in the early eighteenth century. In titrimetry we add a reagent, called the titrant, to a solution containing another reagent, called the titrand, and allow them to react. The type of reaction provides us with a simple way to divide titrimetry into the

following four categories: acid–base titrations, in which an acidic or basic titrant reacts with a titrand that is a base or an acid; complexometric titrations based on metal–ligand complexation; redox titrations, in which the titrant is an oxidizing or reducing agent; and precipitation titrations, in which the titrand and titrant form a precipitate.

Table 1.5: Reagent and product formula used for assay of some important bulk elements [75]

Ion	Reagent	Product formula	Special conditions
Th	Sebacic acid	ThO ₂	Ignite at 700-800 °C
Ti	Tannic acid and phenazone	TiO ₂	Dry at 100 oC then ignite at 700-800 °C
U	Cupferron	U ₃ O ₈	Dry at 100 °C and ignite at 1000 °C
Zr	Mandelic acid	ZrO ₂	Ignite at 900-1000 °C
REEs (M)	Oxalic acid	M ₂ O ₃	Ignite at 850

For accurate titration we must combine stoichiometrically equivalent amount of titrant and titrand. We call this stoichiometric mixture the equivalence point. Unlike precipitation gravimetry, where we add the precipitant in excess, an accurate titration requires knowledge of exact volume of titrant at the equivalence point, V_{eq} . The product of the titrant's equivalence point volume and its molarity, M_T , is equal to the moles of titrant reacting with the titrand.

$$\text{Moles of titrant} = M_T \times V_{eq}$$

From the knowledge of the stoichiometry of the titration reaction, one can calculate the moles of titrand. Precise quantification of many elements using titrametric method has been discussed in reports [76-78].

1.5.5. Isotopic composition and Oxygen/ metal ratio determination

Precise determination of isotope ratios is required for the characterization of radioactive waste materials from nuclear reactors and for dating of geological materials in geochronology (based on the decay of natural long-lived radionuclide, e.g., ^{87}Rb , ^{187}Re , or ^{235}U and ^{238}U). Isotope ratio measurements of long lived radionuclides is also applied in isotopic dilution methods (e.g., the accurate determination of uranium, thorium or iodine concentration spiked with ^{235}U or ^{233}U , ^{230}Th and ^{129}I respectively). Conventional radiochemical methods for the determination of isotopic ratios of long-lived radionuclide at low level concentration require a careful and often time consuming chemical separation of the analyte. Sometimes radioanalytical methods are unsuitable, e.g. for isotope analysis of plutonium, where the radionuclides, such as, ^{239}Pu and ^{240}Pu cannot be distinguished due to their similar α energies. In contrast, in comparison to classical radioanalytical measurements ICP-MS provides high isotopic selectivity and sample preparation is often easier. ICP-MS has proved to be an extremely efficient and sensitive analytical mass spectrometric method in ultra trace analysis and this technique has been applied for the precise determination of isotopic compositions of long-lived radionuclides in aqueous solutions [79-81]. The highest precision for isotopic ratio measurements down to 0.002% relative standard deviation (RSD) is possible using the thermal ionization mass spectrometry (TIMS) with a multiple collector ion detection system. Accelerator mass

spectrometry (AMS) is used to determine highly accurate isotopic ratios of U and Pu in nuclear reactor fuels and environmental samples. AMS combines a highly specific particle accelerator with highly sensitive mass analyzers to remove molecular isobaric interferences and achieve much lower detection limits.

Oxygen amounts other than the specified values may change the oxygen to metal ratio (O/M) of the oxide fuel resulting in changes in the physical and chemical properties of the fuel [82, 83]. O/M ratio affects the thermal conductivity, melting point, diffusion coefficients and vapour pressure. Apart from this, the O/M controls the chemical state of the fission product and their interaction with fuel.

1.6 Importance of the thesis work

Uranium silicide is a high density intermetallic nuclear fuel based on low enriched uranium (LEU). There are limited reports in literature on U_3Si_2 fuels [84-87] the discussed the physical, chemical and irradiation properties. The only report available for chemical characterization of U_3Si_2 is [88], does not discuss the trace impurities determination. India, is using first time U_3Si_2 as nuclear fuel in new reaserch reactor at Trombay. Hence a thorough knowledge of chemical characterization for trace, minor and major elements is essential. A method has developed for quantification of trace and ultra trace impurities in U_3Si_2 using ICP-MS.

U-Mo alloy is a metallic fuel, which has higher density than U_3Si_2 . The report has discussed physical, chemical, and irradiation properties [89-93]. Quantification of trace

impurities in U-Mo nuclear fuel using ICP-MS is reported [94], where only few elements have been analyzed, and is less useful for routine analysis due to memory effect of matrix elements. In this work, a chromatography method has been developed for separation of trace elements from the U-Mo alloy. The developed method quantitatively separated thirty three elements which were quantified by ICP-MS. The method has been validated using standard addition and gamma spectrometry method.

U-Zr and U-Pu-Zr alloys are preferred metallic nuclear fuel. Fabrication and properties of this fuel has discussed elsewhere [95-99]. Only limited reports are available where trace elements has been analyzed [94,100], and only few elements in the matrix have been reported. There are no reports for simultaneous separation of both matrix elements (U&Zr). In the present work a solvent extraction method has been developed for quantitative separation of of U and Zr for determination of 36 trace elements in U-Zr alloy. The method has been validated using standard addition method and sample has analyzed.

Dysprosium-titanate is an alternative control rod material for boron based control rods. It is advantageous compared to boron in many respect [101-103]. However, it is a refractory material and dissolution method is not available in the literature. Also chemical characterization of major, minor and trace element is not available. In the present work, a microwave dissolution method has optimized and precise gravimetric method has been

developed for estimation of dysprosium and molybdenum. Titanium has been estimated using UV-Visible spectroscopy. The trace elements have been estimated using ICP-MS.

Alumina is a ceramic material used as insulating material in nuclear reactors [104,105]. Al is used as clad material in the research reactors working at low temperature [106-109]. The dissolution of refractory alumina powder is reported [110], but it was not possible to dissolve the grains of alumina. A microwave method is optimized in the present work to dissolve the alumina. A gravimetric method has been developed to separate the trace and ultra trace level of rare earth elements from Al matrices. The method has been validated using standard addition method and ICP-MS.

Chapter 2

Experimental methods and Techniques

2.1 Introduction

Characterization of nuclear materials can be carried out using several instrumental techniques. Each technique has its advantages and disadvantages. The different techniques are used depending upon the nature of material and the type of characterization required. Several analytical techniques, such as, Neutron Activation Analysis (NAA), Graphite Furnace Atomic Absorption Spectrophotometry (GFAAS), Inductively Coupled Plasma Atomic Emission Spectroscopy (ICP-AES), Total Reflection X-Ray Fluorescence (TXRF), UV - Visible spectrophotometry, gamma spectrometry, Inductively Coupled Plasma Mass Spectrometry (ICP-MS) etc., are in practice for determination of trace impurities in the nuclear materials. Mass spectrometry is used for major, minor, trace and ultra trace analysis. In the present thesis ICP-MS, UV-Visible spectrophotometry, gamma spectrometry, solvent extraction, ion chromatography and gravimetry have been used for characterization of major and trace elements. Microwave dissolution system has been used to dissolved refractory materials such as, Dy_2TiO_5 and Al_2O_3 . Muffle furnace was used to bring precipitates into corresponding oxides for major analysis. Analytical balance has been used for weighing the samples.

The ICP-MS analysis is possible if total dissolved solid is less than 0.2%. Accordingly trace element analysis by ICP-MS requires matrix separation which has been carried out using solvent extraction, anion exchange and precipitation. The details of ICP-MS, gamma spectrometry, UV-Visible Spectrophotometry, Microwave dissolution system,

solvent extraction, anion exchange and precipitation gravimetric method have been discussed in this chapter.

2.2 Mass spectrometry

In mass spectrometry (MS), the mass-to-charge ratio (m/z) is measured as a dimensionless number. Sometimes the unit known as the Thomson (Th), in honor of J. J. Thomson who in 1906, received Nobel Prize in physics for discovery of electron and determination of its m/z ratio. Thomson's early work on cathode rays laid the foundation of the MS field. Thomson, with the help of his student Francis Aston (Nobel Prize in Chemistry in 1922), built the first mass spectrometer to measure the masses of charged atoms. In 1885 Goldstein discovered the anode rays, which are positively charged gas-phase ions in a discharge tube. This method for generating positively charged ions was used in the early mass analysis measurements by Wien [111], Thomson [112] and Aston [113]. Discovery of isotopes of elements by mass spectrometry was started when Thomson found that neon has two different isotopes of mass numbers 20 and 22. Few years later Aston found another isotope of neon of mass 21. Thomson is accepted as the father of the mass spectrometry.

F. W. Aston and other scientists redesigned the instruments to improve resolving power and began using them to separate and prove the existence of elemental isotopes. Alfred Nier, an electrical engineer, made significant contribution in building mass spectrometry; including the 60° sector field instrument, which greatly reduced the size and power

consumption of the magnet. He later produced a design that still bears his name and that of his colleague E. G. Johnson: the Nier-Johnson mass spectrometer, which combines electrostatic and magnetic analyzers in a unique conformation. A variant of this design was commercially developed into one of the highest-resolving-power instrument. Nier helped biologists by preparing ^{13}C -enriched carbon. He also assisted geochemists in determining the age of the earth by measuring $^{207}\text{Pb}/^{206}\text{Pb}$ in the planet's crust, among other achievements. One of Nier's most notable accomplishments was his contribution to U enrichment efforts as a part of Manhattan project. Nier was able to separate nanogram quantities of the ^{235}U isotopes by MS and John Dunning of Columbia University confirmed that ^{235}U was the isotope responsible for the slow neutron fission.

By the 1940s, mass spectrometers were commercially available, and it was firmly established as a useful technique among physicists and industrial chemists. The trio of Fred McLafferty, Klaus Biemann, and Carl Djerassi, brought mass spectrometry to the chemistry community and laid the ground- work for modern biological MS research [114]. With the introduction of the spark ion source by Dempster in 1934 [115,116] significant progress in inorganic mass spectrometry was made for the direct solid analysis of electrically conducting solids (e.g., metals, alloys). Finnigan introduced the first commercial quadrupole mass spectrometer in 1968. Yost and Enke built the first triple quadrupole mass spectrometer as an important tandem mass spectrometric instrument for structure analyses in 1978 [117]. Paul and coworkers developed a quadrupole ion trap, which can trap and analyze ions separated by their m/z ratio using a 3D quadrupole radio-

frequency electric field [118-120]. For the development of the ion trap technique Paul was honored with the Nobel Prize in 1989.

In 1946, Stephens presented his concept of the linear time-of-flight mass spectrometer (ToF-MS) as the simplest mass separation technique. Goldsmith improved mass determination with accuracy to the third decimal place for xenon isotopes employing ToF-MS [121]. Major progress in inorganic mass spectrometry was made possible by the development of ICP-MS in 1980 by Houk, Fassel and co-workers [122]. ICP-MS has grown exponentially and today plays the dominant role among the inorganic mass spectrometric techniques for trace, ultratrace and isotope analysis [123]. The coupling of a laser ablation system to ICP-MS was proposed by Gray in 1985 [124] and has been commercially available since 1990. Nowadays, LA-ICP-MS is the most versatile and sensitive solid mass spectrometric technique for direct trace, ultra-trace and surface analysis and is extremely useful for isotope ratio measurement.

All types of mass spectrometric systems for analysis of inorganic and organic compounds use the same basic principle. A schematic of a mass spectrometer and the principle of operation for the qualitative and quantitative analysis of inorganic or organic compounds is given in Figure 2.1. In this thesis work trace and ultra trace elements were quantified using inductively coupled plasma orthogonal- time-of-flight mass spectrometry (ICP-ToF-MS) of GBC 8000R model.

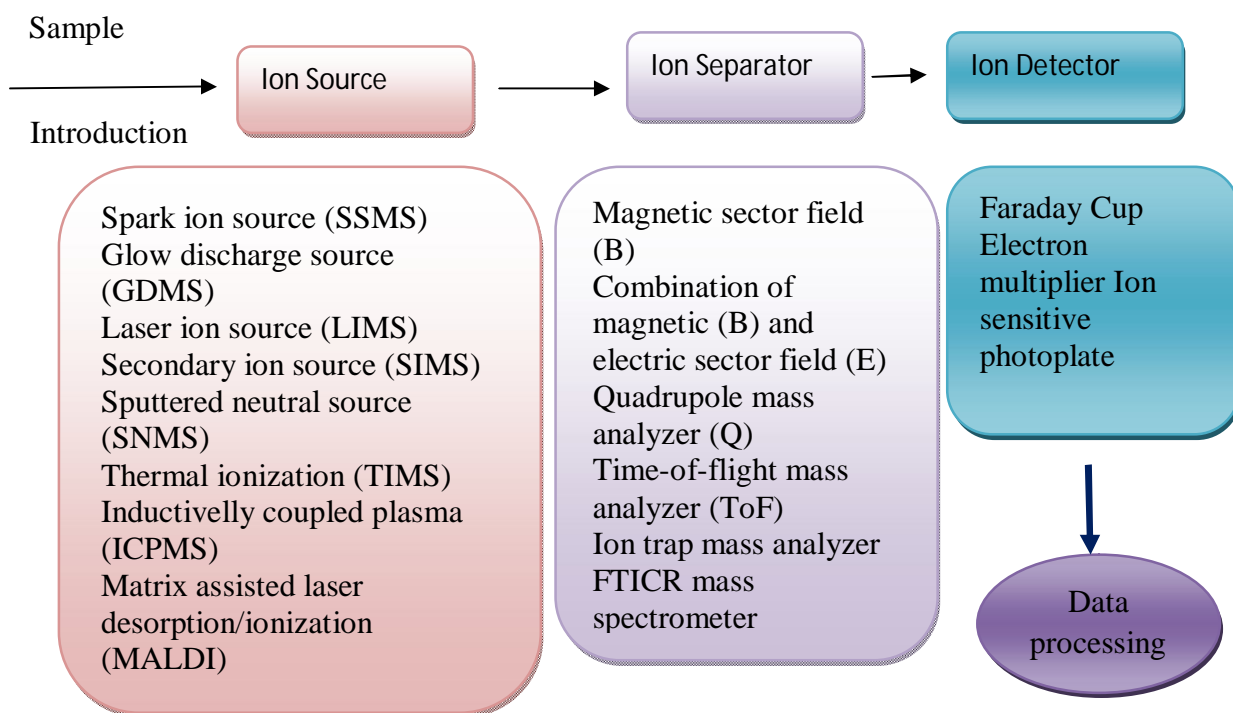


Fig. 2.1: Basic diagram of mass spectrometry: generation of ions, separation of these ions by their mass-to-charge ratio in the mass separator and detection of ions in the ion detector.

2.2.1 Inductively Coupled Plasma Time-of-Flight Mass Spectrometry (ICP-tof-MS)

In 1964 Greenfield et al. [125] introduced inductively coupled plasma source (ICP) for the excitation of atoms and molecules in inductively coupled plasma optical emission spectrometry (ICP-OES). It is currently the most commonly used plasma ion source in inorganic mass spectrometry due to its excellent thermal properties. The ICP source was first successfully coupled to a quadrupole mass analyzer by Gray, Houk and Date [126-

127]. ICP-MS has greater speed, precision, and sensitivity. An ICP-MS from GBC Australia has been used in the present thesis work, the diagram is given in Figure 2.2.

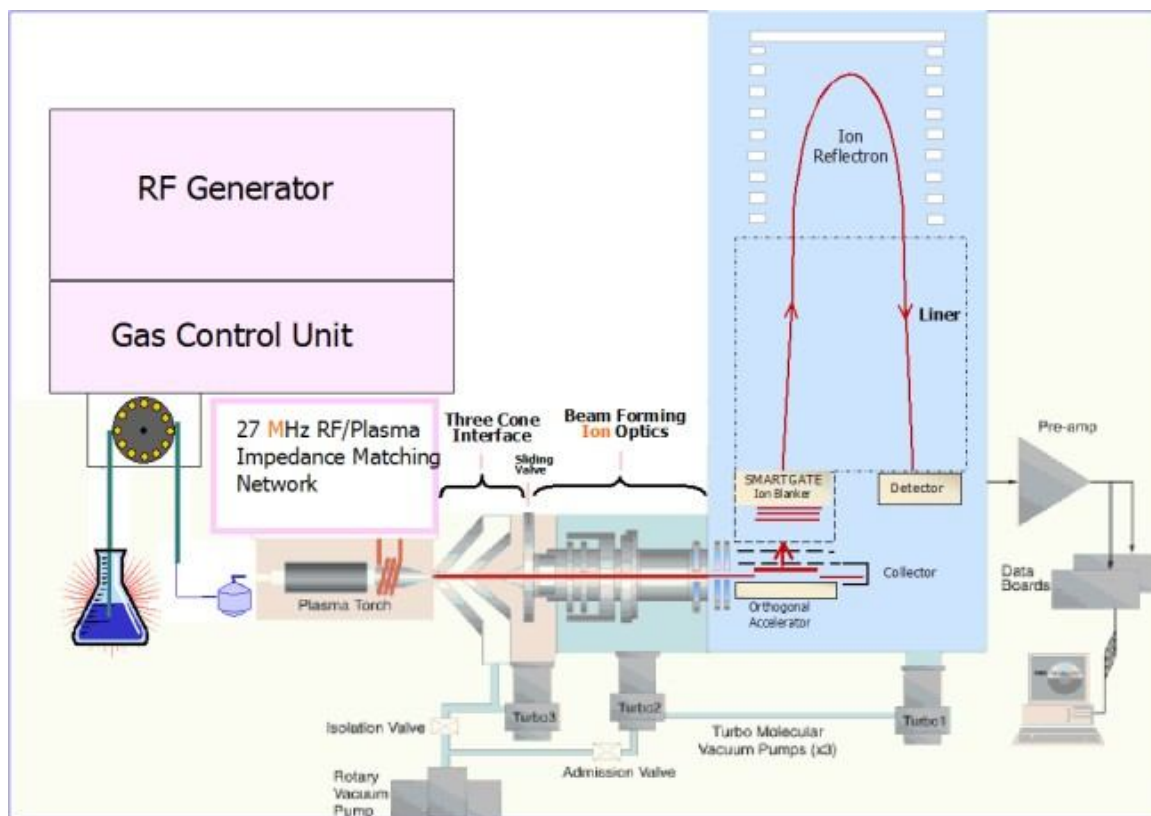


Fig. 2.2: Block diagram of orthogonal accelerated time-of-flight mass spectrometer
(GBC 8000R Model)

The different components of the instrument are:

- i. Sample Introduction System
- ii. Sample Ionization
- iii. Ion Sampling/ Extraction
- iv. Ion Focusing
- v. Mass analyzer
- vi. Detector

2.2.1.1 Sample Introduction System

There are several approaches to introducing samples into an ICP. The particles must be 10 μm or less in diameter to be atomized in the plasma. Gaseous samples meet this criterion and can be injected directly. Samples in solution form require nebulisation to create the particles of desired size (aerosols). Concentric glass pneumatic (Meinhard) nebulisers are frequently used [128,129]. A picture of such a nebuliser is shown in Figure 2.3. It consists of an outer glass tube through which gas (typically argon) flows at a rate of 0.5 – 1.5 L min^{-1} . The gas rushing across the end of the inner tube causes a drop in pressure, which leads to the liquid sample being drawn through the sample tube.

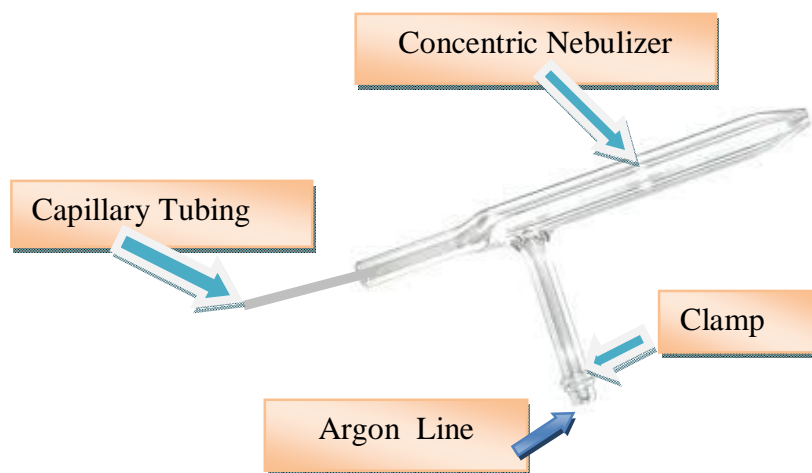


Fig. 2.3: Concentric glass pneumatic (Meinhard) nebuliser

The pneumatic nebulizer works on the principle of the interaction of a high velocity gas stream with a steady flow of analyte solution. Energy is transferred from the gas to the liquid stream causing disruption of the liquid stream into aerosol. This process is known as Venturi effect. This is an automatic process, that is, the sample is sucked in

automatically. Best long term stability of Meinhard nebulisers is generally obtained with a pump, which is necessary to remove the waste solution from the spray chamber. The solution uptake rate can be controlled by adjustment of the pump speed and through the choice of pump tubing. The main drawback of such nebulisers is that they are blocked very easily if solutions with high dissolved solids content are analyzed and requires the total dissolved solid concentration in the liquid sample to be less than 0.2%.

The aerosol from the nebuliser is allowed to pass through a water cooled (at 15°C) cyclonic spray chamber which acts as a drop size filter. The purpose of the spray chamber is to ensure that only the smallest solution droplets (less than 10 µm diameter) reach the plasma, to ensure uniform loading of the plasma for blank, standard and sample. A cooling water jacket is provided on the spray chamber to lower the water loading in the plasma. The improved temperature stabilization of the spray chamber obtained allows the instrument sensitivity to stabilize more quickly. A typical spray chamber is shown in the Figure 2.4. The nebulisation efficiency of the pneumatic nebuliser combined with spray chamber is only 1 to 2 % which is a constraint on the sensitivity of the instrument.

The laser ablation has also been used as a means of sample introduction, though less commonly. In this method, a laser is focused on the sample and creates a plume of ablated material which can be swept into the plasma. This is particularly useful for solid samples, though difficulty to create standards is a challenge in quantitative analysis.

Other methods of sample introduction include electro thermal vaporization (ETV) and in torch vaporization (ITV) hot surfaces (graphite or metal, generally). These require very

small amounts of liquids, solids, or slurries. Other methods like vapor generation are also known.

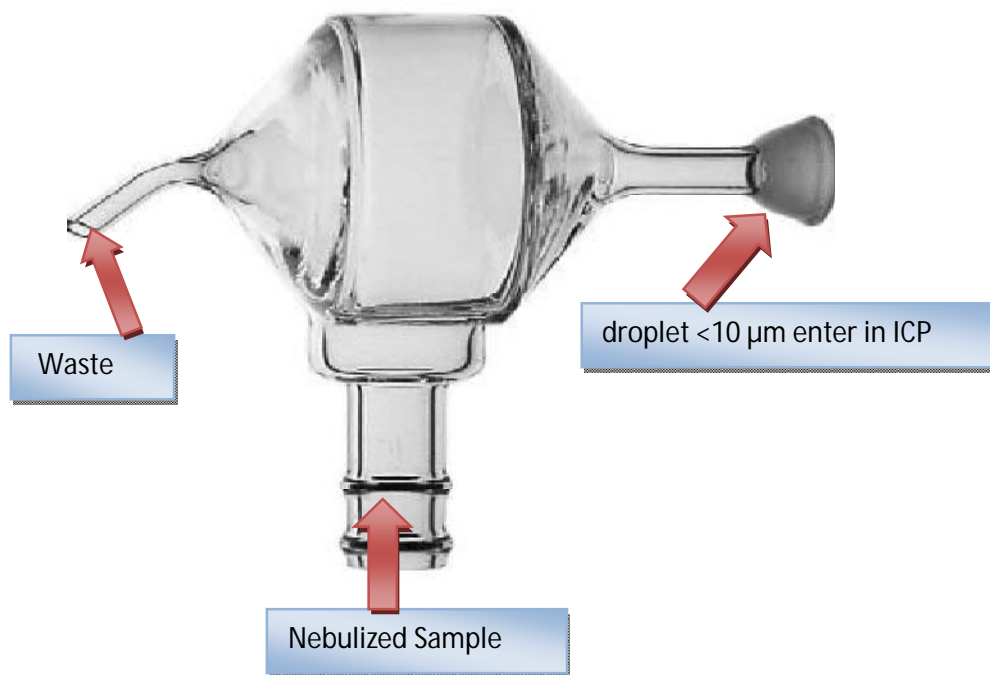


Fig. 2.4: Cyclonic spray chamber

2.2.1.2 Sample Ionization

Once the sample passes through the nebulizer and is partially de-solvated, the aerosol moves into the torch body and is mixed with more argon gas. A coupling coil is used to transmit radio frequency to the heated argon gas, producing an argon plasma "flame" located at the torch. The techniques used for interfacing the plasma source (ICP) to a mass spectrometer were first developed by Dr. Alan Gray [130,131]. An atmospheric inductively coupled plasma is formed when an inert gas usually argon, is introduced into a quartz torch (Fassel torch) [132] that consists of three concentric tubes of varying diameter. The inner tube carries the sample aerosol (nebulizer gas) in a flow of argon, the

intermediate (auxillary gas), which forms and sustains the plasma and the outer (cool gas) that cools the torch as shown in Figure 2.5.

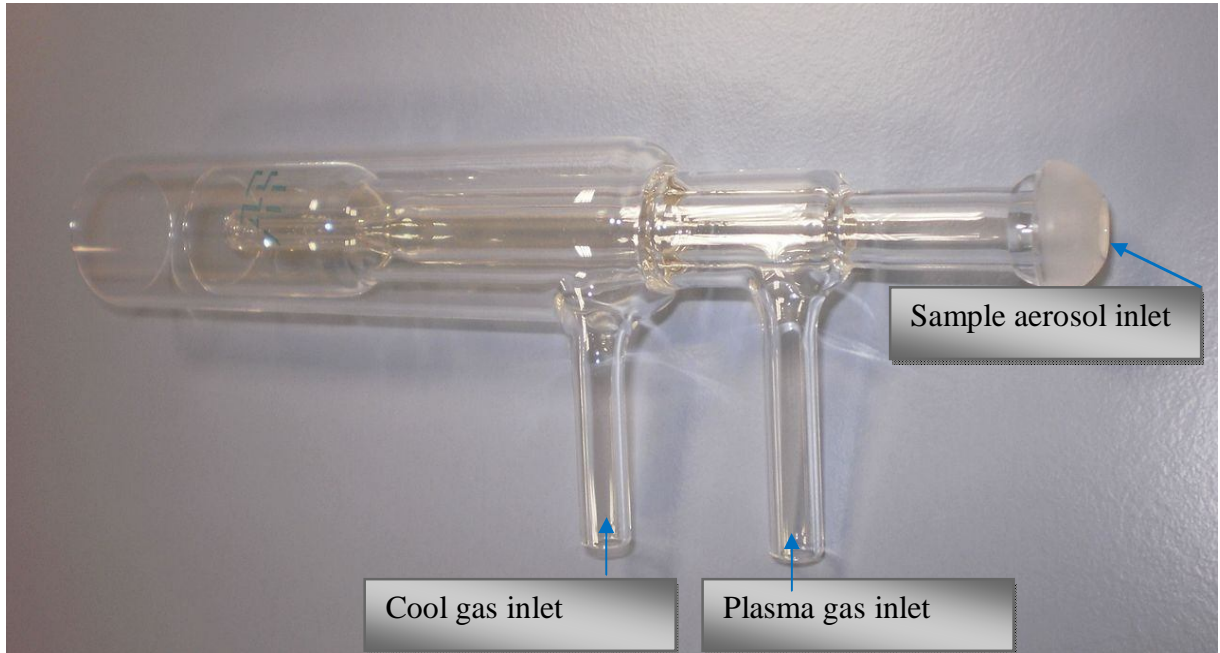


Fig. 2.5: A Typical picture of Plasma Torch

On entering the torch the argon gas is seeded with electrons by initial excitation with a Tesla coil. Radiofrequency energy is applied to the three turns of a coaxial water cooled induction copper coil surrounding the torch. The high frequency current flowing in the induction coil generates oscillating magnetic fields whose lines of force are axially oriented inside the quartz tube and follow closed elliptical paths outside the tube. Induced magnetic fields, in turn, induce electrons in the gas to flow in closed annular paths inside the quartz torch. These electrons (eddy current), accelerated by the time varying magnetic field collide with the neutral argon atoms and ionize them and resistive heating occurs. Then through the process of radiative recombination, the argon ions are recombined with electrons to lead to excited argon atoms and a significant optical background in the UV

region ($e^- + \text{Ar}^+ \rightarrow \text{Ar} + h\nu$). The ions, electrons and neutral atoms continuously collide and as long as the rf field and gas flow is maintained the plasma is sustained.

The resulting plasma is a dense annular shaped ball of highly excited atoms, ions, meta-stable and neutral species. The operating temperature of an ICP is between 5000 to 10000 K [133]. Figure 2.6 shows some approximate temperatures at various positions in the plasma [134].

Measurements of plasma temperature by optical means generally show gas temperature of about 6000 K in the central channel, while excitation temperatures are found to be 7000 – 7500 K and the ionization temperature about 8000 K at 10 mm beyond the load coil.

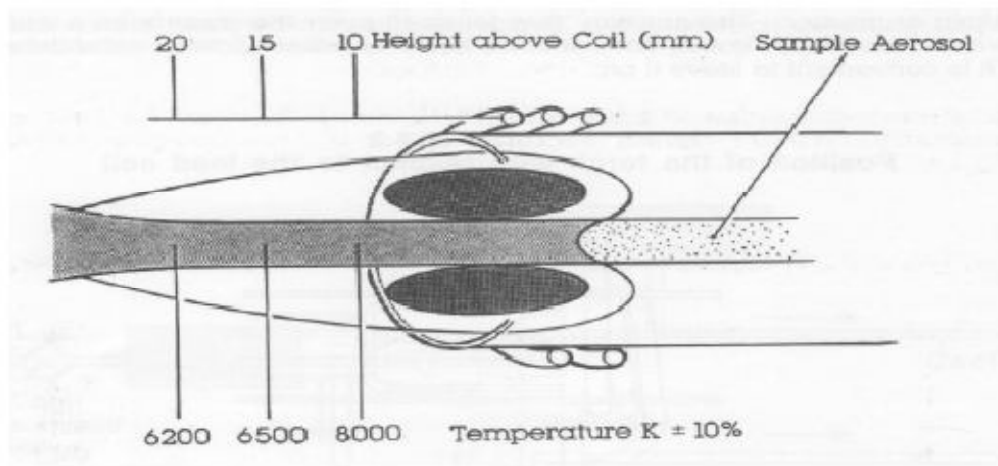


Fig. 2.6: Temperature profile of Plasma

The ICP source has two roles. The first is the volatilization, dissociation and atomization of the sample to be analyzed in order to obtain free analyte atoms, usually in the ground state, and the second is a partial ionization of the analyte atoms and the excitation of the atoms and ions to higher energy states. The plasma acts as a reservoir of energy provided by the RF field and transfers this energy to the analyte. Various ionization processes [135,

136] have been suggested resulting from species that are obtained during the plasma generation. The main modes of ionization by ICP [137] are:

- 1) Charge transfer ionization: $Ar^+ + M \rightarrow M^+ + Ar$
- 2) Thermal ionization: $M + e^-(fast) \rightarrow M^+ + e^-(slow)$
- 3) Penning ionization: $M + Ar^m \rightarrow M^+ + Ar + e^-$

Where Ar^m is meta-stable argon.

In the ICP the principal mechanism by which ionization occurs is thermal ionization. The degree of ionization of an element can be calculated from the Saha equation:

$$\frac{M^+}{M^0} = \frac{1}{n_e} \left(\frac{2\pi m_e kT}{h^2} \right)^{\frac{3}{2}} \frac{Q^+}{Q^0} e^{\left(\frac{-E_{IP}}{kT} \right)}$$

.....(1)

Where M^+ , n_e and M^0 are the number densities of the ions, free electrons and neutral atoms respectively, Q^+ and Q^0 are the ionic and atomic partition functions, respectively, m_e is the electron mass, k is the Boltzmann constant, T is the temperature, h is the planck's constant and E_{IP} is the first ionization energy of the element.

At such high temperatures (5000 to 10000K) using the above equation it has been calculated that most of the elements in the periodic table that have first ionization energies of less than 9 eV are singly ionized to the extent of 90% and there is negligible molecular species or doubly charged ions. Ions are produced in a reproducible manner and ion characteristics of dissolved solids are formed. Hence multi-elemental analysis can be carried out by ICP-MS [138]. Most elements are efficiently ionized in the high

temperature (7500 K) atmosphere of the normal analytical zone and it is generally the region from which ions are sampled in ICP-MS. The position of the normal analytical zone is dependent on the aerosol gas flow rate and, to a lesser extent, on the power supplied to the coil.

The gas that is commonly used to generate the plasma is argon. Like any noble gas, argon is a mono-atomic element with high ionization energy (15.76 eV), has meta-stable energy states (11.55 and 11.75 eV) and is chemically inert. Consequently argon has the capability to excite and ionize most of the elements of the periodic table. Argon is also the cheapest noble gas owing to high concentration in air.

2.2.1.3 Ion Sampling/ Extraction

The ICP reaches temperatures of 5000 – 10000 K at its core, operates with 10 -20 L/min of argon support gas and, of course, operates at atmospheric pressure. The mass spectrometer, on the other hand, operates at 10^{-5} to 10^{-6} Torr or below and, obviously, cannot be subjected to the heat of the plasma. The coupling is achieved by interposing an interface between the two. The differentially pumped interface [139] between the ICP and mass spectrometer is a critical part of any ICP-MS system. The interface essentially consists of two orifices [126, 140,141] and a slide valve to produce three stage expansion chambers – an initial expansion stage (1 torr), an intermediate stage (10^{-3} torr) and an analyzer stage (10^{-6} torr). The first orifice, known as the sampler cone, is a water cooled metal cone with a circular hole of ~ 1.0 mm diameter [142]. A second metal cone known as the skimmer (0.75 mm dia.) is placed behind the sampler and divides an initial expansion chamber (1 torr) from the vacuum region that contains the focusing ion lenses

(10^{-3} torr) and the mass analyzer (10^{-6} torr). The sampler is immersed in the normal analytical zone of the plasma, 5-15 mm from the RF load coil.

2.2.1.4 Ion Focusing

In order to collect as many ions as possible into a beam to pass into the mass analyzer, the skimmer is followed by a series of electrostatic lenses. Before the lens a slide valve is used, which enables the path into the high vacuum region to be closed behind the skimmer. When this is shut, the aperture and skimmer may both be removed without interfering with the pressure in the vacuum region. This valve is then not reopened until the pressure in the extraction stage is re-established. The ion focusing lenses are crucial for the overall sensitivity of the instrument because scattered ions will not be detected. Ion focusing is achieved by subjecting the charged ions to constant electric fields. The system consists of a number of axially symmetric electrostatic lens elements on the system axis and lens supply unit.

2.2.1.5 Mass analyzer

The mass analyzer sorts the ions extracted from the ICP source according to their mass to charge ratio [143]. The mass spectrum is a record of the relative number of the ions of different m/z , which is characteristic of the analytes present in the specimen. Successful operation, of the mass analyzer requires a collision free path for ions. To achieve this, the pressure in the analyzer section of the spectrometer is maintained below 10^{-6} torr [144]. In the mass analyzer the ions are sorted into discrete m/z values depending on the energy, momentum and velocity. Each mass analyzer has its own special characteristics and applications and its own benefits and limitations. The choice of mass analyzer should be

based upon the application, cost, and performance desired. There is no ideal mass analyzer that is good for all applications. The mainly used mass analyzers in ICP-MS are as:

- i. Time of flight (TOF)
- ii. Magnetic (B) and/or Electrostatic (E)
- iii. Quadrupole (Q)

The Instrument used in the present thesis is based on time of flight mass analyzer. The basic principle time of flight based mass analyzer is given below:

Time of flight (TOF) Mass Analyzer

A time of flight mass spectrometer measures the mass-dependent time taken by ions of different masses to move from the ion source to the detector. The kinetic energy (T) of an ion leaving the ion source is:

$$T = eV = \frac{mv^2}{2} \dots\dots\dots(2)$$

where, e is the charge, V applied voltage, m the mass and v is velocity of the ion. The velocity of ion (v), is the length of the flight path, L, divided by the flight time, t:

$$v = \frac{L}{t} \dots\dots\dots(3)$$

Substituting this expression for v into the kinetic energy relation, we can derive the working equation for the time-of-flight mass spectrometer:

$$\frac{m}{e} = \frac{2Vt^2}{L^2} \dots\dots\dots(4)$$

or, rearranging the equation to solve for the time-of-flight:

$$t = \sqrt{\frac{m}{e}} \frac{1}{2V} \dots \dots \dots (5)$$

The ions leaving the ion source of a time-of-flight mass spectrometer have neither exactly the same starting times nor exactly the same kinetic energies. Various time-of-flight mass spectrometer designs have been developed to compensate for these differences. A reflectron is an ion optic device in which ions in a time-of-flight mass spectrometer pass through a "mirror" or "reflectron" and their flight is reversed. A linear-field reflectron allows ions with greater kinetic energies to penetrate deeper into the reflectron than ions with smaller kinetic energies. The ions that penetrate deeper will take longer to return to the detector. If a packet of ions of a given mass-to-charge ratio contains ions with varying kinetic energies, then the reflectron will decrease the spread in the ion flight times, and therefore improve the resolution of the time-of-flight mass spectrometer. A typical diagram of orthogonal-accelerated-time of flight mass analyzer is given in Figure 2.7.

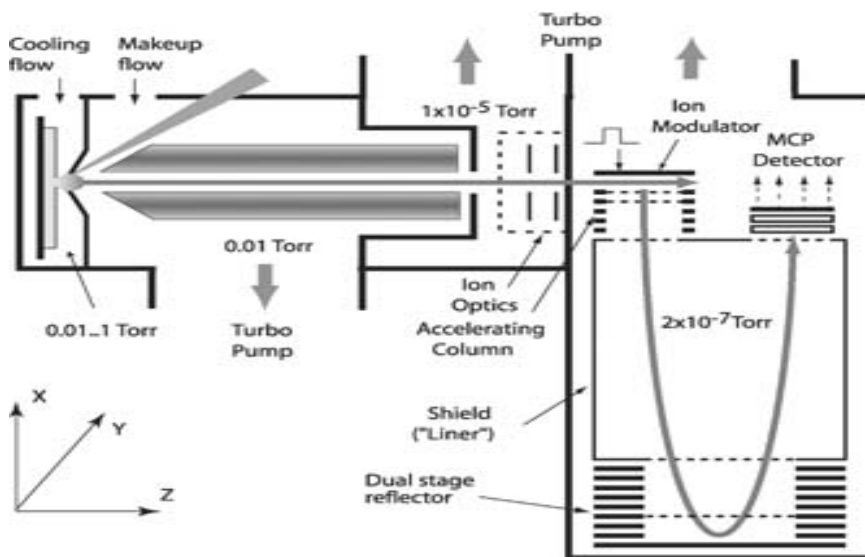


Fig 2.7: Orthogonal Accelerated time of flight mass analyzer

2.2.1.6 Detector

An electron multiplier is used to detect the presence of ion signals emerging from the mass analyzer of mass spectrometer. The task of the electron multiplier is to detect every ion of selected mass passed by the mass filter. The basic physical process that allows electron multiplier to operate is called secondary electron emission. When a charged particle (ion or electron) strikes a surface it causes secondary electrons to be released from atoms in the surface layer. The number of secondary electrons released depends on the type of incident primary particle, its energy and characteristics of the incident surface. There are two basic forms of electron multipliers that are commonly used in mass spectrometry: the discrete-dynodes electron multiplier and continuous-dynodes electron multiplier (often referred as a channel electron multiplier or CEM). A typical discrete-dynode electron multiplier has between 12 and 24 dynodes and is used with an operating gain of between 10^4 and 10^8 depending on the application. Figure 2.8 shows the typical diagram of the detectors. A typical mass spectra is given in Figure 2.9.

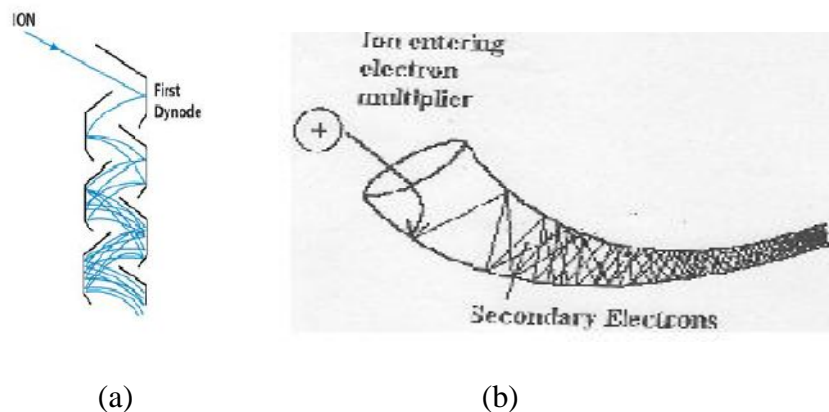


Fig. 2.8: Electron multipliers : (a) Discrete- dynodes electron multiplier and (b) continuous-dynodes electron multiplier.

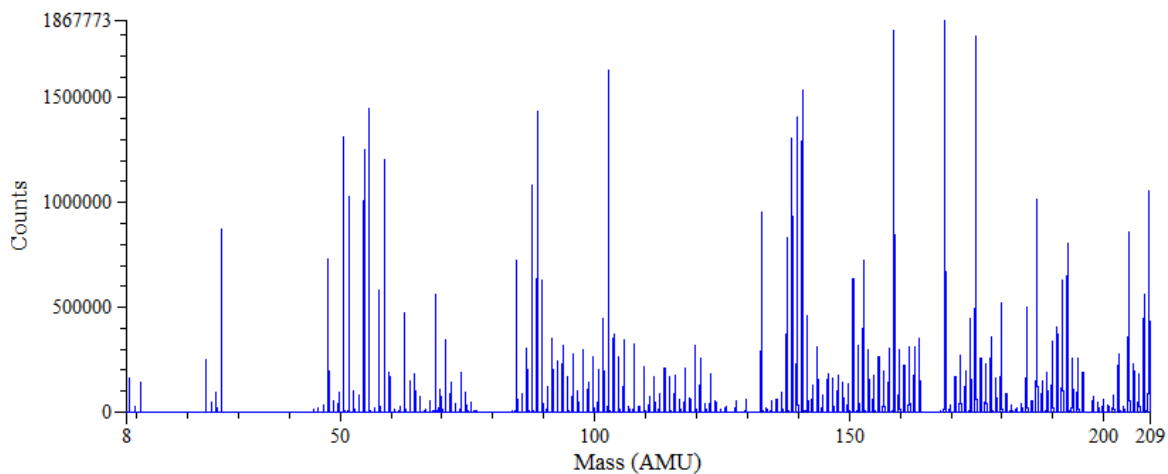


Fig. 2.9: A typical mass spectrum (50 ppb multi-element standard solution).

2.2.2 Interferences in ICPMS

Interferences in ICP-MS are of three types – spectroscopic, non spectroscopic and memory effects. Spectral overlaps are probably the most serious types of interferences seen in ICP-MS. The most common type is known as a polyatomic or molecular spectral interference, which is produced by the combination of two or more atomic ions. They are caused by a variety of factors, but are usually associated with either the plasma and nebulizer gas used, matrix components in the solvent and sample, other analyte elements, or entrained oxygen or nitrogen from the surrounding air. For example, the $^{40}\text{ArO}^{16}$ has a significant impact on the major isotopes of Fe at mass 56, $^{40}\text{ArCl}^{35}$ interfere with ^{75}As , $^{40}\text{ArC}^{12}$ interferes with ^{52}Cr , $^{40}\text{ArNa}^{23}$ interferes with ^{63}Cu etc. Another type of spectral interference is produced by elements in the sample combining with H, ^{16}O , or ^{16}OH (either from water or air) to form molecular hydride (H), oxide (^{16}O), and hydroxide

(^{16}OH) ions, which occur at 1, 16, and 17 mass units higher than its mass [145]. The final classification of spectral interferences is called “isobaric overlaps,” produced mainly by different isotopes of other elements in the sample that create spectral interferences at the same mass as the analyte ,e.g. ^{54}Fe and ^{54}Cr , ^{144}Sm and ^{144}Nd etc. Few ionic species formed from used mineral acids (HNO_3 , HCl , HClO_4 , and H_2SO_4) and their overlap with analyte is given in Table 2.1. Isobaric interference can be overcome by selecting a different isotope of the concerned element or employing interference correction equations [146].

Table 2.1 Some background ions observed from mineral acid solvents

Acid	Ions	Mass	Interfere with
HNO_3	N^+	14	--
	ArN^+	54	$^{54}\text{Fe}^+$, $^{54}\text{Cr}^+$
	NO^+	30	$^{30}\text{Si}^+$
	N_2^+	28	$^{28}\text{Si}^+$
HCl , HClO_4	Cl^+	35,37	--
	ClO^+	51	$^{51}\text{V}^+$
		53	$^{53}\text{Cr}^+$
	Ar Cl^+	75	$^{75}\text{As}^+$
		77	$^{77}\text{Se}^+$
ClO_2^+	67	$^{67}\text{Zn}^+$	
H_2SO_4	S^+	32,33,34	
	SO^+	48	$^{48}\text{Ti}^+$

	49	$^{49}\text{Ti}^+$
	50	$^{50}\text{Ti}^+$, $^{50}\text{Cr}^+$, $^{50}\text{V}^+$
SO_2^+	64	$^{64}\text{Zn}^+$, $^{64}\text{Ni}^+$
	65	$^{65}\text{Cu}^+$
	66	$^{66}\text{Zn}^+$

Suppression or enhancement of the analyte signal due to the presence of matrix is known as Non spectral interference [147-149]. Heavy matrix elements cause more severe suppression effects and light analytes are more seriously affected [150,151]. As a mechanism of the mass dependence of the matrix effect, many reports [152,153] explain that the suppression is caused by collision of analyte ions with heavy matrix ions which are enriched on the central axis of the supersonic expansion region behind the sampler. Tan and Horlick [151] and Gillson et al. [154] reported that the ion transmission through the skimmer is affected by space charge repulsion with heavy ions being transmitted most efficiently. The GBC 8000R model has introduced a blanker option, where unwanted masses could be deviated from the path of their flight and stop to reach the detector. It increase the life time of the detector.

Memory effects arise due to the deposition of the analytes or their compounds at the sampler or skimmer orifice or at the focusing lenses and may continue to show some signal at the analyte mass even after removal of the analyte solution. The memory effects can be minimized by rinsing the system with blank solution (1% HNO_3) for about a minute or two so that the deposited traces are eliminated.

2.2.3 Optimization and Calibration of ICP-MS

A complete optimization of the Opti Mass 8000R involves the adjustment of 24 parameters as follows:

Orthogonal Accelerator (OA) and Reflectron:	8 parameters
Ion Optics	8 parameters
Plasma	8 parameters

The full optimization is required only after maintenance operations on the OA, reflectron or detector or after every six months. A 5 ppb solution of Li, Sr, In, La and Bi in 1.0% HNO₃ has been used to optimize the parameters. A systematic block diagram of optimization is given in Figure 2.10. The mass calibration and blanker calibration is done at every week. The optimized parameters of ICP-MS after one hour ignition of the plasma is given in Table 2.2

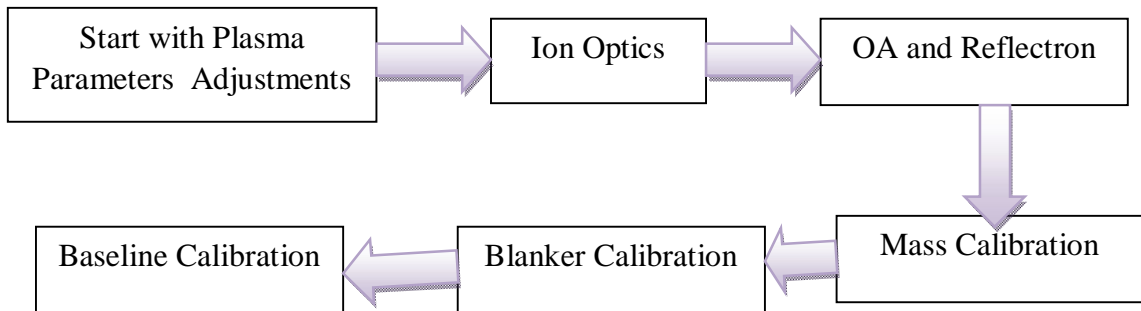


Fig. 2.10: A systematic block diagram of optimization and calibration of ICPMS

Table 3.2: Optimized operating conditions of ICP-MS

ICP-MS parameters	Values
RF power	1200 W
Frequency	27.2 MHz
Plasma gas flow rate	11.0 L min ⁻¹
Auxiliary gas flow rate	0.60 L min ⁻¹
Nebulizer gas flow rate	0.75 L min ⁻¹
Sample uptake rate	0.5 mL min ⁻¹
Measurement mode	Dual (PC/analog)
X-Position	10.0 mm
Y-position	-2.2 mm
Z-position	-1.6 mm
Skimmer voltage (V)	-1200
Extraction (V)	-950
Z1(V)	-900
Y Mean (V)	-265
Y deflection (V)	4
Fill (V)	-38.0
Blanker (V)	150
Z Lens mean (V)	-870
Z Lens deflection (V)	-40
Lens body (V)	-180

Fill Bias (V)	1.25
Fill Grid (V)	-12.0
Pushout plate (V)	655
Pushout Grid (V)	-495
Reflectron (V)	670
Multiplier gain (V)	2500

2.2.4 Advantage and disadvantage of ICP-MS

The ICP-MS has following advantages:

- i. Detection limits are 10-100 times superior to those of ICP-AES.
- ii. Ability to provide elemental isotopic ratio information.
- iii. Almost all elements can be analyzed in duplicate and with good precision in 1-2 minutes.
- iv. Large linear dynamic working range.
- v. The effective combination of different types of ICP-MS instruments coupled with the many varied types of sample introduction allow for customization of techniques for a specific sample type or form of analyte.

Disadvantage of the techniques are:

- i. The high-cost of ICP-MS systems.
- ii. Lower knowledge and insufficient understanding about the technique compared to the other techniques.
- iii. Elements such as Ca and Fe are difficult to determine by conventional ICP-MS because of mass spectral interferences by argides.

- iv. Ni cones, due to which chances of nickel from cones is always there and nickel quantification at ultra trace level becomes difficult. This can be alleviated by switching to more expensive Pt cones.

2.3 Gamma Spectroscopy

Gamma spectroscopy helps in identification and/or quantification of radionuclides. The γ -rays emitted from radionuclides have energy range from a few keV to 3 MeV, corresponding to the typical energy levels in nuclei. The equipment used in gamma spectroscopy includes an energy-sensitive radiation detector, electronics to process detector signals produced by the detector, such as a pulse sorter (i.e., multichannel analyzer), and associated amplifiers and data readout devices to generate, display, and store the spectrum. A basic block diagram of gamma spectrometer is given in Figure 2.11.

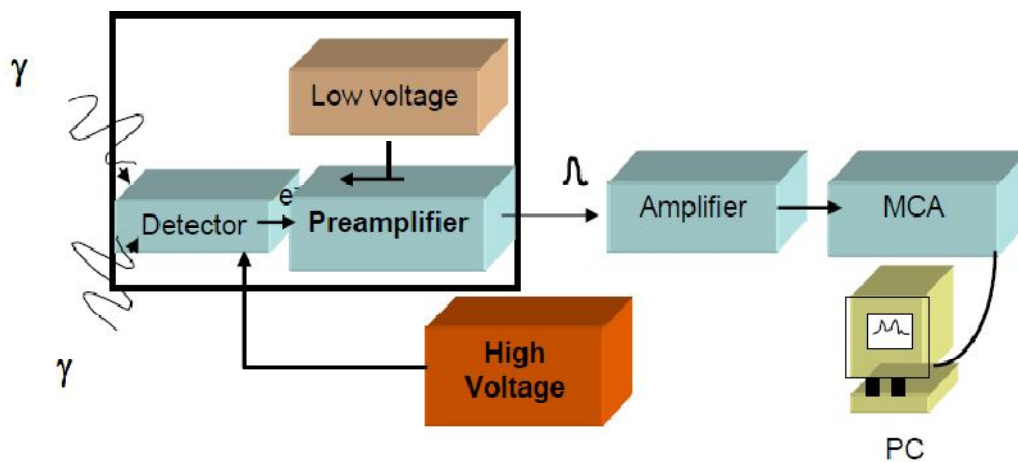


Fig. 2.11: Block diagram of basic gamma spectrometry system

The most common detectors include sodium iodide NaI(Tl) scintillation detectors and high-purity germanium detectors. γ -rays interact with detector material by photoelectric absorption, the Compton scattering, and pair production.

The photoelectric absorption is predominant for low energy rays and results in absorption of all of the energy of the incident gamma ray. Full energy absorption is also possible when a series of these interaction mechanisms take place within the detector volume.

The photoelectron is emitted with an energy (E_e) given by:

$$E_e = h\nu - E_b \dots\dots\dots(6)$$

Where E_b is the binding energy of the photoelectron in its original shell, and $h\nu$ is the energy of incident γ -photon.

The probability of photoelectric absorption depends on the gamma ray energy, the electron binding energy and the atomic number of the atom. The probability of photoelectric absorption is given approximately by the equation below:

$$\tau \propto Z^n / E\gamma^{3.5}, (n = 4 - 5)\dots\dots\dots(7)$$

Where Z is the atomic number of the detector material and E is gamma rays energy.

In the case of Compton scattering, the photon collides with an electron and is scattered, transfers a small fraction of its energy to the electron. As all angles of scattering are possible, the energy transferred to the electron varies from zero to a large fraction of the gamma ray energy. It could be shown by writing equations for conservation of momentum and energy. The energy of the scattered photon is given by:

$$E' = h\nu' = \frac{h\nu}{1 + \frac{h\nu}{m_0c^2(1 - \cos\theta)}} \dots\dots\dots(8)$$

Where, E' is energy of scattered photon, m_0c^2 is the rest mass energy of the electron (0.51MeV), and θ is the scattering angle [155]. The probability of Compton scattering per atom of the absorber depends on the number of atoms available as scattering targets and therefore increases linearly with Z .

In case of pair production the photon energy is converted to a pair of electron and positron (e^- and e^+) in the vicinity of the nucleus. The photon must have higher energy than the sum of the rest mass energies of an electron and positron ($2 \times 0.511 \text{ MeV} = 1.022 \text{ MeV}$) for the pair production to occur. A typical gamma spectrum is given in Figure 2.12.

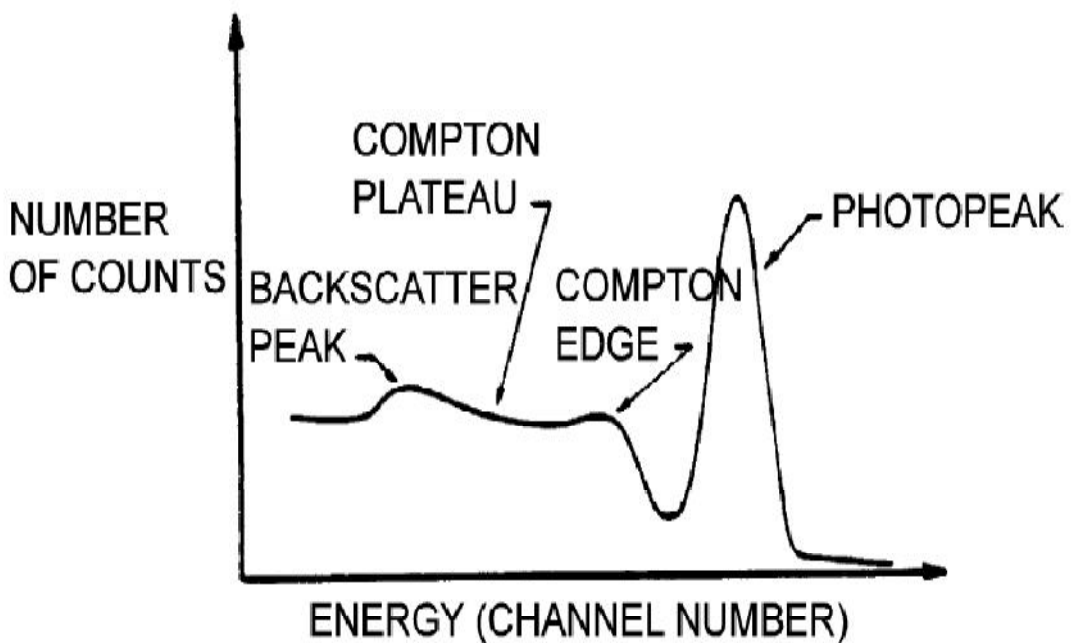


Fig. 2.12: A typical gamma-ray spectrum

2.3.1 NaI (Tl)- scintillation counters

Different types of detectors are used for detection of γ - rays. One common method of converting the energy of the gamma rays photons is called scintillation, which involves turning the energy into visible light. Many materials are used for this detection including inorganic crystals and organic plastics, but the most commonly used are alkali halide viz. NaI(Tl) [158]. the doping of a small quantity ($\sim 0.1\%$) of Tl in NaI creates active sites in the band gap and results in high fluorescence yield of the detector at the same time the wavelength of the fluorescence light falls in the visible region which is the response for a PMT. Other common scintillation detectors include CsI(Na or Tl) and bismuth germanate (BGO) crystals and various organic plastic materials. The operation of a gamma scintillation detector can be summarized as follows. Radiation produces a flash of light in the scintillator which is coupled to the PMT to derive electrical signal. The light photons strike the photocathode of the PMT and release photoelectrons. The photoelectrons are multiplied by factors of 10^5 to 10^7 and produce a voltage pulse at the anode. The basic processes involved in scintillation counting are:

- i) The absorption of radiation within the scintillator resulting in the excitation and ionization of atoms or molecules.
- ii) Photons are emitted when excited atoms or molecules return to their ground state.
- iii) Photons are absorbed by the photocathode of the photomultiplier tube (PMT) and result in the emission of photoelectrons.
- iv) The number of photoelectrons is amplified by the dynode series of the

PMT. The photoelectrons are collected at the anode and produce a voltage pulse.

- v) The pulse produced at the anode, which is proportional to the energy transferred to the scintillator, is amplified, analyzed and counted by scaler.

2.3.2 Detector Counting Efficiency and energy Resolution of NaI (TI)

The detector counting efficiency (DE) relates to the ratio of the no. of photons recorded by the detector to that emitted by the source. It can vary with the volume and shape of the detector material, absorption cross-section in the material, attenuation layers in front of the detector, and distance and position from the source to the detector [157].

In the radioactivity measurement the absolute efficiency of the detector must be known. It is defined as the ratio of the number of counts recorded by the detector (N_c) to the number of radiation (N_s) emitted by the source (in all directions) as represented in the following formula:

$$\epsilon_{abs} = \frac{N_c}{N_s} \dots\dots\dots(9)$$

Absolute efficiency of the detector depends not only on detector properties but also on the details of the counting geometry. Various experimental and calculation works have been reported for the detection efficiency work [158,159].

The energy resolution of a detector system is obtained from the peak full width at one-half of the maximum height (FWHM) of a single peak using the following equation:

$$R = \frac{FWHM}{E_0} \times 100 \dots\dots\dots(10)$$

Here R is energy resolution in % and is the related energy E_0 . It determines the separation for two adjacent energy peaks which will lead to identification of different nuclides in spectrum. The energy resolution of the NaI(Tl) detector is nominally 5-10% for 0.662 MeV gamma energy of ^{137}Cs .

2.4 UV-Visible Spectrophotometry

2.4.1 Basic principle

UV-Visible spectroscopy deals with the electromagnetic spectra within 200-800 nm (ultraviolet 200-400 nm and visible 400-800 nm). When electromagnetic radiation falls upon a homogeneous medium, fraction of this is radiation reflected from the medium while some fraction of incident radiation gets absorbed and the rest transmitted from the medium. Thus intensity of the incident radiation (I_0) is given as:

$$I_0 = I_a + I_t + I_r \dots\dots\dots (11)$$

where I_a , I_t , and I_r are intensities of absorbed, transmitted and reflected radiation respectively. If we eliminate the reflected fraction for a given air-quartz interface, we get I_0 as:

$$I_0 = I_a + I_t \dots\dots\dots (12)$$

Absorption of visible and ultraviolet (UV) radiation is associated with excitation of electrons, in both atoms and molecules, from lower to higher energy levels. Since the energy levels of matter are quantized, only light with the precise amount of energy can cause transitions from one level to another. The possible electronic transitions are given in Figure 2.13. In each possible case, an electron is excited from a occupied (low energy, ground state) orbital into an empty (higher energy, excited state) anti-bonding orbital. Absorption of light in the UV-visible region will only result in $\pi \rightarrow \pi^*$ and $n \rightarrow \pi^*$ transitions. In order to absorb light in the region from 200 - 800 nm, the molecule must contain either π bonding or non-bonding orbitals.

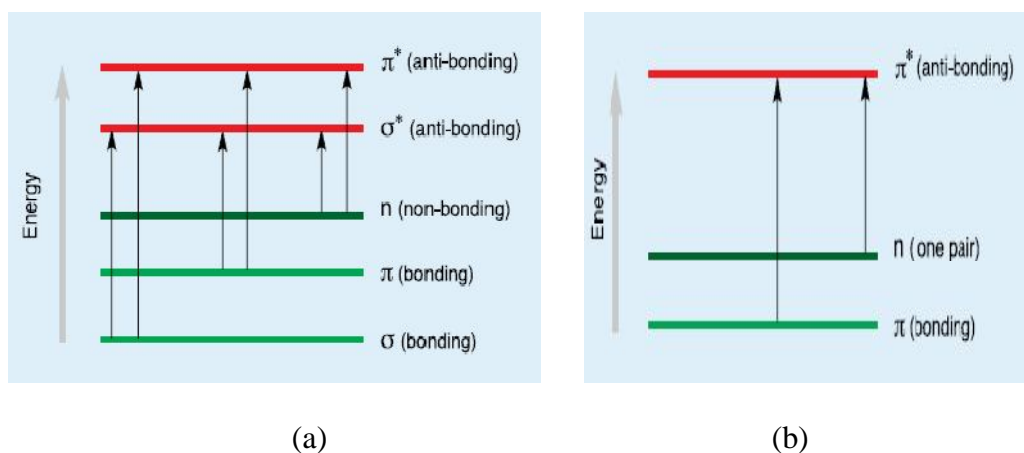


Fig. 2.13: Electronic transitions: (a) Possible electronic transitions (b) Transitions in UV-Visible region

UV-visible spectrophotometers can be used to measure the absorbance of ultra violet or visible light by a sample, either at a single wavelength or perform a scan over a range in the spectrum. The technique can be used both quantitatively and qualitatively. A schematic block diagram of a UV-visible spectrophotometers is shown in Figure 2.14.

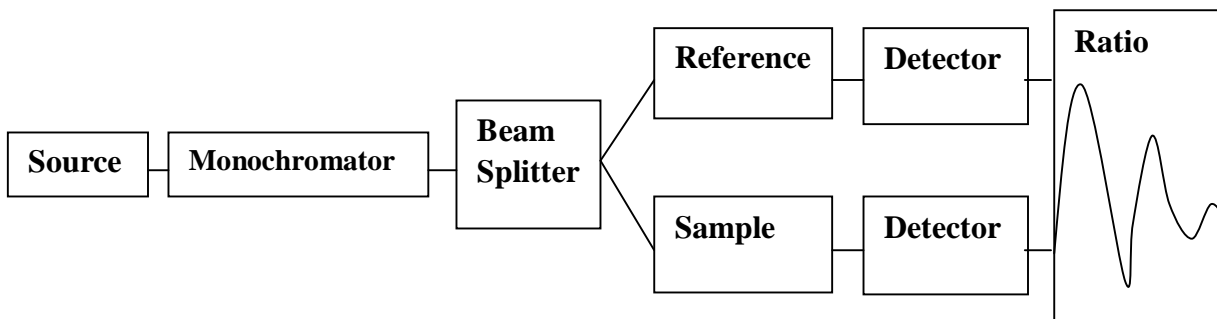


Fig. 2.14: A schematic block diagram of a UV-visible spectrophotometer

The spectrophotometer works on the principle of **Beer-Lambert law**.

Lambert's law states that when a monochromatic radiation passes through a transparent medium, the rate of decrease in intensity with the thickness of the medium is proportional to the intensity of the radiation. In other words, the intensity of the emitted light decreases exponentially as the thickness of the absorbing medium increases arithmetically. The law may be expressed by the differential equation

$$-dI/dl = kI \quad \dots\dots (13)$$

where I is the intensity of the incident light of wavelength λ , l is the thickness of the medium and k is a proportionality factor for the wavelength and the absorbing medium used. Integrating and putting $I = I_0$ when $l = 0$, we obtain

$$\ln (I_0/I_t) = kl$$

or $I_t = I_0 e^{-kl} \quad \dots\dots (14)$

Beer's law states that the intensity of a beam of monochromatic radiation decreases exponentially as the concentration of the absorbing substance increases. This may be written as

$$I_t = I_0 e^{-k'c} \dots\dots\dots (15)$$

Where c is the concentration. Combining the two equations we get

$$I_t = I_0 e^{-\epsilon cl} \dots\dots\dots(16)$$

The equation can be rearranged into

$$\log(I_0/I_t) = \epsilon cl \dots\dots\dots (17)$$

$\log(I_0/I_t)$ is defined as absorbance (A) of the sample.

This is the fundamental equation of spectrophotometry and is known as the **Beer-Lambert law**. Here, if c is expressed in mol L⁻¹ and l is in cm, ϵ is known as the **molar absorption coefficient or molar absorptivity**. It depends on the wavelength of the incident radiation, the temperature and the solvent employed.

If the absorbance of a series of sample solutions of known concentrations are measured and plotted against their corresponding concentrations, the plot of absorbance versus concentration should be linear if the Beer-Lambert Law is obeyed. This graph is known as a calibration graph. Figure 2.15 gives the calibration plot for titanium determined by hydrogen peroxide method. A calibration graph can be used to determine the concentration of unknown sample solution by measuring its absorbance.

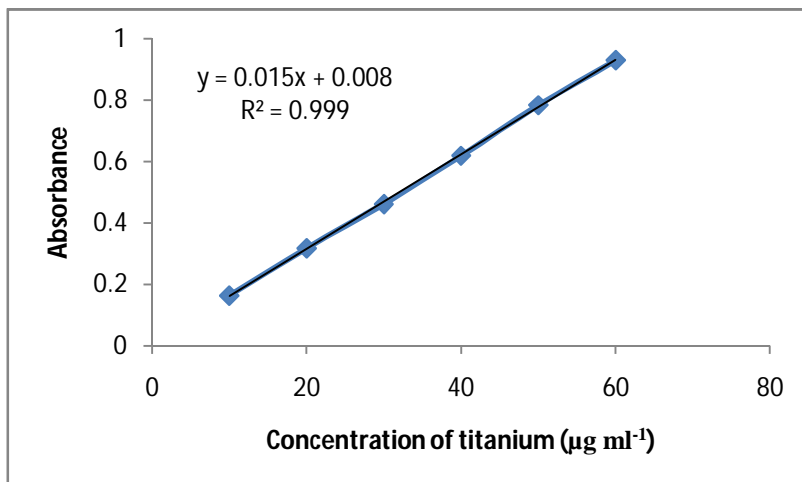


Fig. 2.15: Calibration plot for absorption spectra of titanium
(in 2.5N H₂SO₄ and 3% H₂O₂)

2.4.2 Advantage and disadvantage of UV-Visible Spectrophotometry

Advantages :

- i. Sample analysis using UV-visible spectroscopy is a very quick process compared to other methods. This rapid analysis is achieved only through proper calibration.
- ii. A light source shutter controls the amount of light from a specialized lamp that passes through the sample. The shutter is the only moving component of a UV-visible spectrophotometer. The advantage of this system lies in the simplistic design of the instrument.
- iii. UV/Vis spectrophotometer is routinely used in analytical chemistry for the quantitative determination of different analytes, such as transition metal ions, highly conjugated organic compounds, and biological macromolecules.

Spectroscopic analysis is commonly carried out in solutions but solids and gases may also be studied.

- iv. The UV-visible technique is non-destructive to the sample and has a high sensitivity for detecting organic compounds.

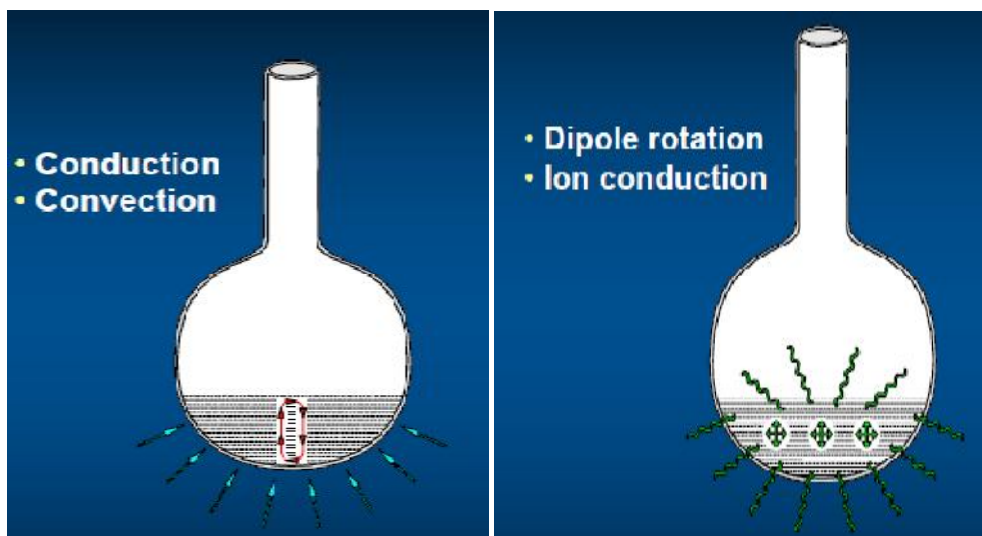
Disadvantages:

- i. Beer law and Lambert law is capable of describing absorption behavior of solutions containing relatively low amounts of solutes dissolved in it (<10mM). When the concentration of the analyte in the solution is high (>10mM), the analyte begins to behave differently due to interactions with the solvent and other solute molecules and at times even due to hydrogen bonding interactions.
- ii. Beer-Lambert law is strictly followed when a monochromatic source of radiation exists. In practice, however, it is common to use a polychromatic source of radiation with continuous distribution of wavelengths along with a filter or a grating unit (monochromators) to create a monochromatic beam from this source.
- iii. Stray radiation or scattered radiation is defined as radiation from the instrument that is outside the nominal wavelength band selected. Usually the wavelength of the stray radiation is very different from the wavelength band selected. It is known that radiation exiting from a monochromator is often contaminated with minute quantities of scattered or stray radiation. Usually, this radiation is due to reflection and scattering by the surfaces of lenses, mirrors, gratings, filters and windows. If the analyte absorbs at the wavelength of the stray radiation, a deviation from Beer-Lambert law is observed similar to the deviation due to polychromatic radiation.

- iv. Since UV-visible spectrophotometer is based on electronic transition, the absorption spectrum of the sample changes with the change in pH of the solvent.

2.5 Microwave Dissolution

Anton Paar multiwave-3000 system has been employed to dissolve the highly refractory materials such as dysprosium titanate and alumina in the present work. Microwaves are the form of electromagnetic radiation with wavelength ranging from one meter to one millimeter; with frequency between 300MHz (100cm) and 300GHz (0.1cm). Microwave promotes the rotation of specific molecules in a reaction mixture. This rotation results in increased molecular collisions and generation of heat.



(a)

(b)

Fig 2.16: Sample dissolution by: (a) Conduction and convection heating and (b) microwave heating

The acid solutions have the capability to interact with microwaves and generate heat. In the conventional conductive heating, the heat is passed through the vessel walls prior to reaching the reactants, which depends upon vessel material thermal conductivity. On the other hand, microwave heating is independent of vessel material thermal conductivity. Figure 2.16 shows how the conventional conduction heating and microwave heating works. Microwave rotor and lip-type seal vessel are as shown in Figure 2.17.

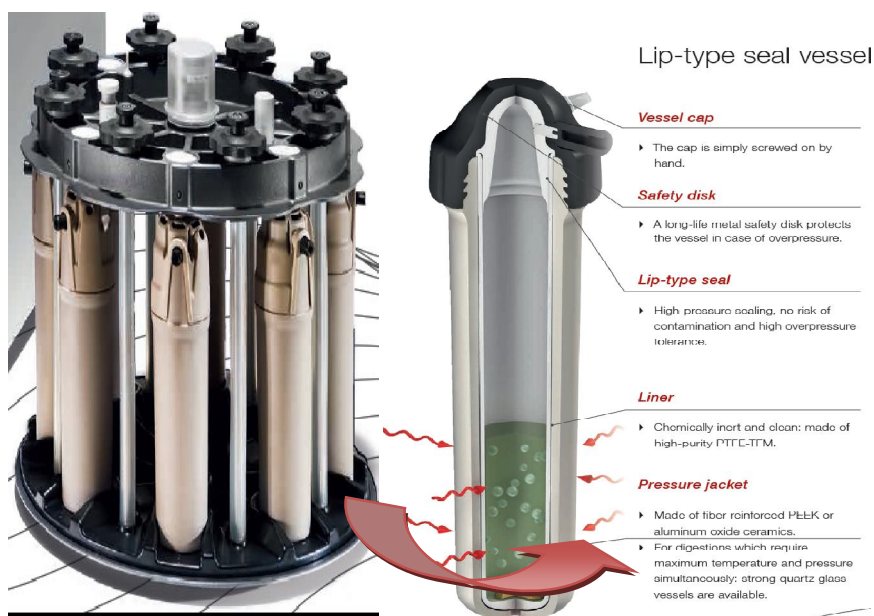


Fig. 2.17: Microwave rotor and high pressure vessel

Microwave-heating techniques are now widely used in many applications of chemical engineering including organic/inorganic synthesis [160-163].

2.6 Matrix separation Methodologies

There are various methods available to separate the matrix from the analyte. In the present work solvent extraction, ion chromatography and precipitation method have been used to separate the matrix. The details of these methods are given below :

2.6.1 Solvent Extraction

In the solvent extraction method a solute is distributed between two immiscible liquid phases. Typical diagram of solvent extraction process is given in Figure 2.18. At equilibrium condition, the ratio of the concentration of the solute in the two phases will be constant and is called as distribution coefficient (K_d). If the K_d value is large, the solute will tend towards quantitative extraction into solvent 1 (organic phase).

$$K_d = \frac{[A]_1}{[A]_2} \dots \dots \dots (18)$$

where $[A]_1$ is concentration of a solute in its single definite form in the liquid phase 1, and $[A]_2$ is concentration of same form in the other phase 2.

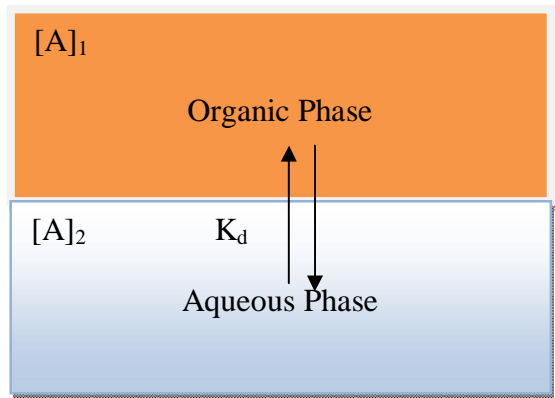


Fig. 2.18: The distribution of a solute between aqueous and organic phase

In practice one measures the distribution ratio (D) defined as the ratio of the total concentration of a solute in the liquid phase 1, regardless of its chemical forms, to its total concentration in the other liquid phase referred as 2. If phase 1 is organic and phase 2 is aqueous then D is given as:

$$D = \frac{[A]_{org}}{[A]_{Aq}} \dots\dots\dots (19)$$

Where $[A]_{org}$ is the total concentration of A in the organic phase and $[A]_{Aq}$ is that in aqueous phase.

D is independent of volume ratio. However, the fraction of the solute extracted will depend on the volume ratio of the two solvents. If a larger volume of organic solvent is used, more solute must dissolve in this layer to keep the concentration ratio constant so as to satisfy the distribution ratio. The percentage of solute extracted into organic phase is given by

$$\%E = \frac{[A]_{org}V_{org}}{[A]_{org}V_{org} + [A]_{Aq}V_{Aq}} \times 100 \dots\dots\dots (20)$$

Where V_{org} and V_{Aq} represent volume of organic and aqueous phase respectively. From equations 19 and 20 we could get the relation between %E and D as:

$$\%E = \frac{100D}{D + \frac{V_{Aq}}{V_{org}}} \dots\dots\dots (21)$$

Often quantitative extraction is not accomplished in a single extraction step even while using an efficient extraction reagent. Extraction can be increased by increasing the

volume of solvent. However, quantitative extraction is most efficiently carried out in batch extraction mode which involves performing multiple extractions with smaller portions of the same volume of solvent. The amount of solute (W_a) left in aqueous phase (V_{Aq}) after “n” multiple batch extractions with organic solvent can be derived from eq. (21) as,

$$W_a = W^o \left(\frac{V_{Aq}}{DV_{org} + V_{Aq}} \right)^n \dots \dots \dots (22)$$

Where W^o is initial amount of solute present in aqueous phase, and n is number of extractions. In the present work the major element (U in U-Zr alloy and in U_3Si_2) has been extracted from the aqueous phase using solvent extraction method, for matrix free analysis of trace elements by ICP- MS.

2.6.2 Ion Exchange chromatography

Ion exchange chromatography (IEX) is used to separate molecules on the basis of differences in their net surface charge. Molecules vary considerably in their charge properties and exhibit different degrees of interaction with the column material according to differences in their overall charge, charge density, and surface charge distribution.

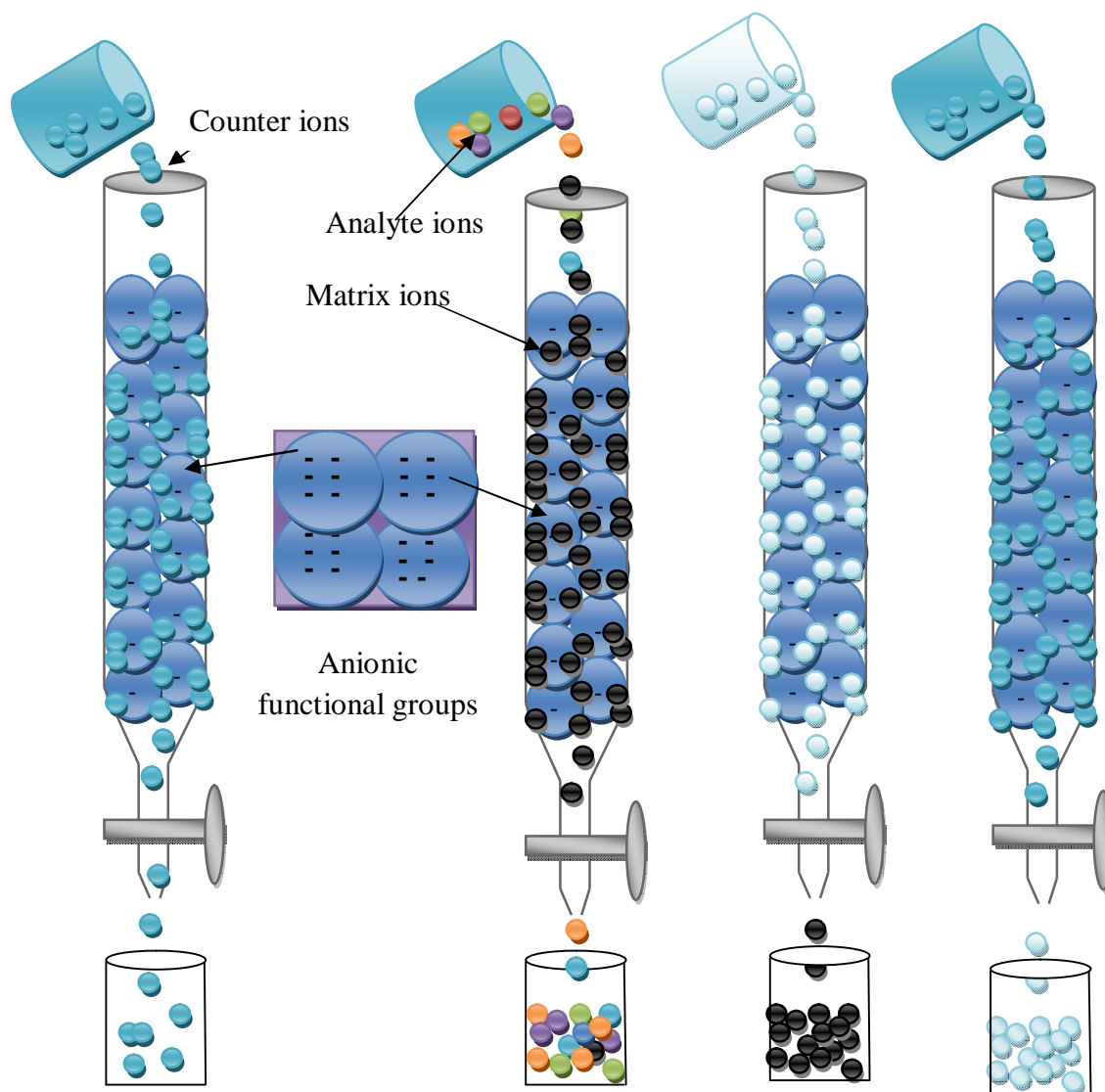
An IEX column comprises a matrix of spherical particles substituted with ionic groups that are negatively or positively charged. Some functional groups substituted onto a chromatographic matrix determine the charge of the IEX medium, that is, a positively charged anion exchanger or a negatively charged cation exchanger. The matrix is usually porous to give a high internal surface area. The medium is packed into a column to form a packed bed.

The majority of the ion exchange resins manufactured in the world today are based on the polymer, styrene, cross linked with divinylbenzene (DVB). Resin properties may be significantly varied by changing the amount of DVB cross linking agent, which alters the porosity of the finished ion exchange resin. Following the formation of the styrene/divinylbenzene copolymer, functionalization of the polymer structure is done to convert the polymer into an ion exchange resin. Functionalities added to the copolymer include sulfonate, quaternary amine, and tertiary amine groups.

The first step in IEX method is the equilibration of the stationary phase to the loading conditions. When equilibrium is reached, all stationary phase charged groups are bound with exchangeable counter ions. Counter ions (salt ions) used in IEX are generally Na^+ for cation exchange and Cl^- for anion exchange.

The second step is sample loading and washing. The goal in this step is to bind the ions of interest and wash out all unbound material. Uncharged molecules, or those with the same charge as the ionic group, pass through the column at the same speed as that of effluent. When all the sample has been loaded and the column washed with loading solvent so that all nonbinding molecules have passed through the column, conditions are altered in order to elute the bound ions

A final wash with high ionic strength buffer regenerates the column and removes any molecules still bound. This ensures that the full capacity of the stationary phase is available for the next run. The column is then re-equilibrated with loading solvent before starting the next run. A systematic diagram of steps has given in Figure 2.19.



Step 1: Conditioning Step 2: Loading Step 3: Matrix elution Step 4: Regeneration

Fig. 2.19: Steps in a ion exchange column chromatography

The sorption characteristics of uranium(VI) on strongly basic anion-exchange resins from hydrochloric acid are extensively reported in the literature [164]. Many elements, such as those in Groups I, II, and part of III, the rare earths, and thorium, do not adsorb at any

HCl concentration. The transition metals show varied adsorption which is often dependent on hydrochloric acid concentration. Thus, many schemes for separating uranium from these elements are possible. Molybdenum(VI) adsorbs on the anionic resin in the hydrochloric acid medium. Hence in the U-Mo alloy matrix, both U and Mo elements were spontaneously separated using an anion exchange resin (tertiary ammonium chloride form of AG 1X4) from the trace impurities. Chemical structure of tertiary ammonium chloride with styrene and DVB is given in Figure 2.20.

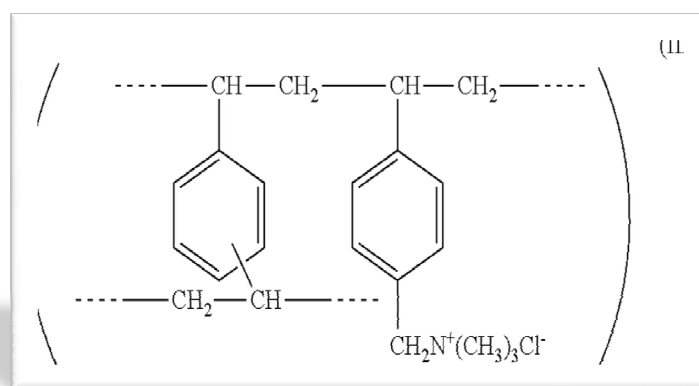


Fig. 2.20: Strong base resin in the form of tertiary ammonium chloride

The ion exchange separation is free from organic waste, hence it is very useful for the routine sample analysis of U-Mo alloy.

2.6.3 Precipitation method

Selective precipitation of matrix element is a common method for analysis of trace elements. Matrix separation and pre-concentration of trace elements using precipitation

method has been reported [165- 169]. In the present work trace amount of rare earth elements have been precipitated from the aluminum matrices. Aluminum and rare earth hydrolyzed in sodium hydroxide solution, but in presence of excess sodium hydroxide solution the aluminum formed soluble sodium aluminates and separated from the rare earth after filtering through the Whatmann 542 filter paper. The method has validated using a standard addition technique. The details has given in chapter 7.

2.7 Gravimetric method of major matrix analysis

Gravimetry includes all analytical methods in which the analytical signal is a measurement of mass or a change in mass. When the signal is the mass of a precipitate, we call the method **precipitation gravimetry**. If signal is based on deposition of analyte as a solid film on an electrode in an electrochemical cell called as **electro-gravimetry**. If the analyte is removed as a volatile species, using thermal or chemical energy the method is called **volatilization gravimetry**. For an accurate gravimetric analysis it is essential that the measured signal (whether it is a mass or a change in mass) should be proportional to the amount of analyte in our sample. A systematic diagram of precipitation gravimetry is given in Figure 2.21.

Sequential steps involved in gravimetric precipitation are:

- i. Preparation of the sample solution
- ii. Precipitation process
- iii. Filtration
- iv. Washing
- v. Drying

- vi. Igniting
- vii. Weighing
- viii. Calculation

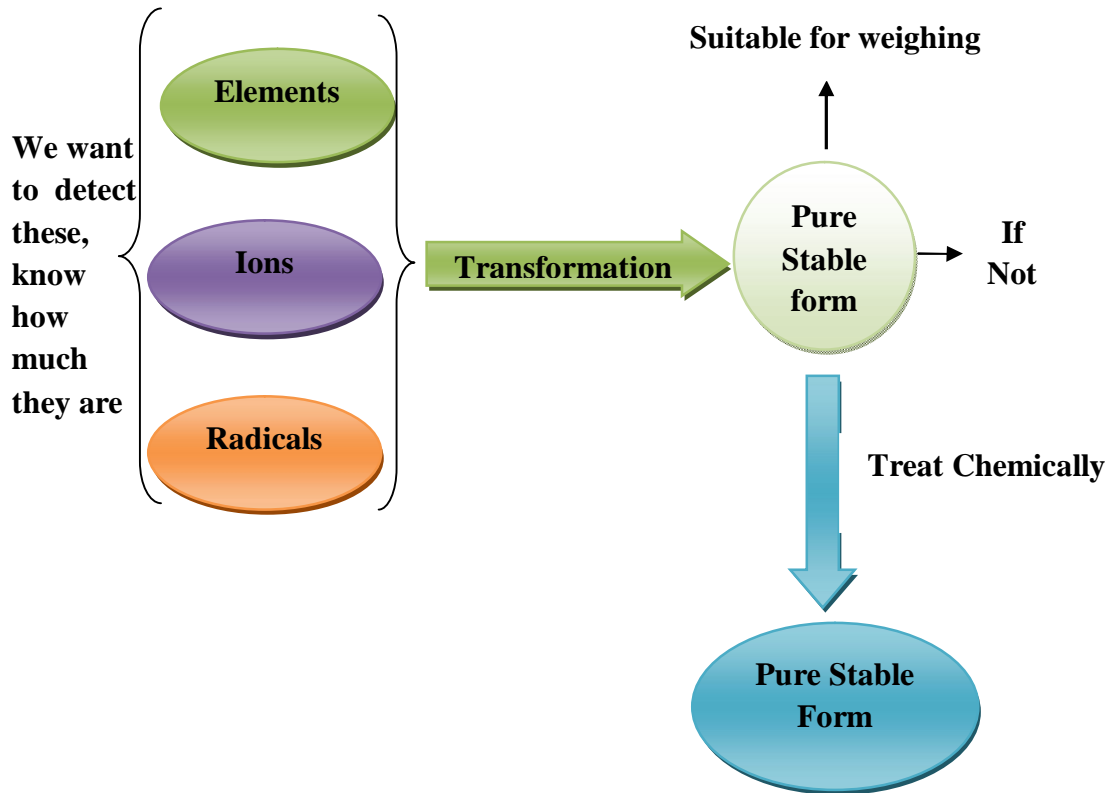


Fig. 2.21: A systematic diagram for precipitation gravimetry

In precipitation gravimetry an insoluble compound forms when we add a precipitating reagent, or precipitant, to a solution containing the analyte. All precipitation gravimetric analysis share two important attributes. First, the precipitate must be of low solubility, of high purity, and of known composition if its mass is to accurately reflect the analyte's mass. Second, the precipitate must be easy to separate from the reaction

mixture. Physical nature of precipitates will be determined by rates of nucleation and particle growth. If rate of nucleation \gg rate of particle formation, then colloidal precipitates form which absorb impurity and also it does not settle easily. Particle size of precipitate is inversely proportional to the relative super-saturation of the solution during precipitation. Von Weimarn defined the relative super saturation (RSS) as:

$$RSS = \frac{(Q-S)}{s} \dots\dots\dots(23)$$

Where, Q is the solute's initial concentration and S is the solute's concentration at equilibrium [170]. A solution with a large, positive value of RSS has a high rate of nucleation, producing a precipitate with many small particles. When the RSS is small, precipitation is more likely to occur by particle growth than by nucleation.

After precipitation and digestion of the precipitate, it is separated it from solution by filtering. The most common filtration method uses filter paper, which is classified according to its pore size and ash content on ignition. Ash less Whatmann filter papers are generally used.

To provide accurate results, the solubility of the compound precipitated must be minimal. Typically accuracy desired in a quantitative analysis, is better than $\pm 0.1\%$, which means that the precipitate must account for at least 99.9% of the analyte. Extending this requirement to 99.99% ensures that the precipitate's solubility does not limit the accuracy of a gravimetric analysis. The loss due to solubility is minimized by carefully controlling the conditions under which the precipitation is carried out. In addition to having a low solubility, the precipitate must be free from impurities. Because precipitation usually

occurs in a solution that is rich in dissolved solids, the initial precipitate is often impure. These impurities must be removed before determining the precipitate's mass.

(i) One common impurity is **inclusion**. A potential interfering ion whose size and charge is similar to a lattice ion, may substitute into the lattice structure, provided that the interferent precipitates with the same crystal structure. The probability of forming an inclusion is greatest when the concentration of the interfering ion is substantially greater than the lattice ion's concentration. An inclusion does not decrease the amount of analyte that precipitates, provided that the precipitant is present in sufficient excess. Thus, the precipitate's mass is always larger than expected.

An inclusion is difficult to remove since it is chemically part of the precipitate's lattice. The only way to remove an inclusion is through re-precipitation. After isolating the precipitate from its supernatant solution, it is dissolved by heating in a small portion of a suitable solvent. It is then allowed to cool, reforming the precipitate. Because the interferent's concentration is less than that in the original solution, the amount of included material is smaller. The process of re-precipitation is repeated until the inclusion's mass is insignificant. The loss of analyte during re-precipitation, however, can be a significant source of error.

(ii) **Occlusions** form when interfering ions become trapped within the growing precipitate. Unlike inclusions, which are randomly dispersed within the precipitate, an occlusion is localized, either along flaws within the precipitate's lattice structure or within aggregates of individual precipitate particles. An occlusion usually increases a

precipitate's mass; however, the mass is smaller if the occlusion includes the analyte in a lower molecular weight form than that of the precipitate.

Occlusions can be minimized by maintaining the precipitate in equilibrium with its supernatant solution for an extended time. This process is called digestion. During digestion, the dynamic process of solubilization-precipitation, in which the precipitate dissolves and reforms, ensures that the occlusion is re-exposed to the supernatant solution. Because the rates of dissolution and re-precipitation are slow, there is less opportunity for forming new occlusions.

(iii) After precipitation is complete the surface continues to attract ions from solution. These surface adsorbates comprise a third type of impurity and can be minimized by decreasing the precipitate's available surface area, which can be done by digesting a precipitate. Surface adsorbates can also be removed by washing the precipitate, although the potential loss of analyte cannot be ignored.

(iv) Another type of impurity is an interferent that forms an independent precipitate under the conditions of the analysis. This can be minimized by carefully controlling the solution conditions. If an interferent forms a precipitate that is less soluble than the analyte's precipitate, the interferent can be first precipitated and removed by filtration, leaving the analyte behind in solution. Alternatively, one can mask the analyte or the interferent to prevent its precipitation.

The scale of operation for precipitation gravimetry is limited by the sensitivity of the balance and the availability of sample. To achieve an accuracy of $\pm 0.1\%$ using an analytical balance with a sensitivity of ± 0.1 mg, we must isolate at least 100 mg of

precipitate. Precipitation gravimetry is usually limited to major or minor analytes. The analysis of trace level analytes or micro samples usually requires a micro-analytical balance. For a macro sample containing a major analyte, a relative error of 0.1–0.2% is routinely achieved. The major limitations are solubility losses, impurities in the precipitate, and the loss of precipitate during handling. For any precipitation gravimetric method the following general equation relating the signal (grams of precipitate) to the absolute amount of analyte in the sample is applied;

$$\text{grams precipitate} = k \times \text{grams analyte}$$

where k , the method's sensitivity, is determined by the stoichiometry between the precipitate and the analyte. The advantage offered by gravimetric analysis are:

- (i) It is accurate and precise when using modern analytical balances.
- (ii) Possible sources of error readily checked, since filtrates can be tested for completeness of precipitation and precipitates may be examined for the presence of impurities.
- (iii) It is an absolute method, i.e. it involves direct measurement without any form of calibration being required.
- (iv) Determinations can be carried out with relatively inexpensive apparatus; the most expensive items are muffle furnace and sometimes platinum crucible.

Disadvantage:

- i. Time consuming process
- ii. Lack of selective precipitants
- iii. Waste generations

Chapter 3

Determination of trace and ultra trace impurities in uranium silicide (U_3Si_2) nuclear fuel employing ICP-MS

3.1 Introduction

Till late seventies the research and test reactors worldwide were using high enriched uranium (HEU >85% U^{235}) plate type dispersion fuel elements, generally consisting of UAl_x (mainly UAl_3) or U_3O_8 dispersed in aluminum matrix and with Al-alloy clad [171]. Nuclear proliferation and diversion are the biggest threats to civilization, and hence, the use of highly enriched uranium which falls in the category of weapons-grade material, has been restricted. In 1978, the Reduced Enrichment for Research and Test Reactor (RERTR) program was initiated by the U.S. Department of Energy for the conversion of worldwide research and test reactor cores from HEU to low enriched uranium-based (LEU <20% ^{235}U) fuels [172]. Since then it has become an international norm for both designing fuels for new reactors and for replacing the existing cores with low enriched uranium fuel.

In order to compensate for the reduced fissile content in LEU-based fuel (meat) extensive research and development programs have been pursued for the exploration of a fuel with maximum metal density [173-175]. Though metallic uranium (U) can provide the highest achievable uranium density, its poor irradiation performance and low melting point restricts its application as a high burn-up fuel [176]. The most widely accepted technical solution to overcome this limitation is the use of uranium silicide (U_3Si_2) fuel dispersed in

an aluminum (Al) matrix. U_3Si_2 was found to perform extremely well even at high burn-ups (19–98% of ^{235}U in LEU) with U densities up to $\sim 5.0 \text{ g cm}^{-3}$.

In 1955, the father of Indian nuclear program, Dr. Homi Jahangir Bhabha conceptualized a pool type reactor using high enriched uranium fuel. The reactor, built with indigenous effort, attained first criticality on August 4, 1956 and this event marked the beginning of the success story of Indian nuclear programme. On January 20, 1957, the reactor was dedicated to the nation and named as Apsara by Pandit Jawaharlal Nehru. The maximum thermal neutron flux at the rated power (1MW) of the reactor was about $1 \times 10^{13} \text{ n/cm}^2/\text{sec}$ [177]. The Apsara reactor has been used extensively to carry out research in a number of areas in basic sciences, production of radioisotopes, neutron radiography, detector testing, shielding experiments, material characterization etc. The reactor has contributed enormously towards training young scientists and engineers. Considering the long service period extending over fifty three years, the reactor has been shut down in June, 2009 and decommissioned.

In the new research reactor, nuclear research facility (NRF), coming up at Trombay, reactor core will consist of low enriched uranium (LEU) in the form of U_3Si_2 dispersed in aluminum matrix as fuel. The core is surrounded by beryllium oxide (BeO) reflectors. The maximum thermal neutron flux is expected to be $6.1 \times 10^{13} \text{ n/cm}^2/\text{sec}$. The higher neutron flux will facilitate production of isotopes for applications in the field of medicine, industry and agriculture. In addition it will provide enhanced facilities for neutron activation analysis, neutron radiography and shielding experiments. The salient features

of the NRF reactor are given in Table 3.1 [174]. The reactor core configurations is given in Figure 3.1.

For safe and smooth reactor operation, chemical quality control (CQC) of every nuclear material is essential. The presence of some trace metallic and non-metallic elements in the nuclear fuel can affect the optimum performance of a reactor [38,178]. These trace elements which get incorporated in nuclear fuel either from the precursors or during various fuel fabrication steps, need to be quantified precisely and accurately.

Table 3.1 Salient Features of the NRF at Trombay [180]

Reactor type	Pool type
Thermal Power	2 MW
Maximum Thermal Neutron Flux	6.1×10^{13} n/cm ² /sec
Maximum Fast Neutron Flux	1.3×10^{13} n/cm ² /sec
Maximum Thermal Neutron Flux in reflector region	4.4×10^{13} n/cm ² /sec
Fuel	Plate type U ₃ Si ₂ dispersed in aluminium matrix Loading density of Uranium 4.3 gm/cc
Reflector	Beryllium Oxide
Coolant / Moderator	Demineralised water
Shutdown system	Fast acting Hafnium shut-off-rods
Shutdown core cooling	Natural convection

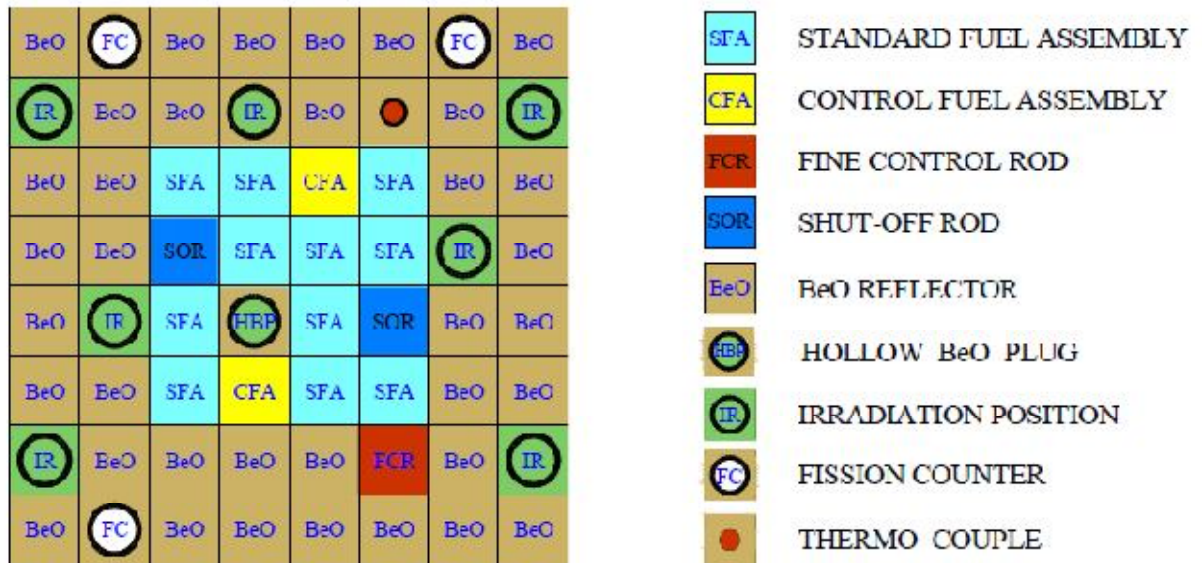


Fig.3.1 Core configuration of new nuclear research facility [8]

The available methods for the determination of trace metallic elements in various nuclear materials are inductively coupled plasma mass spectrometry (ICP-MS) [40-43, 179], inductively coupled plasma atomic emission spectrometry (ICP-AES) [45, 180], flame atomic absorption spectroscopy (FAAS) [46,47], ion chromatography (IC) [48, 49], etc. Among all these techniques, ICP-MS is the most versatile multi-elemental technique with rapid analysis, high sample throughput, long linear calibration range, low detection limit, and fewer spectroscopic interferences, etc. [181-184]. For ICP-MS analysis, it is recommended to analyze solutions with total dissolved solid content $\leq 0.1\%$. Whenever the analyte concentration in the matrix is in the trace/ultratrace level, it is necessary to separate the matrix prior to quantification by ICP-MS as dilution alone may bring down

the analyte concentration below the detection limit of the instrument. In the present work a matrix separation procedure was developed for quantitative separation of thirteen elements (B, Cd, Co, Cr, Cu, Dy, Eu, Gd, Mg, Mn, Ni, Sm, and V) from the U_3Si_2 matrix, followed by their quantification by ICP-MS.

The matrix element, silicon (Si), was removed as its volatile compound (SiF_4) in the presence of HNO_3/HF . This process was carried out in the presence of mannitol to prevent loss of boron [185, 186]. The other matrix element, uranium, was separated by conventional solvent extraction using tri-n-butylphosphate (TBP) in carbon tetrachloride (CCl_4). The raffinate was analyzed by ICP-MS employing the external calibration technique. The method was validated by recovery studies by standard addition technique in the spiked samples due to lack of certified reference materials (CRMs). The separation procedure was cross validated by an independent tracer technique by adding carrier-free ^{51}Cr and $^{152+154}Eu$ tracers before any chemical treatment and finally analyzing the raffinate by gamma spectrometry. Three real U_3Si_2 samples were analyzed for trace and ultra-trace elements by the developed method.

3.2 Experimental Section

3.2.1 Instrumentation

Inductively Coupled Plasma Mass Spectrometry (ICPMS)

An inductively coupled plasma-orthogonal acceleration time of flight mass spectrometer (ICP-*oa*-TOF-MS), Model Optimass 8000R (GBC, Australia), was used for the determination of trace and ultra-trace elements in U_3Si_2 matrix. Details of the instrumental and operating parameters are given in Table 2.2.

Table 3.2: Optimized operating conditions of ICP-MS

ICP-MS parameters	Values
RF power	1200 W
Frequency	27.2 MHz
Plasma gas flow rate	11.0 L min ⁻¹
Auxiliary gas flow rate	0.60 L min ⁻¹
Nebulizer gas flow rate	0.75 L min ⁻¹
Sample uptake rate	0.5 mL min ⁻¹
Measurement mode	Dual (PC/analog)
Acquisition time	5 s

NaI (Tl) gamma spectrometer

A 3”X3” NaI (Tl) well-type detector coupled to a Multichannel Analyzer (Electronic Corporation of India Limited) was used to study the percentage recovery of the tracers (⁵¹Cr and ¹⁵²⁺¹⁵⁴Eu) in the final raffinate. The detector has a resolution of 46.2 keV (FWHM) at 661 KeV. Activities of ⁵¹Cr and ¹⁵²⁺¹⁵⁴Eu were monitored using 320 keV and 122 keV, γ lines respectively.

3.2.2 Reagents and Solutions

Suprapur® HNO₃ and HF (Merck), TBP (Merck), and CCl₄ (Merck) were used for sample preparation. De-ionized water, obtained from a Milli-Q® system (18M Ω cm) was

used for dilution. The ICP standards of 1000 mg L^{-1} (BDH) were diluted appropriately to prepare multi-element standard solutions. Two radio tracers, namely, ^{51}Cr and $^{152+154}\text{Eu}$, were obtained from the Board of Radiation and Isotope Technology (BRIT), India. Eppendorf® micropipettes, Nalgene® PP measuring flask and funnels, and Teflon® PFA beakers were used throughout the experiment.

3.2.3 Dissolution and Matrix Separation

About 1.0 g of U_3Si_2 was taken in a Teflon beaker with 10 mL concentrated HNO_3 and 1 mL of 100 mg L^{-1} manitol solutions. The mixture was then placed under an IR lamp, and concentrated HF was added drop-wise until the solution became clear. The solution was then evaporated to near dryness and brought into 10 mL 4M HNO_3 medium. The typical diagram of dissolution of the sample is given in Figure 3.2. Uranium was then separated from the solution by three contacts with 20 mL 30% TBP in CCl_4 ($\text{O/A} = 2$). The raffinate was again evaporated to near dryness and made up to 25 mL volume in 1% (v/v) HNO_3 medium for ICP-MS analysis.



Fig.3.2 photographs of dissolution apparatus in fume hood

3.2.4 Choice of isotopes

In mass spectrometric analysis, selection of a suitable **isotope** is necessary so as to have better sensitivity, low detection limit, and minimum or no isobaric/polyatomic interferences. The **isotopes** of the elements chosen for our study are listed in Table 3.3, along with their natural abundances and possible interferences.

Table 3.3 List of **isotopes** monitored during mass spectrometric analysis

Monitored Nuclides	Abundance (%)	Possible Interferences
^{11}B	80.2	---
^{114}Cd	28.73	^{114}Sn , $^{98}\text{Mo}^{16}\text{O}$, $^{98}\text{Ru}^{16}\text{O}$
^{59}Co	100	---
^{52}Cr	83.8	---
^{63}Cu	69.17	$^{47}\text{Ti}^{16}\text{O}$
^{163}Dy	24.97	$^{147}\text{Sm}^{16}\text{O}$
^{153}Eu	52.2	$^{137}\text{Ba}^{16}\text{O}$
^{57}Fe	2.2	---
^{160}Gd	21.86	$^{144}\text{Nd}^{16}\text{O}$, $^{114}\text{Sm}^{16}\text{O}$, ^{160}Dy
^{24}Mg	78.9	---
^{55}Mn	100	---
^{60}Ni	26.1	---
^{152}Sm	26.7	^{152}Gd , $^{138}\text{Ba}^{14}\text{N}$
^{51}V	99.75	--

3.2.5 Recovery Studies using Standard Addition Technique

Almost equal amounts (~1.0 g) of a real U_3Si_2 sample from the same batch were taken in four Teflon beakers. One of these was considered as a sample blank, and standard addition was carried out in the other three samples. Individual 1000 mg L^{-1} elemental standards of the analytes were added to the samples after appropriate dilution. The matrix elements (U and Si) from these aliquots were separated. The separated solution was made up to known volume with 1% HNO_3 for quantification of trace elements by ICP-MS.

3.2.6 Gamma spectrometry study

The separation of trace amounts of rare earth and transition elements was studied using radiotracers, ^{51}Cr and $^{152+154}Eu$. These were added in the samples and after separation the aqueous solution were analyzed by NaI(Tl) based scintillation gamma-spectrometry. One stock solution of each tracer was prepared by adding the tracer to the individual solution containing natural Cr and Eu, respectively. The specific activities of these solutions were in the range $1.0\text{--}3.0 \times 10^5 \text{ CPM mL}^{-1}$. The concentration of the chromium solution was $25 \mu\text{g mL}^{-1}$ and that of europium was $1 \mu\text{g mL}^{-1}$. A 0.25 mL aliquot of these stock solutions was mixed in a counting tube, and the volume was made up to 2.5 mL with 4M HNO_3 which would serve as reference. Then, 1 mL stock solution of both tracers was mixed with ~1.0 g of U_3Si_2 and chemically treated in the same manner as discussed earlier. Finally, the raffinate was made up to 10.0 mL in 4M HNO_3 medium. In a counting tube, 2.5 mL of this solution was taken, and both the counting tubes (reference and sample) were counted for ^{51}Cr at 320 keV and for $^{152+154}Eu$ at 122 keV.

3.3 Results and discussion:

The real U_3Si_2 samples were first qualitatively analyzed by ICP-MS which revealed the presence of only 12 elements (B, Cd, Co, Cr, Dy, Eu, Gd, Mg, Mn, Ni, Sm, and V) having specifications in the nuclear fuel. Other elements like Cu and Fe which have specifications in the fuel, but not detected in the real samples, were also considered in the recovery studies. The developed separation procedure ensures quantitative recoveries of the 13 elements (B, Cd, Co, Cr, Cu, Dy, Eu, Gd, Mg, Mn, Ni, Sm, and V) and reduces the total U matrix content to $< 20 \mu\text{g mL}^{-1}$ thereby yielding a decontamination factor of $\sim 10^3$. For the determination of iron, intensity at mass number 57 was monitored due to the presence of isobaric interferences at mass number 54 ($^{40}\text{Ar}^{14}\text{N}$) and 56 ($^{40}\text{Ar}^{16}\text{O}$). However, due to the low abundance of ^{57}Fe , the results were highly irreproducible and hence, iron is not reported.

The quantitative removal of Si as its volatile fluoride compound was confirmed by monitoring the separated solutions. The existing ICP-MS has interference at mass 28 ($^{28}\text{Si}^+$) due to the formation of molecular ion ($^{12}\text{C}^{16}\text{O}^+$) at the same mass. Therefore, Si in the separated solution was quantified by ICP-AES. In the ICP-AES analysis, it is found that only trace amount of Si remains after volatilization. Since boron also form volatile boron trifluoride (BF_3) in presence of hydrogen fluoride. Mannitol was added prior to the sample dissolution step to prevent loss of boron on heating and the consequent HF addition step. The formation of an ester between either $\text{B}(\text{OH})_3$ or BF_4 (Lewis acid) and the mannitol (Lewis base) causes the retention of B in the solution [187]. Addition of HF was done slowly to remove most of the Si as silicon tetrafluoride (SiF_4) because in the

presence of excess HF, SiF₄ gets converted into water soluble hexafluoro silicic acid (H₂SiF₆).

A 10 µg L⁻¹ solution of individual analytes, which are responsible for polyatomic interferences on the monitored **isotopes** was analyzed. It was found that other than oxide ions of Ba and rare earth elements, the signals for other poly- atomic species were less than the detection limit. It has been reported in the literature that in the case of REEs the oxide ion formation yield (MO⁺/M⁺) of the interfering species, relevant to the present study, are very low [188]. Therefore, considering the low concentration of REEs (present in the sub-ppm range) and no detectable Ba in U₃Si₂, the individual analyte intensities were only considered without applying any polyatomic interference correction equations. It can be seen that only ¹¹⁴Cd, ¹⁶⁰Gd, and ¹⁵²Sm have isobaric interferences from ¹¹⁴Sn (0.65%), ¹⁶⁰Dy (2.34%), and ¹⁵²Gd (0.2%), respectively. The intensity of ¹¹⁸Sn (abundance = 24.22%) was monitored in actual sample solutions and was found to be the same as that of the blank value. Since the blank-corrected intensities were considered for every element throughout the analysis, the interference of ¹¹⁴Sn on ¹¹⁴Cd was consequently taken care of. The interference of ¹⁶⁰Dy and ¹⁵²Gd on ¹⁶⁰Gd and ¹⁵²Sm, respectively, was taken care of by applying the following interference correction equations:

$$I^{act}_{160Gd} = I^{obs}_{160} - (I^{act}_{163Dy} \times 2.34/24.97).....(1)$$

and

$$I^{act}_{152Sm} = I^{obs}_{152} - (I^{act}_{158Gd} \times 0.2/24.84) \dots \dots \dots (2)$$

where I^{act} and I^{obs} are the actual intensity of the analyte and the observed intensity at a particular mass number, respectively.

3.3.1 Method validation by Standard Addition Technique

Because of the unavailability of matrix-matched CRMs containing the analytes of interest, recovery studies by standard addition were applied for method validation using a real sample of U_3Si_2 . Individual analyte standards of all the elements of interest were used in the standard addition method and their concentration was varied near their specification limit in the fuel. These specification limits were arrived at by the experience gained from the fuel performance of thermal and research reactors. Analysis of the four solutions, one of which was considered as sample blank and the other three spiked with different concentrations of the analytes, by ICP-MS results in $\geq 92\%$ recovery for the 13 individual analytes, as shown in Table 3.4. The precision indicated in the table is the overall precision calculated by propagation of error, taking into account both the external (N=3) as well as the internal (N=10) standard deviation.

Table 3.4 Results of Recovery Studies using ICPMS (Sample Amount: ~ 1.0 g, Vol. = 25 mL, and N = 10)

Analytes	Specification Limit	Amount Added	Amount Found	Recovery
	($\mu\text{g g}^{-1}$)	(μg)	(μg)	(%)
B	5	0	1.92±0.07	--
		2.5	4.44±0.14	101±6

		5	6.75±0.22	97±5
		10	11.7±0.4	98±4
Cd	2	0	---	---
		1	1.08±0.08	108±7
		2	1.96±0.11	98±6
		4	3.92±0.20	98±5
Co	10	0	4.46±0.13	---
		5	9.55±0.32	102±7
		10	14.4±0.8	99±8
		20	24.3±0.6	99±6
Cr ^a	25	0	14.2±0.6	---
		12.5	26.8±1.1	101±10
		25	38.1±1.6	96±7
		50	64.2±2.4	100±5
Cu ^a	50	0	ND	---
		25	26.3±1.4	101±10
		50	49.5±2.1	96±7
		100	97.3±3.1	100±5
Dy	<3 ^b	0	ND	---
		1	0.92±0.4	92±4
		2	2.04±0.10	102±5
		3	2.92±0.12	97±4

Eu	<3 ^b	0	ND	---
		1	1.00±0.05	100±5
		2	1.98±0.06	99±3
		3	3.10±0.16	103±5
Gd	<3 ^b	0	ND	---
		1	1.10±0.10	110±9
		2	2.040±0.13	102±6
		3	2.95±0.18	98±6
Mg ^a	50	0	15.4±0.42	---
		25	39.5±1.2	96±5
		50	64.7±2.0	99±4
		100	115.2±3.2	100±3
Mn	10	0	2.83±0.14	---
		5	7.65±0.33	96±7
		10	12.6±0.5	98±5
		20	22.7±0.7	99±4
Ni ^a	25	0	12.4±0.56	---
		12.5	24.6±1.1	98±10
		25	37.2±1.4	99±6
		50	62.6±2.3	100±5
Sm	<3 ^b	0	0.28±0.02	---
		1	0.76±0.04	96±9

		2	1.77±0.06	99±4
		3	3.25±0.13	100±5
V	10	0	6.60±0.20	---
		5	11.3±0.3	94±7
		10	16.9±0.5	103±5
		20	26.4±0.8	99±4

^aDetermined by further diluting 1 mL of the solution into 10 mL

^bTotal rare earth element concentration should be less than 3 µg g⁻¹.

ND: Not detected

To enhance our confidence in the separation procedure, recovery studies were also carried out by an independent tracer technique. The results of this exercise are shown in Table 3.5 where it can be seen that the recovery of both Cr and Eu is $\geq 97\%$, thereby cross validating the proposed method for transition metals and REEs.

3.3.2: Recovery Studies by γ -Spectrometry Employing ⁵¹Cr and ¹⁵²⁺¹⁵⁴Eu Tracers

Recovery study by γ -spectrometry is a unique technique to validate any proposed separation procedure as it permits no blank correction on the spiked amount. However, unavailability or restricted availability of radiotracers limits the applicability of this technique. In our case, we used ⁵¹Cr and ¹⁵²⁺¹⁵⁴Eu tracers to validate the separation as representative for transition and rare earth elements. Each sample was counted for 60 seconds and counting repeated for 10 times. The results of the recovery studies are listed in Table 3.5.

Table 3.5 Results of Recovery Studies by γ -Spectrometry (N=10, 60 s Counting)

Sample code	Counts for ^{51}Cr (at 320 keV)	Recovery (%)	Counts for $^{152+154}\text{Eu}$ (at 122 keV)	Recovery (%)
Reference	35776 \pm 248	---	55010 \pm 250	---
Sample-1	34854 \pm 160	97 \pm 1	54130 \pm 170	98 \pm 1
Sample-2	34694 \pm 200	97 \pm 1	54500 \pm 200	99 \pm 1
Sample-3	34900 \pm 225	98 \pm 1	53900 \pm 250	98 \pm 1
Sample-4	34540 \pm 180	97 \pm 1	54710 \pm 300	100 \pm 1
Sample-5	34750 \pm 210	97 \pm 1	54020 \pm 280	98 \pm 1

3.3.3 Detection limits

Both the instrument detection limits (IDLs) and the method detection limits (MDLs) were determined for all 13 elements as per the reported procedure [189-191]. The IDLs were obtained by analyzing the 1% (v/v) pure HNO₃ solution. For the MDL determination, the discussed separation procedure was followed exactly in the absence of the sample, and the solutions were analyzed by ICP-MS. The IDLs and MDLs are tabulated in the Table 3.6.

Table 3.6 Instrumental detection limit (IDL) and method detection limit (MDL) of All the Analytes (N=5)

Analyte	IDL (ng L ⁻¹)	MDL ($\mu\text{g kg}^{-1}$)
B	700	200
Cd	40	10

Co	30	25
Cr	75	8
Cu	42	51
Dy	10	20
Eu	6	10
Gd	14	24
Mg	20	25
Mn	25	15
Ni	200	60
Sm	20	30
V	25	10

3.3.4 Analysis of the real uranium silicide samples

Three real U_3Si_2 samples were analyzed by the proposed method, and the results are listed in Table 3.7. It can also be seen from this table that all of the 13 elements are present well below their respective specification limits in the fabricated fuel. The relative standard deviation (1σ) of the analytes in these samples varied between 3–9%.

Table 3.7 Results of Analysis of Three Real U_3Si_2 Fuel for Metals by ICP-MS

Elements	Sample-1 ($\mu g g^{-1}$)	Sample-2 ($\mu g g^{-1}$)	Sample-3 ($\mu g g^{-1}$)
B	2.23±0.12	1.84±0.08	2.45±0.14
Cd	0.13±0.01	*BDL	0.16±0.01
Co	4.84±0.1	7.34±0.22	6.85±0.6

Cr	10.5±0.5	13.7±0.6	12.6±0.3
Cu	BDL	BDL	BDL
Dy	BDL	0.33±0.02	0.54±0.02
Eu	0.27±0.2	0.23±0.01	0.37±0.02
Gd	BDL	0.16±0.01	0.12±0.01
Mg	13.5±0.4	11.6±0.5	12.7±0.4
Mn	3.47±0.1	2.92±0.15	4.67±0.20
Ni	17.5±0.6	10.7±0.4	13.6±0.6
Sm	0.66±0.02	0.35±0.02	BDL
V	3.62±0.2	4.54±0.22	3.53±0.12

*BDL: Below Detection Limit

3.4 Conclusion

The proposed method effectively separates all 13 elements (B, Cd, Co, Cr, Cu, Dy, Eu, Gd, Mg, Mn, Ni, Sm, and V) from the U_3Si_2 matrix, which could then be quantified precisely and accurately by ICP-MS. The developed separation procedure reduces the matrix concentration to $< 20 \text{ mg L}^{-1}$ in the final solution for ICP-MS analysis. The methodology was validated by the standard addition technique, using ICP-MS, with recoveries of $\geq 92\%$ for all of the elements of interest. An independent tracer technique was also used to cross validate the method. Three real U_3Si_2 samples were analyzed by this developed procedure. The method provides a simple and efficient way of analyzing trace and ultra trace elements in U_3Si_2 fuel.

Chapter 4

Quantification of Trace Metallic Impurities in U-Mo Alloy using ICP-MS

4.1 Introduction

As part of non proliferation of nuclear materials, various nuclear reactors which were using very high U enrichment are being switched over to fuels of lower U-enrichment. However, the resultant loss of power is compensated by raising the fuel densities. Several types of fuels, such as intermetallic and alloys, are being studied which can provide high density of U [192-194]. Two forms of U–Mo alloy fuel have been irradiation-tested in the US GTRI (Global Threat Reduction Initiative) in order to qualify this fuel for the conversion of research and test reactors from highly enriched uranium (HEU) to low enriched uranium (LEU). One form, (dispersion fuel) consists of fuel particles dispersed in an aluminum matrix and the other, (monolithic fuel) is of solid alloy fuel foil directly bonded to aluminum cladding. The geometry for both fuel forms is a thin plate. Schematic cross sectional view of dispersed and monolithic fuel is given in figure 4.1. U–Mo alloy, as a potential fuel for research and test reactors, generally has stable irradiation performance as long as fission product-induced swelling is concerned. Up until very high burnup, fission gas bubbles are small and predictable at temperatures of interest, which are below ~250 °C.

Low-enriched uranium alloys with 6 to 12 wt. % of Mo are under consideration in Indian nuclear program as very high density fuels. Alloying Mo with uranium stabilizes uranium in the γ -phase, which is preferred owing to the advantages related to better

accommodation of fission products and swelling behavior. Reported studies show that the maximum γ -phase stabilization can be achieved with 10% Mo in the U-Mo alloy [178, 195,196].

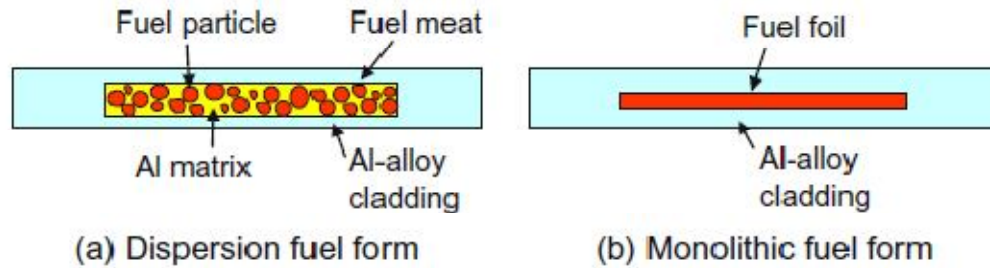


Fig. 4.1: Schematic cross sectional view of U-Mo fuel

There are a number of factors which need to be considered for realizing the designed performance of the nuclear fuel inside the reactor. The fabricated fuels before their final use should be certified for presence of various impurities. Owing to the deleterious effects associated with these trace impurities their maximum limit is specified [182, 197- 199]. Boron, cadmium and some rare earth elements (Sm, Eu, Gd, Dy) have very large neutron absorption cross sections and can affect the neutron economy. Low melting elements such as zinc, if present, may cause liquid metal embrittlement (LME), alter the fuel structure, which in turn may lead to failure. On the other hand, refractory elements, such as tungsten, may cause “creep resistance” resulting in clad damage. Elements, which get incorporated in nuclear fuel either from the precursors or during various fuel fabrication steps, need to be quantified precisely and accurately.

Various methods are available for the determination of trace metallic elements in various nuclear materials, viz., inductively coupled plasma mass spectrometry (ICP-MS) [40-43], inductively coupled plasma atomic emission spectroscopy (ICP-AES) [188], ion chromatography (IC) [48] etc. As discussed in chapter 3 Among all these techniques, ICP-MS is the most versatile multi-elemental technique with rapid analysis, high sample throughput, wide linear calibration range, low detection limit, and fewer spectroscopic interferences, etc. [194-196].

The Mass spectrometry technique cannot be used for samples having high matrix concentration. For ICP-MS analysis it is recommended to analyze solutions with total dissolved solid content $\leq 0.1\%$. Such samples require a pre-analysis matrix separation procedure, which can reduce or eliminate the matrix. The matrix under study contains U and Mo. Several studies are reported where solvent extraction is used to separate the U matrix [200-206]. Similarly organic extractants like Cyanex-923 and oxime (8-diethyl-7-hydroxydodecane-6-oxime) have been used for separating Mo [207-209]. Though the solvent extraction methods have been used successfully, they are laborious, time consuming and involve large volumes of organic solvents, especially when the method is employed on routine basis. It is also possible to separate Mo matrix by precipitation [210], uranium by hydrolytic precipitation or by formation of yellow cake [211, 212]. However, for the matrix under study, use of two different methods for U and Mo, will be cumbersome. It is also important to consider that the separation method should not affect the recovery of analytes. In view of the complexities associated with two different

methods for separation of U and Mo and also to minimize the losses in the recovery of analytes, it was decided to develop a method for simultaneous separation of U & Mo.

Various reports suggest that the, U and Mo can form chloride complexes, which are anionic in nature [213, 214]. The anionic complexes formed with chloride have been utilized for separation of U [215, 216] and Mo [217, 218] separately. It is possible to have a medium where both U and Mo form anionic chloride complexes, which can be separated simultaneously from the matrix. In the current work, anion exchange separation is investigated for simultaneous separation of U and Mo, from the various analytes. Recovery studies are carried out to understand the loss of analytes.

4.2 Experimental Section

4.2.1 Instrumentation

The Inductively Coupled Plasma - orthogonal acceleration- Time of Flight Mass Spectrometer (ICP-*oa*-TOF-MS), Model Optimass 8000R (GBC, Australia) discussed in chapter 3 was employed for quantification of trace and ultra trace elements in U-Mo alloy. Details of the instrumental and operating parameters are given in Table 4.1.

Table 4.1: Optimized operating conditions of ICP-MS

ICP-MS parameters	Values
RF power	1200 W
Frequency	27.2 MHz
Plasma gas flow rate	11.0 L min ⁻¹
Auxiliary gas flow rate	0.60 L min ⁻¹
Nebulizer gas flow rate	0.75 L min ⁻¹

Sample uptake rate	0.5 mL min ⁻¹
Measurement mode	Dual (PC/analog)
Acquisition time	5 s

4.2.2 Chemicals and Solutions

Bio-Rad AG[®] 1X4, chloride form, 200-400 mesh (Bio-Rad) was used for the ion exchange separation studies. Supra-pure HNO₃ and HCl (Merck) were used for sample preparation. De-ionized water having resistivity 18MΩ.cm (Milli-Q[™] system, Millipore) was used for dilution. The ICP standards of 1000 mg L⁻¹ (BDH) were diluted appropriately to prepare multi-element standard solutions. Eppendorf[®] micropipettes, Nalgene[®] PP measuring flask and funnels, and Teflon[®] PFA beakers were used throughout the experiment.

4.2.3 Preparation of anion exchange column

Approximately 2.0 gram resin, AG 1X4 (capacity 1.2 meq/ml resin bed), was mixed with de-ionized water to make slurry. It was filled in the column (OD-4.0 cm, ID-3.9 cm, and height-20.0 cm) to give a resin height of approximately 10 cm as given in Figure 4.2. To ensure a uniform resin bed, about 15 mL of water was placed in the column, and the resin was drawn from the column into the weight-burette and then released. The resin was allowed to settle in the column. This helped to remove any air bubbles formed during loading of the resin, and allowed the resin beads to settle uniformly in the column. The resin bed was conditioned by adding 30 mL 4 M HCl. Glass wool was placed at the top of

the resin bed to prevent the resin from being disturbed during the addition of reagents. The average flow rate measured was 1.0 mL/min.

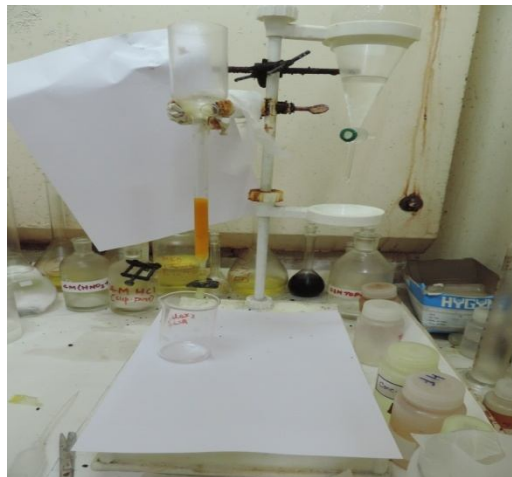


Fig.4.2 A photograph of anion exchange column

4.2.4 Preparation of Synthetic Samples

Due to non-availability of Certified Reference Material (CRM), synthetic samples, having 90% of uranium and 10% of molybdenum in solution form, were prepared after dissolving high purity uranium and molybdenum metal.

4.2.5 Dissolution of U-Mo alloy

In HNO_3 medium the sorption of matrix elements (U & Mo) is not sufficient in the anionic resin column. Chloride medium required to bring U and Mo in the anionic form. Therefore, the alloy was dissolved in HCl medium.. Dissolution of U-Mo alloy in conc. HCl only takes longer time; therefore few drops H_2O_2 were added. The solution was repetitively evaporated near to dryness with addition of 4M HCl, and finally made up-to mark in 25ml class-A volumetric flask using 4M HCl.

4.2.6 Column studies

The solutions were passed through the anion exchange column preconditioned with 4M HCl. Three bed volumes of 4M HCl were passed through the column to ensure attainment of equilibrium. The collected solution was evaporated and dissolved in 1% HNO₃ for estimation of un-retained elements using ICP-MS. The column was re-generated using 1M HNO₃ and 4M HCl before loading new sample.

4.3 Results and discussion

4.3.1 Retention Study of U and Mo

For the desired separation of matrix from the trace impurities it is important to optimize the separation procedure such that the matrix is retained completely on the column and the analytes are recovered in the eluent. It is reported that retention of U and Mo, on anion exchange column increases with increasing HCl concentration and the conditions are optimum at 9 M HCl for U [219] and 4 M HCl for Mo [217, 218]. On the other hand some of the analytes of interest may also form anionic complexes with chloride at higher concentration of HCl, in view of this 4 M HCl was chosen for the anion exchange column separation experiments.

Initially column studies were carried out to understand the capacity of the column for dissolved U and Mo separately. The U or Mo sample was loaded to the column, and their presence in the eluent was observed using reported spectrophotometry method for U [220] and ICP-MS for Mo. The experiments were repeated by gradually increasing the loaded sample mass. It was observed that upto 125 mg of U and 120 mg of Mo could be loaded separately on the column without detecting their presence in the eluent.

Similar experiment was performed using synthetic U-Mo sample. The experiment showed upto 120 mg loading of the sample with the concentration of U and Mo in the eluent being below the detection limit of the methods used. However on loading of additional 10 mg (U+Mo) sample, traces of U were found in the eluent. These observations helped in optimizing the maximum sample loading (~120mg) possible during the actual matrix separation experiments.

4.3.2 Retention of analytes

With the optimized conditions required for complete retention of matrix experiments were carried out to determine the recovery of 52 different analytes. The column was loaded with a standard solution containing different elements (200 ppb each). The recoveries of different elements studied are indicated in the Table 4.2.

Table 4.2: Retention studies of 52 elements (each having 200 ppb) in the absence of matrix

Recovery (%)	Analytes
90-100	Ba, Ce, Cr, Co, Cs, Cu, Dy, Eu, Er, Gd, Hf, Ho, La, Lu, Mn, Mg, Nd, Ni, Pr, Rb, Sc, Sm, Sr, Tb, Tm, V, W, Yb, Zr
75-90	Al, As, Ir, Pb, Rh, Y
25-50	Nb, Se and Zn
<10	Ag, Au, Bi, Cd, Fe, Ga, Ge, Hg, Os, Pd, Pt, Re, Ru, Sb, Sn, Ta, Ti

The column experiment was further repeated with standard solution containing analytes (200 ppb each) and U- Mo (equivalent to alloy concentration of 1 mg/ml). This time the recovery was checked by performing standard addition method. In addition to recovery study the standard addition method also helped in validating the method. Table-4.3 shows that thirty three elements (Al, As, Ce, Cr, Co, Cs, Cu, Dy, Eu, Er, Gd, Hf, Ho, La, Lu, Mg, Mn, Nd, Ni, Pb, Pr, Rb, Rh, Sc, Sm, Sr, Tb, Tm, V, W, Y, Yb, and Zr) were quantitatively separated from the matrix, whereas, twenty one elements (Ag, Au, Ba, Bi, Cd, Fe, Ga, Ge, Hg, Ir, Nb, Os, Pd, Pt, Re, Ru, Sb, Se, Sn, Ta, and Zn) were retained significantly on the column. The precision indicated in the table is the overall precision obtained by propagation of errors, taking into account both the external (triplicate sample, N=3) as well as the internal (no. of ICP-MS analysis of each sample, N=10) standard deviation.

Table 4.3 Recovery of trace elements in synthetic U-Mo Sample

(Sample Amount =0.1g, Volume=25mL, N=10)

Elements	Added (μg)	Determined (μg)	Recovery (%)
Al	0	17.53 \pm 1.41	--
	5	21.83 \pm 1.97	86.0 \pm 10.4
	10	26.52 \pm 2.52	89.9 \pm 11.2
	15	31.42 \pm 3.10	92.6 \pm 11.8
As	0	2.85 \pm 0.15	--
	5	7.15 \pm 0.21	86.0 \pm 5.2
	10	12.06 \pm 0.45	92.1 \pm 5.9

	15	17.25±0.69	96.0±6.3
Ce	0	0.27±0.01	---
	5	4.15±0.08	77.6±3.2
	10	8.43±0.13	81.6±3.3
	15	13.08±1.01	85.4±7.3
Cr	0	2.86±0.10	---
	5	6.87±0.15	80.2±3.3
	10	11.43±0.27	85.7±3.6
	15	16.24±1.12	89.2±6.9
Co	0	0.39±0.02	---
	5	4.38±0.09	79.8±4.4
	10	8.74±0.25	83.5±4.9
	15	13.31±1.05	86.1±8.1
Cs	0	0.28±0.01	--
	5	4.11±0.06	76.5±3.0
	10	8.45±0.23	81.7±3.7
	15	13.03±1.10	85.2±7.8
Cu	0	6.33±0.23	--
	5	11.15±0.38	96.4±4.8
	10	16.08±0.45	97.5±4.5
	15	21.23±1.21	99.3±6.7
Dy	0	0.27±0.01	---

	5	4.62±0.10	86.9±3.7
	10	9.45±0.25	91.8±4.1
	15	14.30±1.05	93.5±7.7
Eu	0	0.22±0.01	---
	5	4.35±0.10	82.6±4.2
	10	8.79±0.18	85.7±4.3
	15	13.59±1.12	89.1±8.4
Er	0	0.36±0.03	--
	5	4.22±0.26	80.0±8.3
	10	8.71±0.52	84.9±8.7
	15	13.65±1.01	89.5±9.9
Gd	0	0.23±0.01	---
	5	4.30±0.21	81.4±5.3
	10	8.82±0.51	85.9±6.2
	15	13.96±0.85	91.5±6.8
Hf	0	0.23±0.01	--
	5	4.54±0.22	86.1±5.6
	10	9.20±0.58	89.7±6.9
	15	14.00±0.91	91.8±7.2
Ho	0	0.33±0.04	--
	5	4.21±0.19	77.5±10.0

	10	8.31 ± 0.52	79.8 ± 10.9
	15	12.62 ± 1.01	81.9 ± 11.9
La	0	0.25 ± 0.01	--
	5	4.11 ± 0.22	77.2 ± 7.4
	10	8.23 ± 0.51	79.8 ± 8.1
	15	12.66 ± 0.95	82.7 ± 9.1
Lu	0	0.24 ± 0.01	--
	5	4.54 ± 0.25	85.9 ± 5.9
	10	9.02 ± 0.55	87.8 ± 6.5
	15	14.01 ± 0.88	91.8 ± 6.9
Mg	0	2.85 ± 0.15	---
	5	7.53 ± 0.29	93.6 ± 6.1
	10	12.30 ± 0.57	94.5 ± 6.6
	15	17.41 ± 1.15	97.1 ± 8.2
Mn	0	4.27 ± 0.32	---
	5	9.24 ± 0.65	99.4 ± 10.2
	10	13.98 ± 0.61	97.1 ± 8.4
	15	19.22 ± 1.21	99.7 ± 9.8
Nd	0	0.22 ± 0.01	---
	5	4.20 ± 0.28	79.6 ± 6.4
	10	8.57 ± 0.53	83.5 ± 6.4
	15	13.11 ± 1.09	85.9 ± 8.1

Ni	0	10.24±0.49	---
	5	14.46±0.82	84.4±6.3
	10	19.36±1.01	91.2±6.5
	15	24.65±1.58	96.1±7.7
Pb	0	0.62±0.06	--
	5	4.38±0.35	75.2±9.4
	10	8.26±0.74	76.4±10.1
	15	12.14±1.33	76.8±11.2
Pr	0	0.24±0.01	--
	5	4.23±0.25	79.8±5.8
	10	8.67±0.58	84.3±6.6
	15	13.25±0.79	86.7±6.3
Rb	0	0.30±0.02	--
	5	4.05±0.27	75.0±7.1
	10	8.05±0.65	77.5±8.1
	15	12.32±1.11	80.1±9.0
Rh	0	0.28±0.03	--
	5	4.13±0.30	77.0±9.9
	10	8.06 ±0.71	77.8±10.8
	15	12.21±1.31	79.5±12.1
Sc	0	0.32±0.03	--
	5	4.15±0.35	76.6±9.7

	10	9.35±0.86	90.3±11.9
	15	14.19±1.21	92.5±11.7
Sm	0	0.22±0.01	---
	5	4.35±0.28	82.6±6.5
	10	9.65±0.63	94.3±5.1
	15	14.81±1.18	97.3±8.9
Sr	0	0.34±0.03	--
	5	4.12±0.29	75.6±8.5
	10	7.94±0.65	76.0±9.1
	15	11.95±1.18	77.4±10.2
Tb	0	0.24±0.02	---
	5	4.96±0.33	94.4±10.1
	10	10.10±0.61	98.6±10.2
	15	14.95±1.11	98.1±10.9
Tm	0	0.24±0.02	--
	5	4.65±0.26	88.2±8.9
	10	9.61±0.59	93.7±9.7
	15	14.15±1.18	92.7±10.6
V	0	0.49±0.03	--
	5	4.25±0.25	75.2±6.4
	10	8.11±0.62	76.2±7.5
	15	12.24±1.21	78.3±10.8

W	0	5.70 ± 0.46	--
	5	9.45 ± 0.76	75.0 ± 8.5
	10	13.52 ± 1.49	78.2 ± 10.7
	15	17.64 ± 1.78	79.6 ± 10.3
Y	0	0.38 ± 0.04	--
	5	4.20 ± 0.27	76.4 ± 9.4
	10	8.19 ± 0.59	78.1 ± 10.0
	15	12.41 ± 1.17	80.2 ± 11.3
Yb	0	0.22 ± 0.03	--
	5	4.34 ± 0.28	82.4 ± 12.4
	10	9.01 ± 0.53	87.9 ± 13.1
	15	13.95 ± 1.19	91.5 ± 14.7
Zr	0	5.63 ± 0.29	--
	5	9.43 ± 0.71	76.0 ± 6.9
	10	13.36 ± 1.05	77.3 ± 7.3
	15	17.62 ± 1.65	79.9 ± 8.9

Recovery of the nineteen elements was < 10%, therefore results not tabulated. Reports shows that these elements (Fe, Zn [221], Pd [222], Bi [223], Cd [224], Au [225], Nb, Ta [226,227], Ir [228], Os [229], Pd, Pt [230], Re [231], Ru [232], Sb [233], Se [234], Sn [235], Ag [236], Ga [237], and Ge [238]) formed strong anionic complexes in presence of hydrochloric acid and get absorbed in the anionic resin. On the other hand, thirty-three

elements, have a good recovery because either they do not form anionic complexes or have very small distribution coefficient. On the basis of the reports, it could be said that the spread in the recoveries is due to their different affinity with anionic resin in the given conditions [239-242].

4.3.3 Study of Isobaric Interferences

The instrument was optimized on daily basis and stability of plasma was studied after two hours ignition of the plasma. Spectroscopic interferences due to isobaric and polyatomic ions were corrected according to the reports [243, 244]. Considering the low concentration of REEs (present in sub-ppm range) and no detectable Ba in U-Mo alloy, the individual analyte intensities were only considered without applying any polyatomic interference correction.

4.3.4 Detection limit

Most analytical instruments produce a signal even when a blank (matrix without analyte) is analyzed. This signal is referred to as the noise level. The instrumental detection limit (IDL) or limit of detection (LOD), is the analyte concentration that is required to produce a signal greater than three times the standard deviation of the noise level. The IDL is determined using 1% supra pure HNO₃ solution. It is analyzed ten times and the standard deviation is calculated. The method detection limit (MDL) is defined as the minimum concentration of a substance that can be measured and reported with 99% confidence that the analyte concentration is greater than zero and is determined from analysis of the sample in a given matrix containing the analyte. It is determined using the standard solution having 2.5 to 5 times the values of the LOD for the analytes. It is mixed with 5.0

ml supra pure concentrated HCl (i.e. the amount of acid used in dissolution of 0.1g sample) , evaporated, and the residue is re-dissolved in 10 ml 4M HCl. This solution passed through the anion exchange column and additional 20 ml 4M HCl used to collect the analytes. Finally, it is evaporated to dryness, and dissolved in 10 mL 1% HNO₃ for ICP-MS analysis. Standard deviation (σ) of ten analysis is used to calculated the MDL of the analytes. The procedure has reported somewhere in [245]. The IDLs and MDLs are tabulated in Table 4.4.

Table 4.4 Instrument detection limit (IDL) and Method detection limit (MDL) of all the analytes (N=10)

Elements	IDL(ngL^{-1})	MDL($\mu\text{g Kg}^{-1}$)	Elements	IDL(ngL^{-1})	MDL($\mu\text{g Kg}^{-1}$)
Al	200	10	Nd	10	1
As	150	15	Ni	80	3
Ce	15	1	Pb	30	4
Cr	100	1	Pr	10	1
Co	20	6	Rb	50	2
Cs	120	5	Rh	50	5
Cu	150	7	Sc	25	5
Dy	5	1	Sm	7	1
Eu	10	1	Sr,	50	10
Er	20	1	Tb	10	1
Gd	10	1	Tm	20	1
Hf	30	1	V	25	2

Ho	25	1	W	100	5
La	10	2	Y	50	5
Lu	15	2	Yb	25	2
Mg	75	10	Zr	100	10
Mn	30	2			

4.3.5 Analysis of Real Samples

Analysis of real samples of different lots was carried out following the methodology described above. The flow diagram for the final optimized procedure is given in Figure 4.4. The results are given in the Table 4.5. As is evident from the table, the concentrations of trace metallic impurities are well below the specification limit for ASTM nuclear grade uranium metal specification. The fabrication procedure for U-Mo alloy has been developed. The trace metallic impurity concentrations determined in different lots by this method will help in understanding the lowest possible impurities during the fabrication. This in turn will help in deciding the specification limits of trace metallic impurities for the alloy.

4.4 Conclusion

Anion exchange separation was used for the simultaneous separation of U and Mo from the analytes. It was possible to recover 33 analytes (Al, As, Ce, Cr, Co, Cs, Cu, Dy, Eu, Er, Gd, Hf, Ho, La, Lu, Mg, Mn, Nd, Ni, Pb, Pr, Rb, Rh, Sc, Sm, Sr, Tb, Tm, V, W, Y, Yb, and Zr) from the sample quantitatively. The chromatography separation procedure is simple, fast, and cheap; it can be employed for routine analysis of U-Mo samples. The

generation of organic and radioactive liquid waste is reduced significantly. The method was successfully employed for the analysis of trace impurities in several real samples.

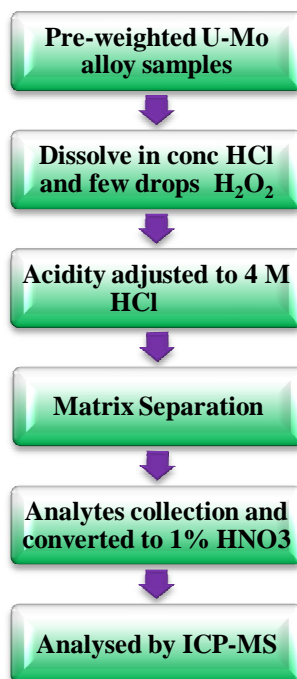


Fig. 4.3: Systematic diagram for the analysis of U-Mo alloy

Table 4.5: Trace element concentrations in the U-Mo Samples of different lots (in $\mu\text{g/g}$)

Elements	Sample I	Sample II	Sample III
Al	220.6 \pm 19.5	159.4 \pm 7.8	183.5 \pm 9.5
As	9.9 \pm 1.2	15.3 \pm 0.9	1.5 \pm 0.2
Ce	2.6 \pm 0.16	0.20 \pm 0.01	<BDL
Cr	28.8 \pm 2.3	36.3 \pm 1.6	23.8 \pm 0.6
Co	3.9 \pm 0.3	<BDL	<BDL
Cs	2.8 \pm 0.2	<BDL	<BDL

Cu	63.7 ± 5.1	62.3 ± 3.1	49.6 ± 1.3
Dy	2.2 ± 0.2	0.3 ± 0.02	0.06 ± 0.01
Eu	2.3 ± 0.2	<BDL	<BDL
Er	3.7 ± 0.3	<BDL	1.0 ± 0.11
Gd	2.4 ± 0.2	<BDL	<BDL
Hf	2.3 ± 0.2	7.4 ± 0.3	0.10 ± 0.01
Ho	3.4 ± 0.3	0.2 ± 0.05	1.5 ± 0.33
La	2.5 ± 0.2	0.2 ± 0.02	<BDL
Mg	28.7 ± 1.7	18.6 ± 1.0	13.8 ± 0.6
Mn	42.9 ± 3.0	59.9 ± 6.5	56.3 ± 4.5
Nd	2.2 ± 0.2	<BDL	<BDL
Ni	103.2 ± 6.2	73.5 ± 3.1	98.5 ± 5.6
Pb	83.8 ± 7.4	7.5 ± 0.3	3.2 ± 0.3
Pr	2.4 ± 0.2	<BDL	<BDL
Rb	3.0 ± 0.2	<BDL	<BDL
Rh	2.7 ± 0.2	<BDL	<BDL
Sc	3.2 ± 0.2	1.8 ± 0.1	1.4 ± 0.1
Sm	2.2 ± 0.2	<BDL	<BDL
Sr	3.2 ± 0.3	0.7 ± 0.05	<BDL
Tb	2.4 ± 0.2	0.06 ± 0.01	<BDL
Tm	2.4 ± 0.2	<0.01	<0.01
V	7.1 ± 0.6	69.2 ± 3.6	0.6 ± 0.04

W	75.5±6.9	57.5±2.8	49.5±2.9
Y	3.8±0.3	1.7±0.06	0.1±0.01
Yb	2.2±0.2	<BDL	<BDL
Zr	70.8±6.8	299.5±15.4	6.1±0.5

BDL: Below Detection Limit

Chapter 5

Quantification of trace and ultra-trace impurities in U-Zr alloy using ICP-MS

5.1 Introduction

The metallic nuclear fuels based on U-Zr and U-Pu-Zr alloys are preferred in fast breeder reactors compared to conventional oxides and carbides owing to their high fissile density, high breeding ratio, less doubling time, good fuel-clad compatibility, high thermal conductivity, and inherent passive safety. Fast reactors generally have an excess of neutrons (due to low parasitic absorption), the neutrons given off by fission reactions can “breed” more fuel from otherwise non-fissionable isotopes or can be used for other purposes (e.g. transmutation of spent nuclear fuel) [246]. The most common breeding reaction is a neutron absorption reaction on uranium-238, yielding ^{239}Pu as shown in Figure 5.1.

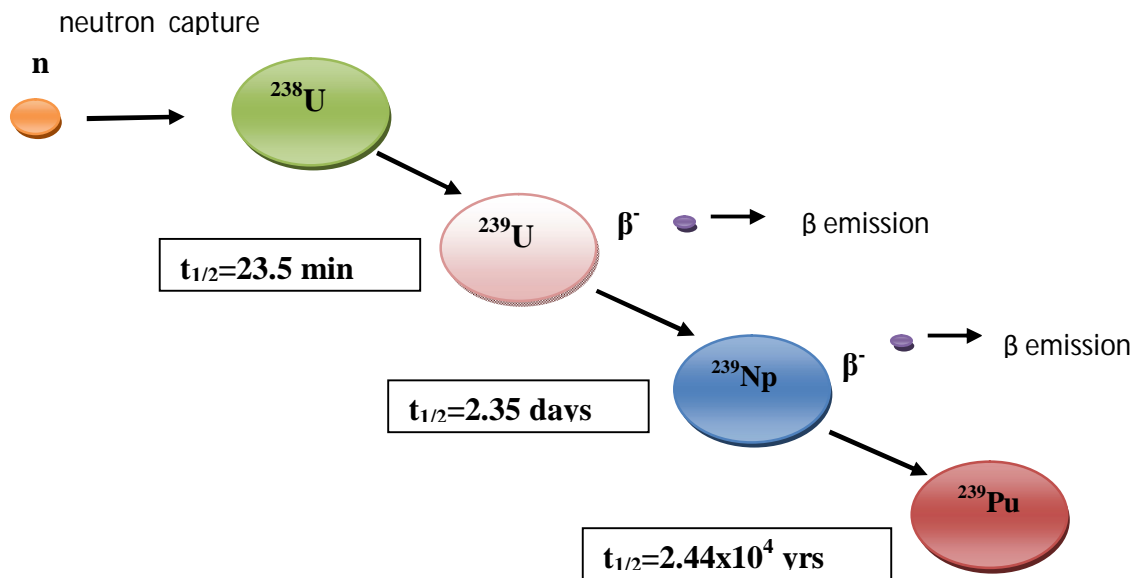


Fig.: 5.1 Formation of fissionable ^{239}Pu from ^{238}U

The term “breeder” refers to the types of configurations which provide the breeding ratio higher than 1. That means such reactors produce more fissionable fuel than they consume.

In India, fabrication and irradiation studies are being pursued in order to develop metallics fuel based fast breeder reactors (FBR) [247]. Metallic fuels have been used in nuclear reactors in the past (EBR I&II USA) and are also proposed for advanced nuclear reactors, such as, traveling wave reactor (TWR), fusion-fission hybrid reactor (FFHR), sodium cooled fast reactors (SFR) etc. [248, 249]. Systematic diagram of sodium cooled fast breeder reactor is shown in Figure 5.2. In the fast breeder reactors U-Pu-Zr is proposed as fuel in the main core, with U-Zr as blanket material for breeding

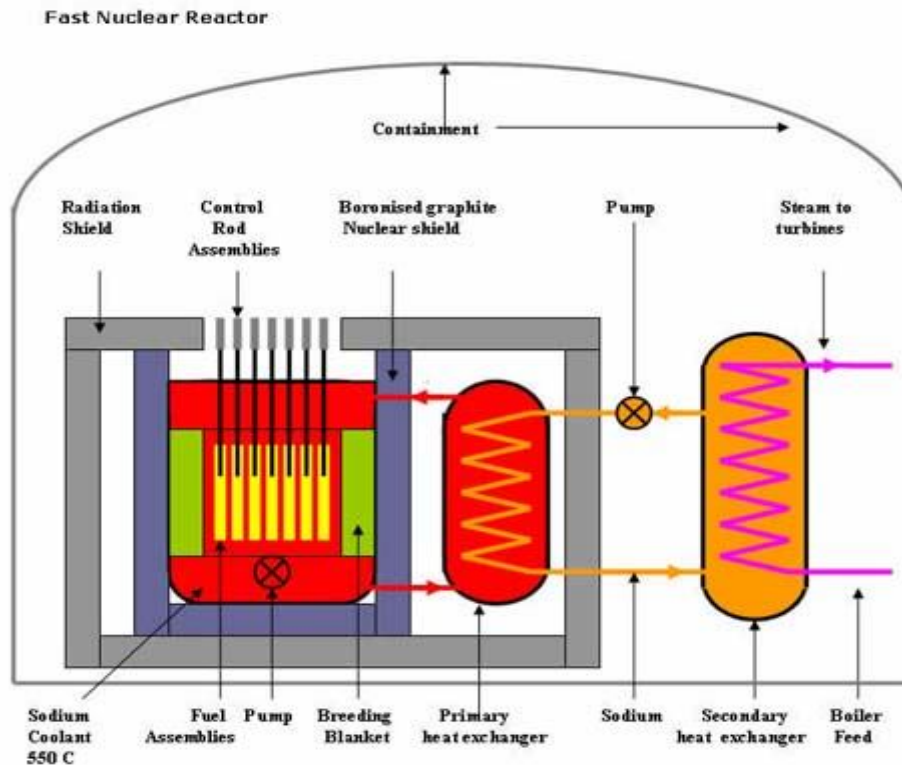


Fig.5.2 Block diagram of sodium cooled FBRs

Chemical characterization of nuclear fuels for major, trace and ultra-trace elements is very important to ensure the desired behavior of fuels during reactor operation. The elements, whose presence above the specification limit could lead to detrimental effects, have very stringent specifications [250, 251]. Hence, it is essential to have precise and accurate knowledge of their concentrations, in the starting raw materials and fabricated fuel, prior to their loading in the nuclear reactors. Several analytical techniques, i.e. neutron activation analysis (NAA), graphite furnace atomic absorption spectroscopy (GFAAS), inductively coupled plasma atomic emission spectroscopy (ICP-AES), total reflection X-ray fluorescence (TXRF), UV - visible spectroscopy, inductively coupled plasma mass spectrometry (ICP-MS) etc. are in practice for determination of trace impurities in the nuclear fuels [39, 252,253]. Each technique has its advantages and disadvantages. However, the sensitivity and the matrix interference are the two key elements in determination of trace impurities in uranium based nuclear materials. Selection of technique depends upon sample size, detection limit, sensitivity, and sample throughput.

Quantification of 12 elements (B, Ce, Cd, Co, Eu, Dy, Gd, Mn, Nd, Ni, Sm and Tb) by ICP-MS has reported where only one matrix element (uranium) has separated and the matrix effect due to zirconium has studied using common analyte internal standard (CIAS) method [94]. This method is tedious and only few elements has analyzed, it is not suitable for routine analysis. In another ICP-MS report where both matrix elements (U & Zr) has separated used sequential separation of U and Zr, and only rare earth elements has reported for analysis [254]. Quantification of 16 elements (Al, B, Cd, Co, Cr, Cu, Dy,

Eu, Gd, Fe, Mn, Na, Ni, Sm, and Zn) using ICP-AES has reported where high concentration (7M) of nitric acid is used [100]. Trace amount of chlorine and fluorine has determined by ion chromatography (IC) after pyrohydrolysis (PH) of U-Zr and U-Pu-Zr samples [255]. These reported methods are not suitable for quantification of trace impurities by ICP-MS. In the present work a method has developed for determination of trace element impurities in U-Zr.

Owing to the very low detection limit, low spectroscopic interference, high sample throughput, high sensitivity, and multi-element capability, ICP-MS is the technique of choice for the trace analysis in U-Zr matrix. However, analysis of trace and ultra-trace elements with high concentration of matrix elements leads to non-spectroscopic interference and memory effect, as the sample solution is passed through a fine capillary of nebulizer, and ions are transmitted to detector through small orifice of sampler and skimmer cones. The sample solutions having high total dissolved solid (TDS) choke the capillary of nebulizer, and orifice of sampler and skimmer, which introduce significant systematic and random error in the measurements. Further, long washing time is required to remove the memory effect from the matrix elements. Considering these problems it is important to separate the matrix before the quantification of traces using ICP-MS.

Extraction of uranium has been reported using dibenzo-24-crown-8 [256] benzyloctadecyldimethylammonium chloride [225], cyanex-272 [229], cyanex-301 [257], di-2-ethylhexyldithiophosphoric acid [228], N,N'-dihexanoylpiperazine [258], dicyclohexyl-18-crown-6 [259], octaethyltetraamidopyrophosphate [260], 1-(4-tolyl)-2-methyl-3-hydroxy-4-pyridone [261], tri-butyl phosphate [262], tri-n-octyl phosphine

oxide [227, 226] etc. Similarly extraction of zirconium has been reported using aliquat-336 [263], tri-2-ethyl hexyl amine [264], cynax-923 [265], tri-butyl phosphate [266], tri-n-octyl phosphine oxide [267, 268] etc. For the matrix under study both U and Zr are to be separated. It is important to have a single solvent extractant which can separate both the species present in the sample simultaneously. As listed above, TBP can be used for both U and Zr. However the experimental conditions required for the complete separation are different for U and Zr. It is also possible to utilize the synergistic solvent extraction procedure, where more than one extractant are used simultaneously as discussed in a review by R.Sarkar et al. [269]. TBP is used in PUREX process for separation of uranium from nitric acid medium, while TOPO is known to extract Zr from HCl medium [302, 303]. In the present work simultaneous extraction of U and Zr was investigated using a combination of tri-n-butyl phosphate (TBP) and tri-n-octyl phosphine oxide (TOPO). A detailed study was carried out to optimize the experimental conditions for simultaneous extraction of U and Zr, leaving the impurities in the solution. The trace analysis of sample prepared using the developed separation method was carried out by ICP-MS and due to the unavailability of certified reference material (CRM) of U-Zr, validation was carried out using standard addition method.

5.2 Experimental

5.2.1 Instrumentation

An inductively coupled plasma - orthogonal acceleration- time of flight mass spectrometer (ICP-oe-TOF-MS), model optimass 8000R (GBC, Australia) was employed for the quantification of trace and ultra trace elements in U-Zr alloy. Details of the

instrumental operating parameters are chapter 2. A 3''X3'' NaI(Tl) well-type detector coupled to a multichannel analyzer (Electronic Corporation of India Limited) was used to validate separation procedure using $^{152+154}\text{Eu}$ as tracer. Details of the spectrometer are given in chapter 2. Eppendorf[®] micropipettes, Nalgene[®] PP measuring flask, and separating funnels, and Teflon[®] PFA beakers were used throughout the experiment.

5.2.2 Chemicals and Solutions

TBP (Merck), TOPO (Aldrich), toluene (SRL), supra-pure HNO_3 and HCl (Merck) were used for solvent extraction and preparation of the sample. De-ionized water having a resistivity of $18\text{M}\Omega\cdot\text{cm}$ (Milli-QTM system, Millipore) was used for dilution. The ICP standards of 1000 mg L^{-1} (BDH) were diluted appropriately to prepare multi-element standard solutions.

5.2.3 Preparation of Aqueous and Organic Medium

The aqueous phase medium was optimized to be a mixture of 4M HCl and 4M HNO_3 . The final volume was made up to 100ml using water. In general, the concentration of TBP and TOPO is expressed in percentage (v/v) and molar (M) values respectively. Therefore, organic phase was prepared by adding weighed amount of TOPO to 30% TBP(in toluene) so as to make the TOPO concentration as 0.1 M.

5.2.4 Preparation of Synthetic Solutions

Due to non-availability of certified reference material (CRM) for U-Zr alloy, a synthetic solution of U-Zr was prepared. Nuclear grade Uranium and Zirconium metals were dissolved separately and mixed together, so as to prepare working standards of

concentration 94 mg mL^{-1} U and 6 mg mL^{-1} Zr. Aliquots of this solution were spiked with known amount of trace elements in this study.

5.2.5 Dissolution of U-Zr alloy

U-Zr could be dissolved in concentrated HCl and HNO_3 , however the dissolution was slow. 100 mg of U-Zr alloy took around 1-1.5 hours for the complete dissolution in HNO_3 medium, which was accelerated by addition of a few drops of HF. On completion of the dissolution HF was removed by repetitive evaporation of solution to near dryness with addition of HNO_3 -HCl (4M) solution. Finally, the dissolved sample was made in HNO_3 -HCl (4M) medium for solvent extraction studies.

5.2.6 Separation of Matrix Elements

In order to develop a solvent extraction based separation procedure, a detailed study was carried out using TBP and TOPO. For the separation studies toluene was selected as the diluent. Many authors have used carbon tetrachloride as diluent [100, 254], however, it is carcinogenic and aids in ozone depletion [271, 272]. Further, it forms $\text{CCl}_4 \cdot 2\text{TBP}$ with TBP, which decreases the extraction efficiency due to decrease in effective concentration of TBP in organic phase. Experiments were performed in fume hood using separating funnels. The volume of aqueous and organic phases taken for the equilibration was 5 ml each.

5.2.6 Aqueous Phase Analysis

After the separation the aqueous phase was evaporated near to dryness and re-dissolved in 1% HNO_3 to a known volume. Zr and trace elements were determined by ICP-MS

whereas U was determined by spectrophotometric method using Arsenazo-III as a chromogenic agent [244].

5.3 Results and discussion

5.3.1 Extraction of Zr from HCl and HNO₃ Medium in TBP

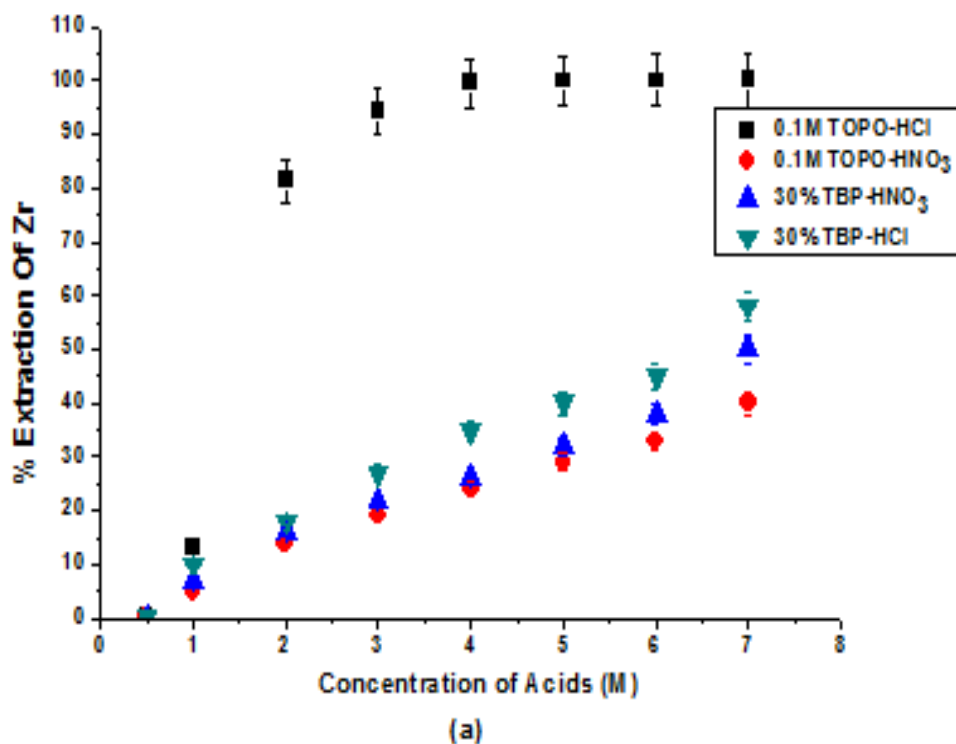
The extraction of U in TBP is reported to increase with increasing concentration of hydrochloric acid, with the appearance of third phase (at Uranium concentrations > 1M) at 5M HCl, [273]. In the PUREX process, the extraction of U is carried out from 4M nitric acid in 30% TBP. Therefore it was important to know the extraction of Zr in TBP in the conditions suitable for U extraction.

A set of separation studies were carried out where, Zr was extracted from varying concentration of HCl or HNO₃, in 30% TBP. For acid concentration of 7M, the extraction in both the acid media increases upto 60% (Figure 5.3a). Extraction of zirconium in high concentration of HNO₃ (>8M) with TBP has been reported [274], but excess nitrate concentration promotes the formation of un-extractable anions of uranium such as [UO₂(NO₃)₃]⁻ [275]. Further, at higher concentration of HNO₃ (>5M), probability of extraction of trace analytes increases [276, 277]. Though both U and Zr can be extracted in the TBP, the conditions required for their individual satisfactory extractions are different.

5.3.2 Extraction of Zr in TOPO

In case of TOPO, U extraction from HNO₃ (4-5M) medium is nearly quantitative (~95%), however for the quantitative extraction of Zr, HCl medium is required. Therefore detailed studies were carried out to optimize the conditions for mixture of acids (HNO₃ and HCl)

and that of the extractants (TBP and TOPO). Extraction of zirconium in TOPO was studied individually in HNO_3 and HCl . The condition was optimized using 1000 μg of zirconium with varying concentration of HCl , HNO_3 and TOPO. The results show that Zr is extracted up to 99 % at HCl concentration above 4 M HCl (Figure 5.3a), while in HNO_3 medium Zr extraction increased with acid molarity reaching around 25% at 4M HNO_3 . In a separate study extraction of Zr from a mixture of HNO_3 (4M) and HCl (4M) to TOPO (concentration varied) was carried out (Figure 5.3b), wherein Zr extraction was found to be better than 99% at and above 0.1M TOPO.



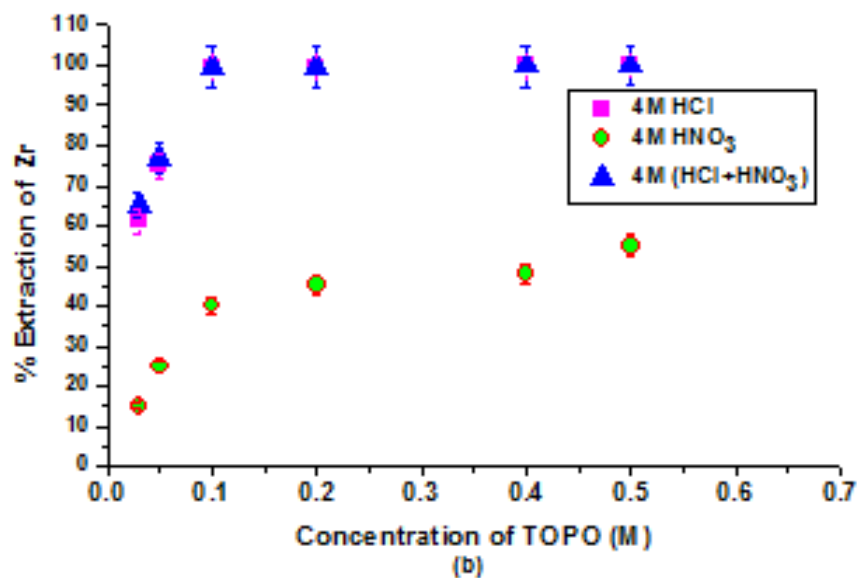
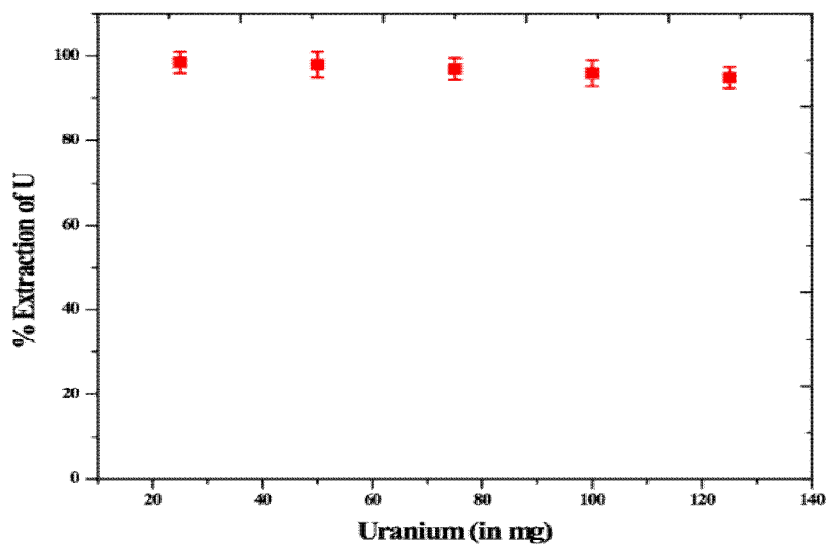


Fig.5.3: Percentage extraction of zirconium: (a) with 30% TBP and 0.1M TOPO at different concentration of HNO₃ and HCl and (b) with different concentration of TOPO at 4M HNO₃, 4M HCl and 4M HNO₃-4M HCl mixture.

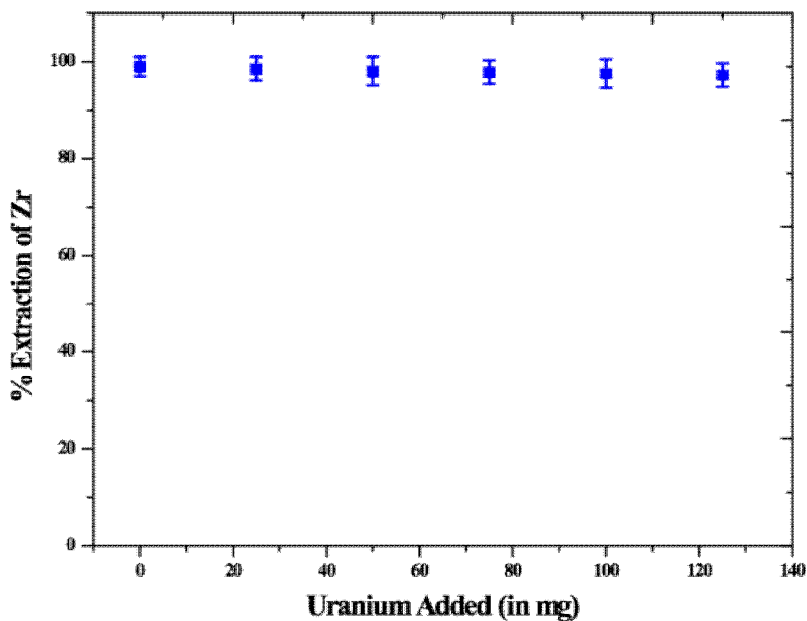
5.3.3 Effect of TBP

In view of the efficient extraction of U in TBP, a set of experiments was carried out by adding 30% TBP to the above optimized organic phase (0.1M TOPO in toluene). Synthetic samples of Zr (6 mg) and varying concentration of U (0-125 mg) in HNO₃- HCl (4M) medium were equilibrated with the organic phase. The amount of U and Zr taken was important because, it represents the U and Zr content in the dissolved U-Zr samples. The percentage extraction of U and effect of increasing U concentration on Zr extraction are plotted in Figure 5.4. It was found that extraction of uranium (up to 125 mg) was

better than 95% as given in Figure 5.4a. On the other hand, the percentage extraction of Zr was above 97% (lower than 99% observed with only Zr) with increasing uranium concentration (Figure 5.4b).



(a)



(b)

Fig. 5.4: Percentage extraction of U (a) and Zr (b) as a function of metal ion concentration in presence of varying amount of U

5.3.4 Non Spectroscopic Interference

As a fraction of U (4-5%) and Zr (2-3%) was still present in the aqueous phase with the trace analytes, it was decided to study the effect of the remaining U and Zr matrix on the analytes of interest. Literature reports show that moderate amounts (0.01-0.5%) of the matrix ions can change analyte signal significantly when analyzed by ICP-MS [153,278, 279].

To study the non-spectroscopic matrix effect, a range of samples were prepared with same concentration of analytes (100 ng mL^{-1} of rare earth and cadmium) and varying concentration of U-Zr (0, 50, 100, 200, 300, 400, 500, 600, and $700 \text{ } \mu\text{g mL}^{-1}$). Each

sample was analyzed for the trace analytes by ICP-MS. The counts of each samples was normalized with 100 ng mL^{-1} standard solution without matrix. It was observed that up to $100 \text{ }\mu\text{g mL}^{-1}$ of matrix had no significant effect on the analyte signal (Figure 5.5) above which the normalized (with respect to the sensitivity in absence of matrix) sensitivity ($\text{counts ng}^{-1} \text{ mL}^{-1} \text{ s}^{-1}$) decreased significantly

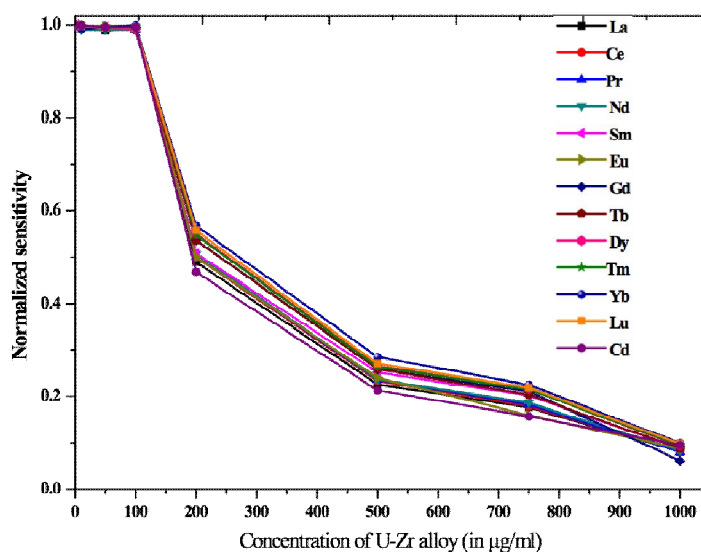


Fig. 5.5: Variation in sensitivity with matrix concentration

In order to have quantitative separation of matrix ($\leq 100 \text{ }\mu\text{g mL}^{-1}$) more than one contact with organic phase was required. The U and Zr content in the aqueous phase after three contacts were found to be 10 and $0.1 \text{ }\mu\text{g mL}^{-1}$ respectively.

5.3.5 Recovery of Analytes

With combination of TBP and TOPO in the organic phase and that of HNO_3 and HCl in the aqueous phase, quantitative extraction was possible for U and Zr. To use this method for matrix separation it was important to study the recovery of analytes during the extraction procedure. The recoveries were studied with and without the matrix. In the first

experiment, 55 elements were studied in absence of U and Zr matrix. Aqueous solutions containing 100 ppb of individual elements in HNO₃-HCl (4M) were equilibrated with equal volume of 0.1M TOPO and 30% TBP (in toluene). Analysis of the aqueous phase ICP-MS showed that thirty six elements were quantitatively retained in the aqueous phase, while the retention was less for the remaining elements as given in Table 5.1. Further studies are required for improving the retention of these elements in the aqueous phase to enable their quantification. In the second experiment, the above procedure was performed in presence of 100 mg synthetic U (94mg) + Zr (6mg) solution. The results indicated that, the retention of analytes were same as observed without the matrix.

Table 5.1 Retention Studies of 55 Elements (each at 100 ppb) in the Absence of the Matrix

Retention (%)	Total elements	Elements
95-100	36	Al, Ba, Bi, Cd, Ce, Co, Cr, Cs, Cu, Dy, Eu, Er, Ga, Gd, Ir, La, Lu, Mg, Mn, Nd, Ni, Pb, Pr, Pt, Rb, Rh, Ru, Sc, Sm, Sr, Tb, Te, Tm, V, Y, and Yb
60-70	2	Pd, Sb,
60-30	10	Ag, As, B, Fe, Mo, Nb, Re, Se, Sn, and Zn
<10	7	Hf, Hg, Ho, Li, Ta, Ti, W,

The reports show that elements such as Ag [280], As [281], B [282], Fe [269], Hg [283], Hf [284], Li [285], Mo [286], Nb [287], Re [288], Ta [289], Ti [290], W [291], and Zn [292] have significant extraction in the organic phase with TBP and TOPO, hence extracted along with the matrix elements (U and Zr). Other elements, such as, Al, Ba, Bi, Cd, Ce, Co, Cr, Cs, Cu, Dy, Eu, Er, Ga, Gd, Ir, La, Lu, Mg, Mn, Nd, Ni, Pb, Pr, Pt, Rb,

Rh, Ru, Sc, Sm, Sr, Tb, Te, Tm, V, Y and Yb [293-299] have very small extraction in hydrochloric acid medium with TBP and TOPO. Reports shows that these elements formed anionic species in presence of chloride medium, therefore, do not extracted with TBP and TOPO.

5.3.6 Standard Addition Method for Validation

The separation method was validated by standard addition method. Four aliquots of the synthetic U-Zr solutions (1.0 ml) were taken in HNO₃-HCl (4M). In the three aliquots multi-element standards of 36 elements (Al, Ba, Bi, Cd, Ce, Co, Cr, Cs, Cu, Dy, Eu, Er, Ga, Gd, Ir, La, Lu, Mg, Mn, Nd, Ni, Pb, Pr, Pt, Rb, Rh, Ru, Sc, Sm, Sr, Tb, Te, Tm, V, Y and Yb) were added, each element having 1, 2 and 5µg and one aliquot was taken as such. The matrix elements (U&Zr) were separated following the developed procedure and retention of analytes in aqueous phase was studied. The instrument was externally calibrated using six multi-element standards having concentration in the range, 50-750 µg L⁻¹. ¹¹⁵In was used as internal standard to monitor any drift during analysis. ICP-MS analysis shows that these analytes were retained in aqueous phase quantitatively (>90%). The recovery results are listed in Table 5.2.

Table 5.2: Recovery of Trace Elements in Synthetic U-Zr Sample

(Sample Amount =0.1 g, Volume=25 mL, N=10)

Elements	Added (µg)	Found (µg)	Recovery (%)
Al	0	0.11 ± 0.01	---
	1	1.10 ± 0.04	99.0 ± 9.7
	2	1.94 ± 0.11	91.5 ± 9.8
	5	4.98 ± 0.19	97.4 ± 9.6

Ba	0	0.12 ± 0.01	--
	1	1.10± 0.04	99.0±9.0
	2	2.1 ± 0.09	98.0±9.4
	5	5.05 ± 0.21	98.6±9.2
Bi	0	1.1±0.05	--
	1	2.05±0.15	95.0±7.0
	2	3.08±0.25	99.0±9.2
	5	5.89±0.25	95.8±6.1
Cd	0	BDL	--
	1	1.00±0.04	99.0 ± 4.0
	2	1.95±0.15	97.0 ± 7.6
	5	4.89±0.25	97.6 ± 5.1
Ce	0	0.10±0.007	--
	1	1.08±0.04	98.0 ± 7.7
	2	2.05±0.10	97.5 ± 8.3
	5	5.08±0.20	99.6 ± 8.0
Co	0	0.11±0.01	--
	1	1.09±0.05	98.0±9.9
	2	1.99±0.09	94.0±9.5
	5	5.10±0.20	99.8±9.9
Cr	0	2.90±0.15	--
	1	3.85±0.25	95.0 ± 7.9
	2	4.89±0.31	99.5 ± 8.1
	5	7.87±0.55	99.4 ± 8.6
Cs	0	0.10±0.008	--
	1	1.09±0.05	99.0 ± 9.1
	2	2.05±0.10	97.5 ± 9.1

	5	4.95±0.25	97.0 ± 9.2
Cu	0	2.91±0.13	--
	1	3.90±0.25	99.0 ± 7.7
	2	4.92±0.30	100.5 ± 7.6
	5	8.00±0.60	101.8 ± 8.9
Dy	0	BDL	--
	1	0.98±0.09	98.0 ± 9.2
	2	1.95±0.15	97.5 ± 7.5
	5	4.99±0.45	99.8 ± 9.0
Eu	0	0.10±0.006	--
	1	1.12±0.03	102.0 ± 6.2
	2	1.99±0.11	94.4 ± 7.7
	5	5.14±0.22	100.8 ± 7.4
Er	0	BDL	---
	1	0.95±0.09	95.0 ± 9.5
	2	1.96±0.15	98.0 ± 7.5
	5	4.85±0.40	97.0 ± 8.0
Ga	0	0.3±0.02	--
	1	1.25±0.09	95.0 ± 9.3
	2	2.21±0.14	95.5 ± 8.8
	5	4.98±0.27	93.6 ± 8.0
Gd	0	BDL	--
	1	1.0±0.02	98.0±5.0
	2	2.01±0.10	99.5±4.9
	5	4.99±0.20	99.4±4.0
Ir	0	BDL	--
	1	0.95±0.08	95.0 ± 8.4

	2	2.01±0.17	100.5 ± 8.5
	5	4.91±0.48	98.2 ± 9.6
Ho	0	BDL	--
	1	0.93±0.07	93.0 ± 7.5
	2	1.91±0.18	95.5 ± 9.0
	5	4.85±0.41	97.0 ± 8.5
La	0	BDL	--
	1	0.95±0.08	95.0 ± 8.4
	2	1.89±0.16	94.5 ± 8.0
	5	4.86±0.41	97.2 ± 8.4
Lu	0	BDL	--
	1	0.97±0.09	97.0 ± 9.0
	2	1.90±0.15	95.0 ± 7.5
	5	4.95±0.45	99.00± 9.0
Mg	0	2.6±0.16	--
	1	3.55±0.28	95.0 ± 8.5
	2	4.52±0.31	96.0 ± 8.4
	5	7.54±0.56	98.8 ± 9.5
Mn	0	1.80±0.15	--
	1	2.75±0.25	95.0± 7.4
	2	3.77±0.35	98.5 ± 7.7
	5	6.70±0.65	98.0 ± 8.1
Nd	0	BDL	--
	1	0.98±0.07	98.0±7.1
	2	1.93±0.15	97.5±7.5
	5	4.95±0.35	99.0±7.1
Ni	0	4.51±0.24	--

	1	5.49±0.30	98.0 ± 7.5
	2	6.48±0.35	98.5 ± 9.2
	5	9.44±0.55	98.6 ± 7.8
Pb	0	0.65±0.05	--
	1	1.59±0.11	94.0 ± 9.7
	2	2.56±0.19	95.5 ± 8.0
	5	5.61±0.35	99.2 ± 9.8
Pr	0	BDL	--
	1	0.98±0.05	98.0 ± 5.1
	2	1.91±0.11	95.5 ± 5.6
	5	4.89±0.25	97.8 ± 5.1
Pt	0	BDL	--
	1	0.89±0.08	89.0 ± 9.0
	2	1.78±0.15	89.0 ± 7.5
	5	4.55±0.48	91.0 ± 9.6
Rb	0	BDL	--
	1	0.91±0.08	91.0 ± 8.0
	2	1.86±0.15	93.0 ± 7.5
	5	5.12±0.49	102.4 ± 9.8
Rh	0	BDL	--
	1	0.98±0.09	98.0 ± 9.0
	2	1.95±0.15	97.5 ± 7.5
	5	5.10±0.45	102.0 ± 9.0
Ru	0	BDL	-
	1	0.93±0.08	93.0±8.6
	2	1.88±0.16	94.0±8.0
	5	4.98±0.42	99.6±8.4

Sc	0	BDL	-
	1	0.95±0.09	95.0±9.5
	2	1.85±0.17	92.5±8.5
	5	4.51±0.45	90.2±9.0
Sm	0	BDL	-
	1	0.98±0.05	98.0±5.1
	2	1.92±0.10	96.0±5.2
	5	4.89±0.26	97.8±5.3
Tb	0	BDL	-
	1	0.92±0.07	92.0±7.6
	2	1.88±0.11	94.0±5.8
	5	4.79±0.27	95.8±5.6
Te	0	0.51±0.02	-
	1	1.48±0.15	97.0±8.1
	2	2.41±0.13	95.0±6.3
	5	5.39±0.29	97.6±6.5
Tm	0	BDL	-
	1	0.91±0.09	91.0±9.9
	2	1.85±0.16	92.5±8.0
	5	4.80±0.42	96.0±8.6
V	0	0.10±0.005	-
	1	1.08±0.05	98.0±6.8
	2	2.06±0.11	98.0±7.2
	5	5.01±0.25	98.2±6.9
Y	0	0.25±0.02	-
	1	1.22±0.07	97.0±9.5
	2	2.21±0.12	98.0±9.5

	5	5.21±0.31	99.2±9.9
Yb	0	BDL	-
	1	0.95±0.09	95.0±9.4
	2	1.88±0.15	94.0±7.5
	5	4.92±0.48	98.4±9.6

5.3.7 Study of Isobaric Interferences

The details of elements forming oxides, hydroxides, and doubly charged species which can cause interference are given in literature [300-302]. Spectroscopic interferences of the analytes in the present studies is given in Table 5.3. A discussion for correction of such kind of interferences can be found in [303, 304]. In the reports the metal oxide to metal ratios, and ratio of doubly charged to singly charged species, have determined. Based on these procedures the ratios of metal oxide to metal (MO^+/M^+), double charged to singly charged (M^{++}/M^+), were determined for the interfering elements. For this 10-100 $\mu\text{g L}^{-1}$ of each element were independently analyzed by ICP-MS and the signal intensities of M^+ , M^{++} , MO^+ and MOH^+ were determined. These signal intensities were used to determined the ratio as given in Figure 5.6. The ratios were used for correction for spectroscopic interferences. The mathematical equations were defined for correction, for example, the signal intensity at mass 114 is given as:

$$I(m/z\ 114) = I(^{114}\text{Cd}) + I(^{114}\text{Sn}) + I(^{98}\text{Mo}^{16}\text{O}) \quad (1)$$

Rearranging terms we have

$$I(^{114}\text{Cd}) = I(m/z\ 114) - I(^{114}\text{Sn}) - I(^{98}\text{Mo}^{16}\text{O}) \quad (2)$$

To figure out the contribution of ^{114}Sn to the signal at m/z 114, we take into account the natural abundance of both ^{114}Sn and ^{118}Sn and the signal intensity of ^{118}Sn :

$$I(^{114}\text{Sn}) = [A(^{114}\text{Sn})/A(^{118}\text{Sn})] \times I(^{118}\text{Sn}) \quad (3)$$

where A is the abundance. Substituting the abundance values we have

$$I(^{114}\text{Sn}) = [0.65/24.23] \times I(^{118}\text{Sn}) \quad (4)$$

$$\text{or } I(^{114}\text{Sn}) = 0.0268 \times I(^{118}\text{Sn}) \quad (5)$$

Similarly the contribution of $^{98}\text{Mo}^{16}\text{O}^+$ was calculated as:

$$I(^{98}\text{Mo}^{16}\text{O}) = [^{98}\text{Mo}^{16}\text{O}/^{98}\text{Mo}] \times I(^{98}\text{Mo}) \quad (6)$$

$$\text{or } I(^{98}\text{Mo}^{16}\text{O}) = 0.0019 \times I(^{98}\text{Mo}) \quad (7)$$

Putting the values of ^{114}Sn and $^{98}\text{Mo}^{16}\text{O}$ we get

$$I(^{114}\text{Cd}) = I(m/z \text{ 114}) - 0.0268 \times I(^{118}\text{Sn}) - 0.0019 \times I(^{98}\text{Mo}) \quad (8)$$

Similarly mathematical equations for other elements was defined and corrections were incorporated.

Table: 5.3: Spectroscopic interference of the analytes due to isobaric, doubly charged and oxide species.

Elements	Monitored mass (abundance)	Spectroscopic Interference	
		Isobaric	Polyatomic
Al	27(100)	--	--
Ba	138(71.9)	$^{138}\text{Ce}(0.25)$, $^{138}\text{La}(0.09)$	--
Bi	209(100)	--	--
Cd	114(28.9)	$^{114}\text{Sn}^+(0.65)$	$^{98}\text{Mo}^{16}\text{O}$
Ce	140(88.48)	--	$^{124}\text{Sn}^{16}\text{O}$

Co	59(100)	--	$^{43}\text{Ca}^{16}\text{O}$
Cr	52(83.79)	--	--
Cu	63(69.1)	--	$^{47}\text{Ti}^{16}\text{O}$
Dy	164(28.2)	$^{164}\text{Er}^+(1.56)$	$^{148}\text{Nd}^{16}\text{O}$
Eu	153(52.2)	--	$^{137}\text{Ba}^{16}\text{O}$
Er	166(33.4)	--	$^{150}\text{Nd}^{16}\text{O}, ^{150}\text{Sm}^{16}\text{O}$
Ga	69(60.2)	$^{138}\text{Ba}^{++}$	$^{53}\text{Cr}^{16}\text{O}$
Gd	158(24.5)	$^{158}\text{Dy}^+(0.09)$	$^{142}\text{Ce}^{16}\text{O}, ^{142}\text{Nd}^{16}\text{O}$
Ir	193(61.5)	--	$^{177}\text{Hf}^{16}\text{O}$
Ho	165(100)	--	--
La	139(99.91)	--	$^{123}\text{Sb}^{16}\text{O}$
Lu	175(97.4)	--	$^{159}\text{Tb}^{16}\text{O}$
Mg	24(78.8)	$^{48}\text{Ca}^{++}$	--
Mn	55(100)	--	--
Nd	146(17.19)	--	--
Pb	208(52.40)	--	--
Pr	141(100)	--	$^{125}\text{Te}^{16}\text{O}$
Pt	195(33.80)	--	$^{179}\text{Hf}^{16}\text{O}$
Rh	103(100)	--	$^{87}\text{Sr}^{16}\text{O}, ^{86}\text{Sr}^{16}\text{OH}$
Rb	85(72.2)	$^{170}\text{Er}^{++}, ^{170}\text{Yb}^{++}$	--
Ru	102(31.6)	$^{102}\text{Pd}^+(0.96)$	$^{86}\text{Sr}^{16}\text{O}$
Sc	45(100)	$^{90}\text{Zr}^{++}$	--
Sm	152(26.6)	$^{152}\text{Gd}^+(0.21)$	$^{136}\text{Ba}^{16}\text{O}, ^{136}\text{Ce}^{16}\text{O}$
Sr	88(82.5)	$^{176}\text{Lu}^{++}$	--
Tb	159(100)	--	$^{143}\text{Nd}^{16}\text{O}$

Te	130(33.80)	$^{130}\text{Xe}()$	$^{114}\text{Sn}^{16}\text{O}, ^{114}\text{Cd}^{16}\text{O}$
Tm	169(100)	--	$^{153}\text{Eu}^{16}\text{O}$
V	51(99.75)	--	--
Y	89(100)	--	$^{73}\text{Ge}^{16}\text{O}$
Yb	174(31.8)	$^{174}\text{Hf}^+(0.18)$	--
Zn	64(48.9)	$^{64}\text{Ni}^+(1.16)$	$^{48}\text{Ca}^{16}\text{O}, ^{48}\text{Ti}^{16}\text{O}$

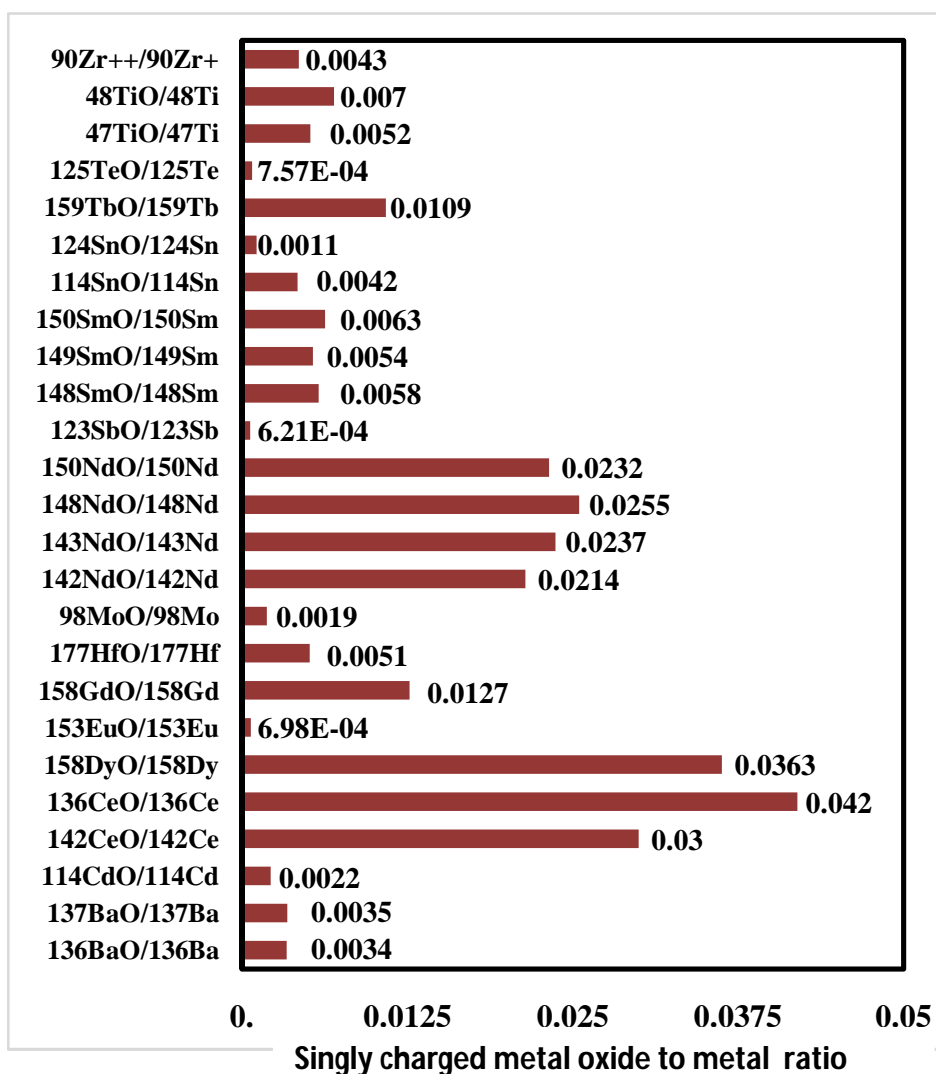


Fig. 5.6: Experimentally determined MO^+/M^+ ratios and $\text{Zr}^{++}/\text{Zr}^+$ ratio by ICPMS at optimized conditions

5.3.8 Detection Limit

Both the instrument detection limits (IDLs) and the method detection limits (MDLs) were determined for the analytes of interest as per the reported procedure [305]. The IDLs were obtained by analyzing the elements in 1% (v/v) pure HNO₃ solution for all these elements. For MDL determination, the discussed separation procedure was followed exactly in the absence of the sample, and the solutions were analyzed by ICP-MS. The IDLs and MDLs are tabulated in Table 5.4.

Table 5.4: Instrument Detection Limit (IDL) and Method Detection Limit (MDL) (N=10)

Elements	IDL ($\mu\text{g L}^{-1}$)	MDL ($\mu\text{g kg}^{-1}$)
Al	0.2	22.0
Ba	0.7	4.1
Bi	1.1	2.3
Cd	0.7	2.2
Ce	0.01	1.4
Co	0.02	2.4
Cr	0.10	1.5
Cs	0.12	5.1
Cu	0.15	11.5
Dy	0.01	4.3
Eu	0.01	1.0
Er	0.05	1.1
Ga	0.26	0.5
Gd	0.01	0.5
Ir	0.01	2.8

Ho	0.05	8.7
La	0.02	0.9
Lu	0.02	0.7
Mg	0.10	25.0
Mn	0.03	6.7
Nd	0.01	1.9
Ni	0.02	17.8
Pb	0.03	3.8
Pr	0.01	0.7
Pt	0.02	1.9
Rb	0.05	1.4
Rh	0.05	1.0
Ru	0.03	1.2
Sc	0.03	14.9
Sm	0.01	1.5
Tb	0.01	0.9
Te	0.3	6.3
Tm	0.02	0.9
V	0.03	7.5
Y	0.05	1.7
Yb	0.03	1.3

5.3.9 Validation of Separation Procedure by γ -Spectrometry Using $^{152+154}\text{Eu}$ Tracer

Recovery study by γ -Spectrometry is unique technique to validate any proposed separation procedure as it does not require any blank correction on the spiked amount. To

validate the recovery of rare earth elements, $^{152+154}\text{Eu}$ tracer was used. The tracer was mixed with natural europium solution in such a manner that concentration of Eu in stock solution becomes $1\mu\text{g mL}^{-1}$. 1.0 mL of the stock solution was taken as reference and 1.0 ml mixed with U-Zr alloy (100mg) after dissolution. The U and Zr matrix was separated by the optimized solvent extraction procedure and the activity of tracer retained in the aqueous phase was determined by measuring 344 keV gamma energy in a NaI (TI) detector. The recovery of tracer was calculated with respect to the reference. The results of the recovery studies are listed in Table 5.5.

Table 5.5 Result of Recovery Studies by γ -Spectrometry (N=10, 60 s Counting)

Sr. No.	Recovery of Eu (%)
Sample-1	98±1
Sample-2	97±1
Sample-3	98±1

5.3.10 Analysis of Real Samples

Analysis of real U-Zr alloy samples of different lots was carried out following the methodology described above. The flow diagram for the final optimized procedure is given in Figure 5.5 and the results are listed in Table 5.6.

5.4 Conclusion

A method, based on solvent extraction of major matrix followed by determination of impurity concentrations using ICP-MS, has been standardized for analysis of trace level impurities in U-Zr. The solvent extraction method is fast and effective for separation of

trace elements from the U-Zr matrix. It is found that thirty six elements can be quantitatively separated from the matrix. The methodology herein proposed led to low detection limit for quantification of trace and ultra-trace elements for U-Zr alloy (1.0-25.0 $\mu\text{g L}^{-1}$). The recovery of trace elements in spiked solution is quantitative (91-102.4%). This method could be used to analyze U-Zr alloy nuclear fuel samples for 36 elements, namely, Al, Ba, Bi, Cd, Ce, Co, Cr, Cu, Dy, Eu, Er, Ga, Gd, Ir, La, Lu, Mg, Mn, Nd, Ni, Nb, Pb, Pr, Pt, Rb, Rh, Ru, Sc, Sm, Sr, Tb, Te, Tm, V, Y, and Yb, with good accuracy and precision.

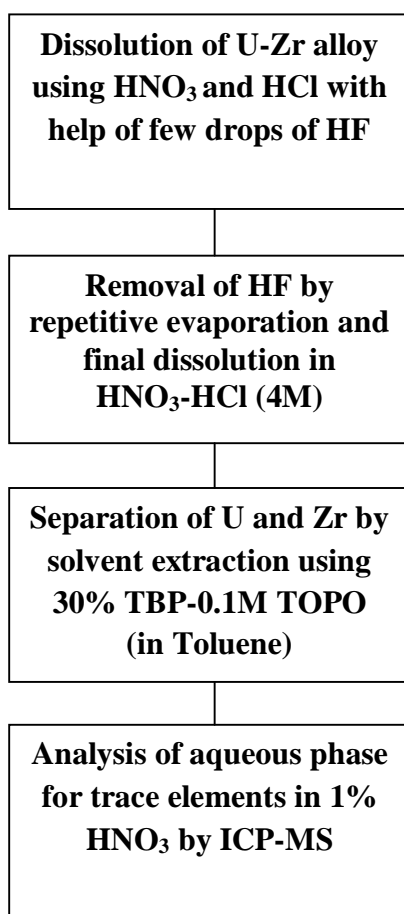


Fig. 5.7: Systematic diagram for analysis of U-Zr alloy

Table 5.6: Trace Element Concentration in the U-Zr Samples of different Lots (in $\mu\text{g g}^{-1}$)

Elements	Sample I	Sample II	Sample III
Al	960 \pm 70	1370 \pm 105	650 \pm 45
Ba	2.81 \pm 1.5	1.77 \pm 0.15	1.32 \pm 0.11
Bi	1.43 \pm 0.10	0.29 \pm 0.02	0.22 \pm 0.02
Cd	0.63 \pm 0.60	0.28 \pm 0.02	0.25 \pm 0.02
Ce	1.24 \pm 0.11	1.36 \pm 0.11	0.63 \pm 0.06
Co	20.72 \pm 1.84	19.47 \pm 1.55	0.49 \pm 0.05
Cr	3000 \pm 150	1100 \pm 65	64.0 \pm 4.5
Cs	20.0 \pm 0.9	15.5 \pm 1.0	5.0 \pm 0.2
Cu	85.16 \pm 7.5	272.74 \pm 25.5	20.86 \pm 2.05
Dy	4.65 \pm 0.41	3.04 \pm 0.30	3.92 \pm 0.31
Eu	BDL*	BDL	BDL
Er	2.44 \pm 0.22	2.31 \pm 0.21	2.05 \pm 0.20
Ga	6.81 \pm 0.55	7.37 \pm 0.72	0.83 \pm 0.08
Gd	0.52 \pm 0.05	0.07 \pm 0.007	BDL
Ir	0.61 \pm 0.06	0.25 \pm 0.02	0.26 \pm 0.02
Ho	3.86 \pm 0.25	3.48 \pm 0.31	2.94 \pm 0.25
La	0.39 \pm 0.04	0.31 \pm 0.03	0.05 \pm 0.005
Lu	BDL	BDL	BDL
Mg	30.58 \pm 2.91	38.15 \pm 3.51	37.83 \pm 3.33
Mn	301.28 \pm 25.5	57.71 \pm 4.89	8.82 \pm 0.75
Nd	0.47 \pm 0.04	0.63 \pm 0.06	0.06 \pm 0.006
Ni	1732 \pm 200	4389 \pm 450	95.5.0 \pm 4.8
Pb	3.15 \pm 0.25	2.55 \pm 0.21	4.37 \pm 0.41

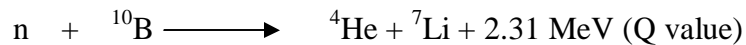
Pr	0.13±0.01	BDL	BDL
Pt	0.03±0.003	BDL	BDL
Rb	0.78±0.07	0.23±0.02	BDL
Rh	0.43±0.04	0.04±0.004	0.01±0.001
Ru	0.66±0.06	0.21±0.02	0.15±0.01
Sc	44.96±4.5	26.44±2.11	18.26±1.55
Sm	0.02±0.002	BDL	BDL
Tb	0.03±0.002	BDL	BDL
Te	3.68±0.31	1.72±0.15	1.51±0.11
Tm	0.09±0.009	BDL	BDL
V	309.12±30.11	383.6±35.55	29.82±2.65
Y	2.03±0.021	121.19±10.51	11.41±1.12
Yb	0.45±0.04	0.13±0.01	BDL

Chapter 6

Chemical Characterization of Dysprosium Titanate (Dy_2TiO_5)

6.1 Introduction

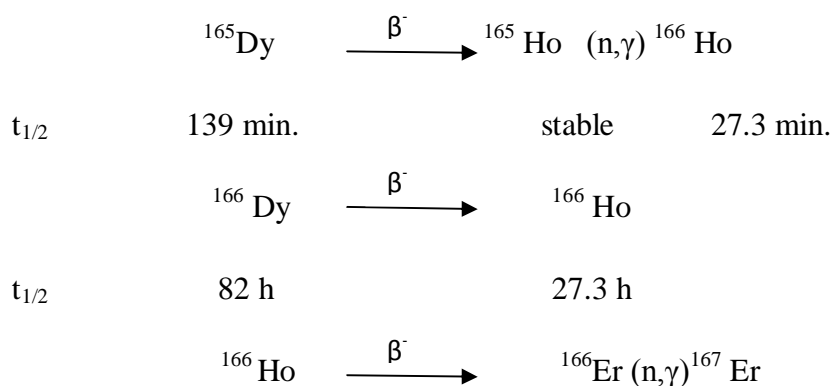
Control rods are used in nuclear reactors to control the fission rate. Boron based control rods are used in several reactors but these control rods are associated with problems like helium formation and swelling of clad material [101, 306]. In addition, formation of tritium is possible in case of fast neutrons which impose additional challenges in nuclear waste management [307]. Significant work has been carried out to explore neutron absorbing materials which do not swell [32] and produce non-radioactive final isotopes. Dysprosium is a strong neutron absorber, and is used as burnable poison in nuclear reactors [308]. The post-irradiation examination demonstrated that lanthanoid oxides ($\text{Ln}_2\text{O}_3 \cdot \text{MO}_2$) with the fluorite structure have the best radiation damage resistance. Dysprosium titanate ($\text{Dy}_2\text{O}_3 \cdot \text{TiO}_2$) is used in control rods of VVER reactors [309]. In addition to lower swelling the matrix has advantages of high melting point ($\sim 1870^\circ\text{C}$), resistance to cladding materials, and ease of fabrication and produces non-radioactive end. The life time of dysprosium titanate is longer than other control rods due to comparable absorption cross section of all the isotopes of Dy. The decay scheme of irradiated boron and dysprosium is given in Figure 1. Dysprosium titanate is fabricated by solid reaction route, using Dy_2O_3 , TiO_2 and Mo oxide. Once fabricated, like other nuclear materials, its chemical quality control is crucial. It is important to certify the major matrix (Dy, Ti and Mo) and the trace level impurities to ensure the desired performance of the material. The nuclear reactions of boron and dysprosium is given below:



Abundance 19.9%

σ 3840 b

	^{160}Dy (n, γ)	^{161}Dy (n, γ)	^{162}Dy (n, γ)	^{163}Dy (n, γ)	^{164}Dy (n, γ)	^{165}Dy (n, γ)	^{166}Dy
Abundance(%)	2.3	18.9	25.5	25.0	28.0	-	-
σ (b)	130	680	240	220	2780	2100	-



173 b

Analysis of any material involves two important steps, namely (i) dissolution and (ii) analysis. However for complex matrices, separation of different constituents is also crucial. The literature reports on Dy_2TiO_5 , viz. its dissolution, separation and determination of matrix composition including trace impurities are scarcely available. The only literature report [310] on its characterization by ICP-MS after dissolution has been as a part of calorimetric studies. However the details of dissolution and matrix separation methods adopted were not reported. Further it is not advisable to use ICP-MS for major matrix determination as it is associated with large RSD.

For quantification of percent level matrix constituents it is important to use a method with high precision. For instance, percentage level of U and Pu are determined using coulometric technique (RSD <0.2%) [311, 312]. Gravimetric method is known for precise quantification of major constituents in a matrix [313]. However application of these or

similar methods becomes difficult for complex matrices such as Dy_2TiO_5 (doped with percent level of Mo), specially owing to (i) difficulty in matrix dissolution and (ii) challenges in separation of the major matrix elements from each other.

In classical methods for dissolution acids and their combinations are used for difficult to dissolve matrices. However considering the complexity of the studied refractory matrix, simple acid dissolution procedures are not adequate. It is important to explore and optimize advanced dissolution procedures such as Microwave dissolution, which has been reported for dissolution of refractory matrices [314, 315]. In the present work a detailed study was carried out to optimize the combination of reagents and operating parameters of microwave for the quantitative dissolution of the Mo doped Dy_2TiO_5 .

For the determination of the major constituents, in Mo doped Dy_2TiO_5 , separation of Mo, Dy and Ti from each other is very crucial. Further the determination of trace constituents would require the separation of matrix from the trace elements. Solvent extraction procedures have been reported for the separation of Dy [316], Mo [317] and Ti [318]. However these procedures involve significant amount of organic solvents and chemicals. In addition, the solvent extraction is tedious and requires additional steps of stripping the analyte into aqueous phase for further analysis [319]. On the other hand precipitation and chromatography have been used for successful separation of matrices, and their combination can reduce the number of steps for preparing samples. In view of this precipitation and chromatography techniques were examined for quantitative of for Dy, Ti and Mo. Gravimetric and spectrophotometric techniques were explored for the final quantification. The developed method was validated by taking appropriate amount of the individual high purity oxides for preparing the synthetic samples.

Developing procedures for the determination of trace impurities in refractory samples is quite challenging. Several types of analytical techniques such as Atomic Absorption Spectroscopy (AAS), Total Reflection X-Ray Fluorescence (TXRF), UV - Visible spectroscopy, Inductively Coupled Plasma Mass Atomic Emission Spectroscopy (ICP-AES), Inductively Coupled Plasma Mass Spectrometry (ICP-MS) [39, 277, 320-322] etc.

are employed for the trace analysis of the nuclear materials. ICP-MS and ICP-AES are advantageous owing to the possibility of multi-elemental analysis, high sensitivity, large linear dynamic range and high sample throughput. In the present work total metallic impurities present in the oxides (Dy_2O_3 and MoO_3 constituents of formed from Dy_2TiO_5) were estimated by ICP-MS to assure the purity of these oxides.

6.2 Experimental

6.2.1 Instrumentation

Microwave-3000 dissolution system (Anton Paar) was used for dissolution of Dy_2TiO_5 . UV-Visible-NIR double beam Spectrophotometer (JASCO V-670) was used to record the absorption spectra. Muffel furnace (META LAB Scientific) was used to heat the precipitate and convert it into oxide form. An analytical balance (A&D Company) was used to record the weights, and ICP-TOF-MS (8000R, GBC Australia) was used to determine trace elements concentration in precipitates. The operating parameters of ICP-MS had been reported elsewhere [304].

6.2.2 Chemicals

Bio-Rad AG[®] 1X4, chloride form, 200-400 mesh (Bio-Rad) was used for the ion exchange separation studies. Supra-pure H_2SO_4 , HNO_3 and HCl (Merck), were used for sample preparation. De-ionized water having resistivity $18\text{M}\Omega\cdot\text{cm}$ (Milli-Q[™] system, Millipore) was used for sample preparation and dilution. The ICP standards of 1000 mg L^{-1} (BDH) were diluted appropriately to prepare standards for titanium and trace elements standard solutions.

6.2.3 Microwave Dissolution of Dysprosium-titanate

The dissolution of Dy_2TiO_5 by conventional methods using different acids and their combination was found to be unsuccessful due to the highly refractory nature of the matrix. Fusion with KHSO_4 was also attempted but the resulting compound was found to

be insoluble in acids. Finally the Microwave route was used for dissolution. The combination of acids and instrumental parameters were varied systematically. A combination of H₂SO₄ and HCl was found to achieve complete dissolution when the acids were in 3:2 ratios by volume. For the dissolution the instrument parameters played the most important role. The optimized conditions of microwave are given in Table 6.1.

Table 6.1: Microwave operating conditions

Power(W)	Ramp(min.)	Hold(min.)
400	20	20
500	10	20
300	20	20
0	10	10

6.2.4 Synthetic Sample Preparation

In order to study the separation and analytical procedures in detail, standard solutions were prepared using high purity dysprosium oxide, molybdenum oxide and titanium metal. The Dy, Ti and Mo in solution forms were mixed together in such a way that the 1.0 mL of this solution contains 68.0 mg of Dy, 11.8 mg of Ti, and 1.8 mg Mo. Three aliquots of this solution in triplicates containing 0.5, 1.0, and 2.0 mL were labeled as SDT-1, SDT-2, and SDT-3 respectively for recovery study of Mo, Dy and Ti.

6.2.5 Separation of Mo from Dy and Ti

Approximately 2.0 gram anionic resin, AG 1X4 (capacity 1.2 meq/ml resin bed) was mixed with de-ionized water to make a slurry. It was filled in the column (OD-4.0 cm, ID-3.9 cm, and hight-20.0 cm) to give a resin height of approximately 10 cm. To ensure a

uniform resin bed, about 15 mL of water was placed in the column, and resin was drawn from the column into the weight-burette and then released. The resin was allowed to settle in the column. This helped to remove any air bubbles formed when loading the column, and allowed the resin beads to settle uniformly in the column. The resin bed was conditioned by adding 30 mL 4 M HCl. Glass wool was placed at the top of the resin bed to prevent the resin from being disturbed during the addition of reagents. The average flow rate measured was 1.0 mL/min. Mo could be separated from a mixture of Dy and Mo using this anion column in 4M HCl.

6.2.6 Precipitation of Molybdenum

The retained Mo was eluted with 1M HNO₃ from the column and precipitated with 2% α -benzoin oxime in alcohol. Precipitate was filtered using whatmann-542 filter paper and converted to oxide after heating at 600°C for 3 hours.

6.2.7 Precipitation of Dy

The eluted solution from the column (in 4M HCl) was diluted (~ 1M HCl) using milli Q water. Titanium and dysprosium were separated by precipitation of Dy (along with other rare earths) with excess amount of 10% oxalic acid. Precipitate was filtered with whatmann-542 filter paper and converted into oxide after heating at 850°C for 3 hours. The filtrate containing titanium was preserved for Ti estimation.

6.2.8 Measurement of Absorbance for Titanium complex

The filtrate was diluted using milli Q water to known volume. Three aliquots of this solution were completely evaporated to dryness and re-dissolved in 2.5N H₂SO₄ and 3% H₂O₂ solution. The titanium formed a yellow color complex having absorbance at 410 nm. The absorbance of the samples and standards were recorded and amount of titanium was calculated using calibration plot.

6.3 Result and Discussion

6.3.1 ICP MS measurement of Dy, Ti and Mo

ICP-MS is widely used for trace and ultra trace measurements, while in some reports it has been used for major element also. Therefore, first of all, ICP-MS was employed for analysis of major elements Dy, Ti and Mo in synthetic dysprosium-titane samples. After appropriate dilution the synthetic samples were analyzed by ICP-MS and the data has been given in the Table 6.2. It was found that the precision and accuracy was not good by ICP-MS analysis. Which could be due to matrix effect and atmospheric plasma, Other drawback of ICP-MS is memory effect, if high concentration of these elements are used. Therefore, in the present work major elements have determined by either the conventional method or the techniques that provide high precision.

Table 6.2: Determination of major elements using ICP-MS in the synthetic samples

Sample Code	Dy Expected (mg)	Dy Found (mg)	Mo Expected (mg)	Mo Found (mg)	Ti Expected (mg)	Ti Found (mg)
SDT-1	34	36.0 ±2.5	0.9	0.8 ±0.1	5.9	5.5 ±0.5
SDT-2	68	62.5 ±6.5	1.8	2.0 ± 0.2	11.8	10.5 ±1.0
SDT-3	136	125.6 ±10.0	2.7	2.5 ± 0.2	23.6	20.5 ±2.0

6.3.2 Determination of molybdenum (Mo)

The conventional gravimetric method was developed for precise quantification of major Mo (~1.8%). Determination of Mo was performed using α -Benzoin oxime, which is known for selective precipitation of Mo [323]. The method was validated using the standard solutions of only Mo, Mo with Dy, Mo with Ti, and Mo with Dy and Ti. This study was important to understand the effect of Dy and Ti on the recovery of Mo. It was

found that recovery of Mo was quantitative with only Mo solution (Table 6.3). However, in the presence of Dy the recovery of Mo increases unexpectedly (Table 6.4). Previous report shows that α -benzoin oxime forms complexes with dysprosium [324]. The method was modified and Dy was precipitated with oxalic acid followed by precipitation of Mo with α -benzoin oxime. However Mo was found to be co-precipitated with dysprosium [325]. This study shows that separation of Mo and Dy is essential prior to their estimation.

Table 6.3 Recovery of molybdenum in pure molybdenum solution (N=3)

Sample Code	Expected Mo (in mg)	Found Mo (in mg)	Recovery (%)
M-1	1.0	0.98±0.02	98.0
M-2	2.0	1.95±0.05	97.5
M-3	3.0	2.94±0.08	98.0
M-4	4.0	3.9±0.10	98.0
M-5	5.0	4.95±0.12	99.0

As per our earlier studies, Mo exists as anionic specie in 4M HCl and can be selectively retained on an anion exchange column [304]. On the other hand Dy and Ti do not form anionic species in the similar conditions and can be separated from Mo completely. The results in Table 6.4 show precise and accurate determination of Mo.

Table 6.4: Effect of Dy in the precipitation of Mo (N=3).

Sample Code	Amount of Dy added (mg)	Mo Expected (mg)	Mo Found (mg)		
			Without separation (mg)	After separation	
				Precipitation of Dy followed by Mo estimation	Anion exchange Separation followed by Mo estimation
DM-1	34	0.9	3.6 ± 0.3	ND	0.9±0.02
DM-2	68	1.8	8.3 ± 0.5	<0.1	1.7±0.05
DM-3	136	2.7	12. ± 0.9	<0.2	2.6±0.08

Effect of titanium in the precipitation of molybdenum was also studied. The results in Table 6.5 shows that Mo could be determined in presence of titanium.

Table 6.5: Recovery of Mo in presence of Ti (N=3).

Sample Code	Amount of Ti added (mg)	Mo Expected (mg)	Mo Found (mg)	
			Without separation	After separation
			MT-1	5.9
MT-2	11.8	1.8	1.7±0.05	1.8±0.05
MT-3	23.6	2.7	2.6±0.08	2.6±0.10

6.3.3 Determination of Dysprosium (Dy)

Reports show that carboxylic acids such as oxalic acid, glycolic acid and malic acid are very good complexing reagents for rare earth elements (REEs) and can be used for their quantitative precipitation [326]. Oxalic acid is better complexing agent for rare earths compared to glycolic and malic acid [327, 328]. Therefore, oxalic acid was selected to

precipitate Dy (along with all REEs). For the complete precipitation it was important to use high pH conditions to increase the de-protonated oxalate ($C_2O_4^{2-}$). However the sample pH cannot be increased due to possibility of hydrolysis Dy and Ti. On the other hand, at lower pH (< 2) the predominant form of oxalic acid is $HC_2O_4^-$. Hence, excess amount of oxalic acid was used for quantitative precipitation of REEs at lower pH. The dysprosium was precipitated using excess amount of 10% (w/v) oxalic acid. The effect of Mo and Ti in the recovery of Dy were studied using synthetic solutions. The results in Table 6.6 show that presence of Mo without separation interferes in the Dy recovery while it is not affected in presence of titanium (Table 7).

Table 6.6: Recovery of Dy in presence of Mo (N=3).

Sample Code	Amount of Mo added (mg)	Dy Expected (mg)	Dy Found (mg)	
			Without separation	After separation
DM-1	0.9	34	35.0±0.5	33.5±0.5
DM-2	1.8	68	69.5±1.0	67.5±1.0
DM-3	2.7	136	137.9±2.0	135.5±2.0

Table 6.7: Recovery of Dy in presence of Ti (N=3).

Sample Code	Amount of Ti added (mg)	Dy Expected (mg)	Dy Found (mg)	
			Without separation	After separation
DT-1	5.9	34	33.5±0.5	33.9±0.5
DT-2	11.8	68	67.9±1.0	67.5±1.0
DT-3	23.6	136	135.5±2.0	136.2±2.0

6.3.4 Determination of Titanium (Ti)

Reports show that spectrophotometric methods can be employed for quantitative estimation of titanium using different complexing reagents such as disodium-1,2-

dihydroxybenzen-3,5-disulfonate[329], N-(2-hydroxybenzylidene)-3-oxobutanehydrazide [330], 2,4-dihydroxy acetophenone isonicotinoylhydrazone [331], 2,3-dihydroxynaphthalene [332] and hydrogen peroxide [333]. Most of these reagents are expensive, difficult to obtain and not eco-friendly. Hydrogen peroxide, being nontoxic, cheap and extremely sensitive, was used in the present work.

ICP standard of titanium was diluted to prepare calibration standard for spectrophotometric determination of titanium. The calibration plot was linear with regression coefficient of 0.9997. The synthetic samples of titanium with Mo and Dy, as discussed above, were also analyzed for titanium using this calibration plot. The results in Table 6.8 and Table 6.9 show that titanium could be estimated in the presence of Mo and Dy without separation.

Table 6.8: Recovery of Ti in presence of Mo (N=3).

Sample Code	Amount of Mo added (mg)	Ti Expected (mg)	Ti Found (mg)	
			Without separation	After separation
MT-1	0.9	5.9	5.8±0.1	5.9±0.1
MT-2	1.8	11.8	11.6±0.2	11.5±0.2
MT-3	2.7	23.6	23.2±0.5	23.1±0.5

Table 6.9: Recovery of Ti in presence of Dy (N=3).

Sample Code	Amount of Dy added (mg)	Ti Expected (mg)	Ti Found (mg)	
			Without separation	After separation
DT-1	34	5.9	5.9±0.1	5.8±0.1
DT-2	68	11.8	11.7±0.2	11.9±0.2
DT-3	136	23.6	23.4±0.5	23.1±0.5

6.3.5 Analysis of Synthetic Dysprosium titanate samples

A synthetic sample of dysprosium titanate was used to validate the developed methodology for estimation of matrix elements Dy, Ti and Mo. The molybdenum was separated using anion exchange resin in 4M HCl and determined as discussed above. The Dy and Ti were also estimated as discussed above. The results in Table 6.10 show that the Dy, Ti and Mo could be quantified by the developed method with very good precision and accuracy.

Table 6.10: Estimation of Mo, Dy and Ti by developed method in synthetic samples

(N=3)

Sample Code	Dy Expected (mg)	Dy Found (mg)	Mo Expected (mg)	Mo Found (mg)	Ti Expected (mg)	Ti Found (mg)
SDT-1	34	34.3 ±0.5	0.9	0.9±0.01	5.9	5.8 ±0.1
SDT-2	68	67.8 ±1.2	1.8	1.7±0.04	11.8	11.7 ±0.2
SDT-3	136	135.6 ±1.8	2.7	2.6±0.07	23.6	23.5 ±0.4

6.3.6 Analysis of real Sample:

Several real samples of dysprosium-titanate were dissolved using the microwave method and the major elements Dy, Ti and Mo were estimated using this method. The trace impurities were also estimated in the oxides of Dy and Mo to assure the purity of oxides. The flow sheet is given in Fig. 6.2. Results of three real samples are given in Table 6.11.

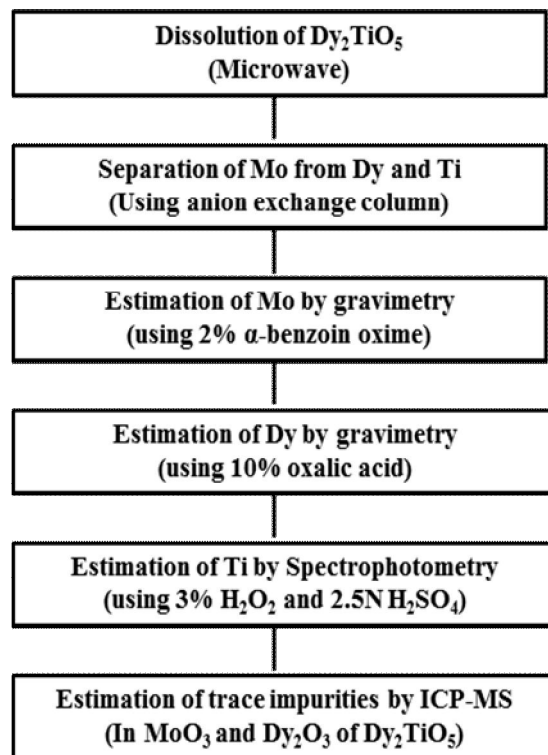


Fig. 6.1: Flow-sheet of separation and estimation of Dy, Ti and Mo in Dy₂TiO₅

Table 6.11: Analysis of real dysprosium titanate samples of different lots

Elements	Amount in (%)		
	Lot 1	Lot 2	Lot 3
Dy	70.1±0.5	69.5±0.8	71.1±1.0
Ti	11.5±0.2	11.8±0.5	11.2±0.5
Mo	1.8±0.1	1.9±0.1	1.7±0.1

6.3.7 Estimation of trace impurities in MoO₃ and Dy₂O₃ by ICP-MS

The purity of oxides formed in the above process was checked by ICP-MS. Known amount of Dy₂O₃ and MoO₃ were dissolved separately and were taken in 1% HNO₃ to estimate trace elements by ICP-MS. The trace impurities in the solution containing major titanium was also analyzed. It was found that most of the elements were present only at ultra trace level (<1µg g⁻¹) and the total impurity was < 10µg g⁻¹ for each lot of the

sample. The amount of trace elements found in both oxides in different lots is given in Table 6.12.

Table 6.12: Estimation of trace impurities in the real samples by ICP-MS

Elements	Impurities in oxides of Dy and Mo ($\mu\text{g g}^{-1}$)					
	Lot 1		Lot 2		Lot 3	
	Dy ₂ O ₃	MoO ₃	Dy ₂ O ₃	MoO ₃	Dy ₂ O ₃	MoO ₃
Al	*BDL	5.4	0.1	4.1	0.2	5.1
As	3.8	BDL	1.2	BDL	1	0.2
Ba	1.9	BDL	1.5	0.1	0.5	0.1
Be	0.7	0.9	0.5	1	0.2	0.1
Cd	0.6	3.3	0.1	0.5	BDL	0.1
Ce	1.3	BDL	1.1	BDL	0.1	BDL
Co	BDL	1.7	BDL	1	0.2	0.5
Cr	12.4	1.4	5.5	0.5	10.5	1.1
Cs	1.1	1.2	0.5	0.6	0.5	0.6
Cu	1	0.5	1.1	0.7	1.3	0.5
Dy	balance	3.5	balance	1.5	balance	2.5
Eu	0.7	BDL	0.1	BDL	1.1	BDL
Fe	12.4	32.4	9.5	15.5	11.5	7.5
Ga	0.5	1.4	0.2	0.1	1.2	0.1
Gd	2.8	0.1	1.5	BDL	1.5	BDL
Ge	BDL	BDL	BDL	0.1	BDL	BDL
Hf	1.5	3.3	0.5	1.1	1	3.9
Hg	1.2	0.2	0.1	BDL	0.2	BDL
Ho	1.2	BDL	0.1	BDL	0.5	BDL
La	1.7	BDL	0.2	0.1	0.2	BDL
Li	BDL	2.6	0.5	3.1	1	10.5
Lu	1.8	BDL	0.2	0.2	1.1	BDL

Mg	4.5	0.9	2.5	0.5	5.6	1.1
Mn	BDL	1.4	BDL	1.2	0.1	2.5
Mo	3.5	balance	2.1	balance	4.1	balance
Nb	19.2	5.4	10.5	3.1	9.5	1
Nd	1.8	BDL	0.1	BDL	1.5	BDL
Ni	BDL	BDL	BDL	BDL	0.5	BDL
Os	BDL	2.6	BDL	1.1	BDL	BDL
Pd	18.5	1.9	5.5	1.2	4.3	<LOD
Pr	2.3	BDL	0.5	BDL	1.5	BDL
Pt	BDL	1.6	BDL	0.5	BDL	BDL
Re	BDL	1.9	BDL	0.1	BDL	0.5
Rh	0.6	1	0.1	0.5	0.5	0.8
Ru	3.4	0.9	1.5	0.2	2.5	1
Sb	4.5	0.3	2.4	0.1	3	0.6
Sc	BDL	BDL	0.1	BDL	BDL	BDL
Sm	2.9	BDL	0.5	BDL	1.5	BDL
Sn	BDL	22.8	BDL	14.5	BDL	12.5
Sr	1.9	1.2	1.1	1	1.1	0.4
Ta	BDL	19.6	0.1	11.5	BDL	7.5
Tb	105.2	1.5	50.5	0.1	25.1	BDL
Ti	0.2	1.1	1	1	0.2	1.5
Tl	16.3	BDL	5.6	0.1	4.6	0.5
Tm	BDL	BDL	0.1	BDL	1	BDL
V	5.5	1.2	3	1.5	3.5	1
W	BDL	10.3	BDL	5.1	BDL	7.5
Y	2.8	1.1	2.1	1.1	3.5	1.4
Yb	2.1	BDL	0.5	BDL	2.1	BDL
Zn	26.6	14.1	20.5	9.5	20.5	8.6
Zr	4.9	1.3	5	1.1	4.5	1.3

Total impurities	273.3	150	139.8	85.2	134.5	82.5
------------------	-------	-----	-------	------	-------	------

*BDL is below detection of the ICP-MS.

(Percentage relative standard deviation (%RSD) for all elements analyzed by ICP-MS was <10)

6.4 Conclusion

A methods has been developed for determination of major constituents of Dy₂TiO₅ following microwave dissolution of the refractory matrix and followed by gravimetry for Dy and Mo and spectrophotometry for Ti. The microwave assisted dissolution of dysprosium titanate is fast and requires small amount of acids. The gravimetric method is an absolute method (standard and calibration not required) with high precision (<2% RSD). In this work Dy and Mo has been determined by this method. After separation the recovery of molybdenum was within 98.0-99.9% with precision 1.0-2.0 (%RSD). The presence of titanium does not affect the recovery of molybdenum and dysprosium. The recovery of dysprosium and titanium were 99.7-100.8% and 98.3-99.9% respectively. Percentage relative standard deviation (%RSD) for dysprosium and titanium were <2%. The total impurities in the oxides of Dy and Mo were estimated below 0.05% using ICP-MS. The three real dysprosium titanate samples were analyzed following this method. The percentage of Dy, Ti and Mo estimated in the real samples were much close to the expected values. The developed method is simple, precise and accurate.

Chapter 7

Chemical Characterization of aluminum oxide (Al_2O_3)

7.1 Introduction

Alumina (Al_2O_3) is an exceptionally important ceramic material which has many technological applications [334-338]. It has several special properties like high melting point, chemical inertness, electrical and thermal properties [339-343]. Alumina occurs in nature as the minerals corundum, diaspore, gibbsite and bauxite. Production of alumina from these minerals has been discussed in [344-346]. The precious stones ruby and sapphire are composed of corundum with small amounts of impurities which give colors. $\alpha\text{-Al}_2\text{O}_3$ is one of the promising insulating ceramic materials for International Thermonuclear Experimental Reactor (ITER) and commercial reactors, owing to its high electrical resistance [105, 347]. The presence of impurities in the alumina changes its properties drastically [348-350]. The rare earth impurities have been studied for grain boundary strengthening in alumina [351].

More than 90% alumina produced worldwide is utilized in the production of aluminum [352]. Aluminum, with its low thermal neutron absorption, high radiation stability, low cost, and good corrosion resistance to air and water in addition to the short half life of its activation product ^{28}Al ($t_{1/2} = 2.24$ min) is ideally suited for use in research and test reactors [353]. Aluminum alloys have been used in fission reactors where the temperature is limited to below 200°C [106]. The chemical compositions of aluminum alloys and their applications have discussed in [107-109]. Various uses of aluminum in nuclear reactors

have been discussed in IAEA report [354]. Aluminum is also used as dispersed phase for uranium-aluminates /uranium-silicide nuclear fuels in research reactors [355].

γ -Alumina is one of the most common crystalline materials used as adsorbents and catalysts or as their support . Industrial applications in many separation and reaction processes require the use of γ -alumina in the granular form. Alumina is used in cosmetic and personal care products as an abrasive , anti-caking agent, anti-bulking agent and as an adsorbent [356, 357] . Aluminum salts are incorporated into some vaccine formulations as an adjuvant to enhance the immune response in the vaccinated individual [358]. Alumina has been approved by the FDA for use in medical devices. The alumina used in these devices must comply with ASTM F603-12 (standard specification for high-purity dense aluminum oxide for medical application) [359]. The use of ceramic femoral heads made up of an alumina/ceramic composite have been approved for use in hip joint replacement in humans. A typical replacement product is reported to be composed of ~75% alumina, ~25% zirconia, and < 1% chromium oxide [360]. Aluminum is poorly absorbed through either oral or inhalation routes and is essentially not absorbed dermally in healthy humans [361].

Chemical purity of nuclear grade aluminum, aluminum alloys and alumina is very important to ensure the desired behavior during reactor operation. The impurities present in nuclear grade aluminum, which form activation product on irradiation during reactor operation have been discussed in [362]. The elements having large neutron absorption cross section such as B , Cd and rare earth elements, have very stringent specifications in nuclear materials [275, 322]. The effect of trace impurities in aluminium matrices have

been reported [363-366]. Hence, it is essential to have precise and accurate knowledge of their concentrations in the aluminum matrices. Determination of trace impurities in aluminum matrix has been reported using several analytical techniques, such as, neutron activation analysis,(NAA) , charged particle activation analysis (CPAA), graphite furnace atomic absorption spectrometry (GFAAS) laser-induced breakdown spectroscopy (LIBS), inductively coupled plasma atomic emission spectroscopy (ICP-AES) and inductively coupled plasma mass spectrometry (ICP-MS) [367-373]. Each technique has its advantages and disadvantages. However, the sensitivity and the matrix interference are the two key elements in determination of trace impurities. In most of the reports, where trace impurities has been determined the dissolution of alumina and matrix separation have not been discussed. The rare earth elements have large neutron absorption cross section for thermal neutron [374] but their quantification is not reported in these reports.

Dissolution of refractory materials by conventional method and fusion method requires large amount of reagent which increase the total dissolved solid and hence solution could not be directly analyzed by ICP-MS. These dissolution methods are very tedious and time consuming. Fusion with alkali salts is used to decompose samples containing refractory oxides which are resistant to acids [375]. The main disadvantage of fusion method is the high level of total dissolved solid (TDS) in solutions. High content of solid decreases the sensitivity of ICP-MS resulting in poor detection limits and hence need frequent cleaning of cones, nebulizer, and spray chamber. It is generally accepted that to achieve good stability, the total dissolved solid (TDS) in the samples should not exceed 0.2% w/v, which can be a severe limitation if analytes concentration is extremely low. High

dilutions are required with fusion prior to analysis, which also results in deteriorations in detection limits.

In the present work microwave dissolution method has developed for quantitative dissolution of alumina. The advantage of microwave dissolution are, it is fast, require only small amount of acids, and no loss of volatile impurities [376, 377]. ICP-MS technique has been used for quantification of trace impurities in Al_2O_3 due to its low detection limit, low spectroscopic interference, high sample throughput, high sensitivity, and multi-element capability. However, analysis of trace and ultra trace elements with high concentration of matrix elements leads to matrix effect. The sample solutions having high total dissolved solid (TDS) choke the capillary of nebulizer, and holes of sampler and skimmer, which introduce significant systematic and random error in the measurements. Further, long washing time is required to remove the memory effect from the matrix elements. Therefore, in this work, a method has been developed to separate the matrix (Al) from the trace amount of rare earth elements prior to analysis by ICP-MS.

7.2 Experimental

7.2.1 Instrumentations

An Inductively Coupled Plasma - orthogonal acceleration- Time of Flight Mass Spectrometer (ICP-*oa*-TOF-MS), Model Optimass 8000R (GBC, Australia) was employed for quantification of trace and ultra trace elements in U-Zr alloy. The operational conditions of the equipment were optimized using a tuning solution (Li, Al, V, Sr, In, Cs, and Bi 5ng ml^{-1}). Details of the instrumental operating parameters are given in Table 7.1. Microwave-3000 dissolution system (Anton Paar) was used to dissolve the

sample. Details of microwave have discussed in chapter 2. Eppendorf[®] micropipettes, Nalgene[®] PP measuring flask, and separating funnels, and Teflon[®] PFA beakers were used throughout the experiment.

Table 7.1: Optimized operating conditions of ICP-MS

ICP-MS parameters	Values
RF power	1200 W
Frequency	27.2 MHz
Plasma gas flow rate	10.0 L min ⁻¹
Auxiliary gas flow rate	0.50 L min ⁻¹
Nebulizer gas flow rate	0.75 L min ⁻¹
Sample uptake rate	0.6 mL min ⁻¹
Measurement mode	Dual (PC/analog)
Acquisition time	5 s

7.2.2 Reagents and Solutions

Supra-pure H₂SO₄, HNO₃ and HCl (Merck) were used for sample preparation. Sodium hydroxide (AR grade, SRL). De-ionized water having resistivity 18MΩ.cm (Milli-Q[™] system, Millipore) was used for dilution. The ICP standards of 1000 mg L⁻¹ (BDH) were diluted appropriately to prepare multi-element standard solutions.

7.2.3 Microwave dissolution of Alumina

Known amount (100-250 mg in each Teflon pressure tube) of the samples were dissolved using 5.0 mL milli Q water, 2.0 mL hydrochloric acid and 3.0 mL sulfuric acid. The optimized operating condition for microwave is given in Table 7.2.

Table 7.2: Microwave operating conditions

Power(W)	Ramp(min.)	Hold(min.)
400	20	20
500	10	20
300	20	20
0	10	10

7.2.4 Dissolution of Aluminium metal

In the case of aluminium metal powder and chips dissolution has performed using conventional dissolution method (hot plate). To weighted amount of samples, 5.0 mL milli Q, 1.0 mL HCl and 1.0 mL HNO₃ was added. The concentrated sulfuric acid (1.0 mL H₂SO₄) was added drop wise to accelerate the reaction rate. The samples were dissolved within 5.0 minutes (~ 200 mg samples).

7.2.5 Separation of Trace elements

The dissolved alumina and aluminium samples were treated with 30% sodium hydroxide solution where almost all metals got hydrolyzed (or precipitated). In presence of excess amount of sodium hydroxide solution aluminium forms soluble sodium-aluminate while the traces of REE impurities could be separated using Whatman-542 filter paper The

precipitates were dissolved in conc. HCl, evaporated and finally taken in 1% HNO₃ for ICP-MS analysis.

7.2.6 Gamma spectrometry study using ¹⁵²⁺¹⁵⁴Eu as tracer

The separation method was validated using tracer, ¹⁵²⁺¹⁵⁴Eu. The separation method was repeated in the presence of tracer and activity was determined using NaI(Tl) based gamma spectrometry.

7.3 Result and discussion

7.3.1 Matrix dissolution and Separation

Microwave dissolution offers a very convenient method to dissolve the refractory oxides. The reported method was followed for dissolution of alumina granules, but was not successful. Therefore, it was modified and optimized for acids combinations and microwave operating parameters. The alumina granules were completely dissolved within 1.5 hours.

In the present study the rare earth elements have been pre-concentrated and separated from the aluminium matrix prior to their estimation. Upon addition of excess amount of ~7.5M NaOH (30% w/v), the aluminum was left in solution as sodium aluminate, while the rare earth impurities were precipitated as hydroxides [378]. The soluble aluminium separated from the rare earth precipitates using Whatman 542 filter paper.

7.3.2 Recovery study of rare earth by standard addition method

Recovery of rare earth elements present in trace amount in alumina were studied by spiked method due to non-availability of certified reference material (CRM). Four aliquots of high purity aluminium solution (~ 1.0 g Al) were taken and in three aliquots 5,

10, and 25 μg of rare earth elements were added. One aliquot was kept as such for blank correction. The separation method was followed as discussed in this work and analytes were collected and estimated by ICP-MS. The results (Table 7.3) show that rare earth quantitatively recovered.

Table 7.3 Recovery of rare earth elements in high purity aluminium metal after matrix separation (Sample Wt.= 1.0 g, Vol.=10 mL, N=10)

Elements	Added (μg)	Found (μg)	Recovery (%)
Ce	0	<BDL	--
	5	4.7 ± 0.3	93.8 ± 6.3
	10	9.6 ± 0.7	95.7 ± 7.0
	25	12.5 ± 0.9	100 ± 7.2
Dy	0	0.1 ± 0.01	--
	5	4.8 ± 0.2	94.0 ± 10.0
	10	10.1 ± 0.5	100.0 ± 11.1
	25	24.8 ± 0.7	98.8 ± 10.4
Er	0	0.1 ± 0.01	--
	5	5.0 ± 0.2	98.0 ± 10.7
	10	10.1 ± 0.6	100 ± 11.6
	25	25.0 ± 1.5	99.6 ± 11.7
Eu	0	<BDL	--
	5	4.8 ± 0.3	96.0 ± 6.3

	10	9.9 ± 0.7	99.0 ± 7.1
	25	24.5 ± 1.6	98.0 ± 6.5
Gd	0	0.1 ± 0.01	--
	5	4.9 ± 0.4	96.0 ± 10.8
	10	10.0 ± 0.5	99.0 ± 11.1
	25	24.9 ± 1.0	99.2 ± 10.7
Ho	0	<BDL	--
	5	4.7 ± 0.3	94.0 ± 6.4
	10	9.9 ± 0.9	99.0 ± 10.0
	25	24.5 ± 2.0	98.0 ± 8.2
La	0	<BDL	--
	5	4.8 ± 0.4	96.0 ± 8.3
	10	9.5 ± 0.9	95.0 ± 9.5
	25	25.0 ± 2.0	99.8 ± 8.0
Nd	0	<BDL	--
	5	4.9 ± 0.3	98.0 ± 6.3
	10	9.7 ± 0.9	97.0 ± 9.3
	25	24.8 ± 1.5	99.2 ± 6.1
Pr	0	<BDL	--
	5	4.8 ± 0.4	96.0 ± 8.3
	10	9.8 ± 0.8	98.0 ± 8.2
	25	25.0 ± 2.0	100.0 ± 8.0

Sm	0	<BDL	--
	5	4.9 ± 0.4	98.0 ± 8.2
	10	9.9 ± 0.7	99.0 ± 7.1
	25	24.2 ± 1.8	96.8 ± 7.4
Tb	0	<BDL	--
	5	4.8 ± 0.5	96.0 ± 10.4
	10	9.7 ± 0.9	97.0 ± 9.3
	25	24.8 ± 1.5	99.2 ± 6.1
Yb	0	<BDL	--
	5	4.8 ± 0.3	96.0 ± 6.3
	10	9.7 ± 0.9	97.0 ± 9.3
	25	24.1 ± 1.5	96.4 ± 6.2

7.3.3 Correction for spectroscopic interferences

The spectroscopic interferences were monitored and corrected as discussed in previous chapter [339, 340], for precise and accurate quantification of trace and ultra trace impurities.

7.3.4 Detection Limits

The instrumental detection limits (IDLs) and the method detection limits (MDLs) of the method were determined as discussed in previous chapters, using the reported method [341]. The results are given in Table 7.4.

Table 7.4: Instrumental detection limits(IDLs) and method detection limits (MDLs)

Elements	IDL ($\mu\text{g L}^{-1}$)	MDL ($\mu\text{g kg}^{-1}$)
Ce	0.01	1.4
Dy	0.01	4.3
Er	0.05	1.1
Eu	0.01	1.0
Gd	0.01	0.5
Ho	0.05	8.7
La	0.02	0.9
Nd	0.01	1.9
Pr	0.01	0.7
Sm	0.01	1.5
Tb	0.01	0.9
Yb	0.03	1.3

7.3.5 Recovery study by gamma spectrometry

Recovery study by γ -Spectrometry is unique technique to validate any proposed separation procedure as it does not require any blank correction on the spiked amount.

Gamma spectrometric techniques have been reported by our group to validate the recovery studies [322]. To validate the recovery of rare earth elements, $^{152+154}\text{Eu}$ tracer was used. The tracer was mixed with natural europium solution in such a manner that concentration of Eu in stock solution becomes $1\mu\text{g mL}^{-1}$. 1.0 mL of the stock solution was taken as reference and 1.0 ml mixed with 100 mg aluminium solution. The aluminium was separated by the optimized procedure and the tracer recovered was determined by gamma spectrometry using NaI (Tl) detector measuring 344 keV gamma energy. The recovery of tracer was calculated with respect to the reference. The recovery of Eu was found to be better than 98% with <2% RSD (Table 7.5).

Table 7.5 Result of recovery studies by γ -spectrometry (N=10, 60 s Counting)

Samples	Recovery of Eu (%)
Sample-1	99±1
Sample-2	98±1.5
Sample-3	99±1

7.3.6 Analysis of Real Samples

Aluminum metal powder, chips and aluminium oxides samples received from user laboratories were dissolved and analysed by ICP-MS following the separation method. The results are given in Table 7.6.

Table 7.6 The impurities in real sample of alumina and aluminium metals

Elements	Al ₂ O ₃ (μg g ⁻¹)	Al-Metal powder (μg g ⁻¹)	Al-metal chips (μg g ⁻¹)
La	0.11±0.01	1.29±0.04	1.24±0.04
Ce	0.32±0.02	1.34±0.05	1.69±0.05
Pr	0.09±0.01	0.20±0.01	0.50±0.04
Nd	0.33±0.02	0.99±0.03	1.65±0.11
Sm	0.39±0.03	0.63±0.03	1.45±0.11
Eu	0.20±0.01	0.29±0.01	0.70±0.06
Gd	0.54±0.03	0.73±0.04	1.60±0.10
Tb	0.09±0.01	0.13±0.01	0.35±0.03
Dy	0.89±0.05	2.42±0.07	3.14±0.12
Ho	0.11±0.01	0.09±0.01	0.15±0.01
Er	0.12±0.01	0.15±0.01	0.014±0.01

7.4 Conclusion

The refractory nature of aluminum necessitated to reduce the total dissolved solid content in the solution. The reported dissolution methods in the literature was not suitable to dissolve the alumina, therefore, the method was modified and optimized. The aluminum

matrix was separated using gravimetric method. Method was validated using standard addition method due to lack of certified reference material of aluminum/alumina. The observed recovery in the synthetic samples were between 93-100% with good precision between 6.1-11.6 (%RSD).The instrumental detection limits and method detection limit were found within 0.01-0.05 ng L⁻¹ and 0.5-8.3 µg kg⁻¹respectively. The gamma spectrometry analysis using NaI(Tl)-scintillation shows that recovery for ¹⁵²⁺¹⁵⁴Eu tracer is >98.0% with very good precision <2% (RSD). The procedure is simple, organic waste free and suitable for routine analysis .

Chapter 8

Summary and future outlook

In the present chapter, the summary of all studies carried out as a part of the thesis have been discussed with possible future outlook. In chapter 1, we have discussed the importance of the nuclear energy and importance of the fuel characterization. In this chapter different types of nuclear fuels used and characterization of major, minor and trace level elements, specification of metallic and non-metallic impurities in nuclear fuels have discussed.

In Chapter 2 the details of the instrumentation used for characterization of nuclear fuels, such as, inductively coupled plasma mass spectrometry (ICPMS), NaI(Tl)-scintillation gamma spectrometry, and UV-visible spectrophotometry have been discussed. Brief discussion of modern microwave dissolution method to dissolved refractory materials is given in this chapter. The various matrix separation methods such as solvent extraction, ion chromatography and gravimetric method have also been discussed in details.

In chapter 3, importance of reduced enrichment for research and test reactor (RERTR) programme and development of analytical methods for characterization of trace metallic impurities in low enriched uranium (LEU) based high density U_3Si_2 fuel has been discussed. The new pool-type research reactor, at Trombay will use U_3Si_2 as fuel. A solvent extraction method has been used to separate the matrix elements and trace elements from the U_3Si_2 fuel. Validation of separation method was done using standard addition and tracer techniques. The proposed method effectively separates 13 elements (B, Cd, Co, Cr, Cu, Dy, Eu, Gd, Mg, Mn, Ni, Sm, and V) from the U_3Si_2 matrix, which

could then be quantified precisely and accurately by ICP-MS. The developed separation procedure reduces the matrix concentration to $< 20 \text{ mg L}^{-1}$ in the final solution for ICP-MS analysis. This method will be very useful in characterizing the fuel of new research reactor facility using U_3Si_2 as fuel.

In chapter 4, the quantification of trace metallic impurities in U-Mo alloy has been discussed. The details of ion chromatography method for quantitative separation of 33 elements (Al, As, Ce, Cr, Co, Cs, Cu, Dy, Eu, Er, Gd, Hf, Ho, La, Lu, Mg, Mn, Nd, Ni, Pb, Pr, Rb, Rh, Sc, Sm, Sr, Tb, Tm, V, W, Y, Yb, and Zr) from the U-Mo nuclear fuel have been discussed. The separation method was validated using standard addition method. The developed method does not involve any organic active waste and hence is useful for routine analysis. U-Mo is the metallic fuel under consideration for Indian research reactors. This developed method could be very useful for characterizing the fuel.

In chapter 5, quantification of trace metallic impurities in the metallic fuel for fast breeder reactors such as U-Zr alloy has been discussed. U-Zr and U-Pu-Zr are preferred metallic nuclear fuels for fast breeder reactors. Solvent extraction method was developed to separate the matrix elements (U and Zr) from the trace amount of metallic impurities. The developed method reduces the matrix concentration ($< 10 \text{ ppm}$) with analyte solution. The recovery studies of trace elements using standard addition method show that minimum thirty three elements could be quantitatively separated from the U-Zr matrix. The separation method was validated using independent gamma spectrometric method. The studies show more than 97% recovery of $^{152+154}\text{Eu}$ with high precision. The real

samples of U-Zr alloy were analyzed , 33 trace metallic impurity were present at below the specification limits .

The developed method could be used for characterization of U-Pu-Zr alloy. Due to presence of Pu, the sample becomes highly radioactive and could be handled only in a glove box. Therefore, a proper ventilated and isolated set up of instrumentation is required. The existing ICP-MS system is not installed in a glove box, therefore, the U-Pu-Zr sample could not be analyzed.

In chapter 6, chemical characterization of dysprosium-titanate(Dy_2TiO_5), an alternate control rod material, has been discussed. Dysprosium-titanate being a refractory material, is very difficult to dissolve by conventional method. Therefore, a microwave dissolution method was developed to dissolved the Dy_2TiO_5 . Initially major elements such as Dy and Ti in dysprosium titanate were quantified using the ICP-MS, but the results obtained were not to the desired accuracy and precision. Therefore, gravimetric and spectroscopic method was developed for dysprosium and titanium estimation. Molybdenum could be determined by ICP-MS, if separated from the matrix. However, in present work, gravimetric method for molybdenum is developed . An ion chromatography method has developed to separate the matrix elements. Gravimetric estimation of Dy and Mo in the synthetic samples provide good accuracy (>99%) and precision (<2% RSD). Spectrophotometric estimation of titanium in synthetic samples was achieved with accuracy >98% and good precision (<2%). The oxides of Dy and Mo obtained from dysprosium titanate were analyzed for trace impurities by ICP-MS. Dy_2TiO_5 is used in

VVER reactors as a control rod material and hence this method could be very helpful for chemical characterization of dysprosium titanate .

Aluminum (Al) and alumina (Al_2O_3) are also very useful materials in nuclear industry. Aluminum is used as dispersion medium for metallic and intermetallic nuclear fuels while alumina is used as insulating material. In chapter 7, a detail study has been discussed for quantitative separation and measurement of ultra trace amounts of rare earth elements in Al and Al_2O_3 . Microwave dissolution method has been developed to dissolve the refractory alumina. The rare earth elements have been separated gravimetrically. The separation factor is quite high, gives a decontamination factor of 10^5 . The study shows that rare earth elements $<1\mu\text{g g}^{-1}$ could be easily quantified by ICP-MS. The separation method was validated using independent gamma spectrometric method. Use of $^{152+154}\text{Eu}$ as tracer shows that more than 98% could be recovered. The separation method does not generate any organic waste and hence is very useful for routine analysis in nuclear industries.

Thus as a part of the present thesis a series of separation procedure have been standardized/ developed for analysis of major, minor, and trace elements in the various nuclear materials used in nuclear industry in India. The procedures were developed as a part of the ongoing chemical quality control of nuclear fuels and other nuclear materials to achieve their desired performance during the operation of the nuclear reactors.

References:

1. N.M. A. Mohamed, A. Badawi, Prog. Nucl. Energy 91 (2016) 49.
2. B. R. T. Frost, R. Inst. Chem., Rev. 2 (1969) 163.
3. M. Jacoby, Chemical and Engineering News, 93 (2015) 44.
4. K. Anantharaman, V. Shivakumar, D. Saha, J. Nucl. Mater. 383(2008) 119.
5. H. M. Mattys, Actinides Rev.1(1968) 165.
6. J. F. Schumar, J. Nucl. Mater. 100 (1981) 31.
7. B. W. Brook, A. Alonso, D. A. Meneley, J. Misak, T. Bles, J. B. van Erp, Sustainable Mater. Technol., 1 (2014) 8.
8. F. Javidkia, M. Hashemi-Tilehnoee, V. Zabihi, Journal of Energy and Power Engineering, 5 (2011) 811.
9. A. Gopalakrishnan, Annual Review of Energy and the Environment, 27 (2002) 369.
10. R. Tongia, V. S. Arunachalam, Current Science, 75(1998)549.
11. P.K. Vasudev, Electrical India, 54(2014) 28.
12. A. Kakodkar, R.K. Sinha, M.L. Dhawan, IAEA-SM-353/54
13. F. A. Settle, J. Chem. Educ., 86 (2009) 316.
14. R. C. Ewing, MRS Bulletin, 33(2008) 338.
15. Nuclear Fuel Cycle, <http://www.dae.nic.in>
16. U. Basak, P.S. Kutty, S. Mishra, S.K. Sharma, et.al., BARC News Letter, 249(2003) 191.

17. L. C. Walters, B. R. Seidel, J. Howard Kittel, Nuclear Technology, 65(1984) 179.
18. B. R. Seidel, L. C. Walters, Y. I. Chang, JOM, 39(1987)10.
19. T. Sofu, Nucl. Eng. Technol. 47 (2015) 227.
20. G.J. Prasad, BARC Newsletter, 332(2013)v.
21. IAEA Nuclear Energy Series No. NF-T-4.1.
22. A. Kumar, International conferences on fast reactors and related fuel cycles: Safe technologies and sustainable scenarios (FR 13) Paris, March 4-7, 2013.
23. R. F. Domagala, T. C. Wiencek, H. R. Tresh, Nucl.Technol. 62 (1983) 353.
24. V. P. Sinha, G. P. Mishra, S. Pal, K. B. Khan, P.V. Hegde, G. J. Prasad, J. Nucl. Mater. 383 (2008) 196.
25. W. E. Lee, M. Gilbert, S. T. Murphy, R. W. Grimes, J. Am. Chem. Soc. 96 (2013) 2005.
26. V. Troyanov, V. Popov, I. Baranaev, Prog. Nucl. Energy, 38(2001) 267.
27. J. A. L. Robertson, J. Nucl. Mater. 100 (1981) 108.
28. D. O. Northwood, Mater Des 6(2) (1985) 58.
29. G. Wikmark, L. Hallstadius, K. Yueh, Nucl. Eng. Technol. 41(2) (2009) 143.
30. F. Thevenot, A review on boron carbide Key Engineering Materials 56-57 (1991) 59.

31. G. J. Prasad, Material group, BARC News Letter 332 (2013)
32. V. D. Risovany, E. E. Varlashova, D. N. Suslov, J. Nucl. Mater. 281 (2000) 84.
33. D. A. Petti, Nucl. Tech. 84 (1989) 128.
34. S. S. Bajaj, A. R. Gore, Nucl. Eng. Desig. 236 (2006) 701.
35. J. M. Beeston, Nucl. Eng. desig. 14 (1970) 445.
36. Book: Nuclear graphite edited by R.E.Nightingale, Academic Press -1962 New York and London.
37. IUPAC Compendium of Chemical Terminology , PAC, 51 (1979) 2243.
38. A. Aziz, S. Jan, F. Waqar, B. Mohammad, M. Hakim and W. Yawar, J. Radioanal. Nucl. Chem. 284 (2010) 117.
39. A. L. de Souza, M. E. B. Cotrim, M. A. F. Pires, Microchem. J. 106 (2013) 194.
40. Z. Varga, R. Katona, Z. Stefánka, M. Wallenius, K. Mayer and A. Nicholl, Talanta 80 (2010) 1744.
41. J. Ignacio , G. Alonso, Anal. Chem. Acta 312 (1995) 57.
42. J. M. B. Moreno, J. I. G. Alonso, P. Arbore, G. Nicolaou ,L. Koch, J. Anal. At. Spectrom. 11 (1996) 929.
43. A. Pitois, L.A.d.L. Heras and M. Betti, Int. J. Mass Spectrom. 270 (2008) 118.
44. R. K. Malhotra ,K. Satyanarayana, Talanta 50 (1999) 601.
45. G. V. Ramanaiah, Talanta 46 (1998) 533.

46. N. T. K. Dung, D.T. Son ,H.V. Trung, *Anal. Sci.* 18 (2002) 1263.
47. D. A. Batistoni, P. N. Smichowski, *Appl. Spectrosc.* 39 (1985) 222.
48. M. Betti, *J. Chromatogr. A* 789 (1997) 369.
49. M.D.H. Amey, D.A. Bridle, *J. Chromatogr. A* 640 (1993) 323.
50. F. J. Langmyhr, P. E. Paus, *Anal. Chim. Acta*, 43(1968) 508.
51. G. J. Oliver, *Proc. Anal. Div. Chem. Soc.* 16(1979) 151.
52. R. Bock, *A Handbook of Decomposition Methods in Analytical Chemistry*, New York Wiley, 1979.
53. Z. Sulcek, P. Povondra, *Methods of Decomposition in Inorganic Analysis*, Boca Ralton, FL: CRC Press 1989.
54. J. A. Dean, *Analytical Handbook*, section 1.7, New York: McGraw-Hill, 1995.
55. H. M. Kingston, S. J. Haswell, *Microwave-Enhanced Chemistry: Fundamentals, Sample Preparation and Applications*, Washington, DC: American Chemical Society, 1997.
56. B. E. Erickson, *Anal. Chem.* 70, (1998) 467A.
57. R. C. Richter, D. Link , H. M. Kingston, *Anal. Chem.* 73, (2001) 31A.
58. J. L. Luque Garcia, M. D. Luque de Castro, *Trends in Analytical Chemistry* 22 (2003) 90.
59. C. A. Lucy, L. Gureli, S. Elchuk, *Anal. Chem.*, 65 (1993) 3320.
60. K. L. Ramakumar, V. A. Raman, V. L. Sant, V. D. Kavimandan, H. C. Jain, *J. Radioanal. Nucl. Chem.*, 125 (1988) 467.

61. R. B. Yadav, B. Gopalan, Chemical characterization of power reactor fuels at Nuclear fuel complex, Characterization and Quality Control of Nuclear Fuels (Eds: C. Ganguli, R. N. Jayaraj), Allied Publishers: New Delhi, (2002) 455.
62. S.V. Godbole, Trace metal assay of nuclear materials, Chemical characterization of nuclear fuel, IANCAS Bulletin, 7 (2008) 169.
63. R. M. Sawant, M. A. Mahajan, P. Verma, D. Shah, U. K. Thakur, K. L. Ramakumar, V. Venugopal, A review, Radiochim. Acta, 95 (2007) 585.
64. M. A. Mahajan, M. V. R. Prasad, H. R. Mhatre, R. M. Sawant, R. K. Rastogi, G. H. Rizvi and N. K. Chaudhuri, J. Radioanal. Nucl. Chem. 148 (1991) 93.
65. U. Basak, M.R. Nair, R. Ramachandran, S. Majumdar, BARC Newsletter, Founder's day special issue October-2001 (<http://www.barc.ernet.in/publications/nl/>).
66. S. R. Pillai, S. Anthonysamy, P.K. Prakashan, R. Ranganathan, P.R.Vasudeva Rao, C.K. Mathews, J. Nucl. Mater., 167 (1989) 105.
67. Glasstone and W. H. Jordan, American Nuclear Society, (1990) 167.
68. Toshiaki Hiyama, Toshio Takahashi, Katsuichiro Kamimura, Anal. Chim. Acta, 345 (1997) 131.
69. Y. A. Sayi, K.L. Ramakumar, V. Venugopal Chemical characterization of nuclear fuel, IANCAS Bulletin, 7 (2008) 180.
70. Zhou Nan, Talanta 46 (1998) 1237.

71. G. R. Ramos ,R. I. Tomas, *Microchemical Journal* 33, (1986) 379.
72. K. Uesugi , T. Kumagai, S. Wada, *Microchemical Journal* 33, (1986) 204.
73. K. S. Kim, J.H. Yang, K. W. Kang, K. W. Song, G. M. Kim, *J. Nucl. Mater.* 325 (2004) 129.
74. O. A. Vita, C. R. Walker, E. Litteral, *Analytica Chemica Acta* 64 (1973) 249.
75. J. Mendham, R. C. Denney, J.D. Barnes, M. J. K. Thomas, *Vogel's, Textbook of Quantitative Chemical Analysis, Sixth Edition.*
76. V. V. Yakshin, M. N. Krokhin, *Radiochemistry* 53 (3) (2011) 327.
77. G. R. Waterbury, C.F. Metz, *Analytical Chemistry* 31 (7) (1959) 1145.
78. K. Chander, S. P. Hasilkar, S. G. Marathe, *J. Radioanal. Nucl. Chem.* 154 (4) (1991) 277.
79. Ge Xiao, R. L. Jones, D. Saunders, K.L.Caldwell, *Radist. Prot. Dosimetry* 162 (4) (2014) 618.
80. T. Prohaska, J. Irrgeher, A. Zitek, *J. Anal. At. Spectrom.* 31 (2016) 1612.
81. Takeshi Ohno, *J. Mass Spectrom. Soc. Jpn.* 62 (2014) 103.
82. C. E. Johnson, I. Johnson, P.E. Blackburn, C.E. Crouthamel, *Reactor technology*, 15 (1972) 303.
83. Toshiaki Hiyama, *Anal. Chim. Acta.*, 402 (1999) 297.
84. M. Ugajin, M. Akabori, A. Itoh, *JAERI-Conf. 96-006* 155.

85. A.T. Nelson, J.T. White, D.D. Byler, J.T. Dunwoody, J.A. Valdez and K.J. McClellan Trans. Am. Nucl. Soc., 110 (2014) 987.
86. J. M. Harp , P. A. Lessing, R. E. Hoggan, J. Nucl. Mater. 466 (2015) 728.
87. L. H. Ortega, B. J. Blamer, J. A. Evans, S. M. McDevitt, J. Nucl. Mater. 471 (2016) 116.
88. R. H. L. Garcia, A. M. S.Silva, E. F.U. Carval, International Nuclear Atlantic Conference - INAC 2013, Recife, PE, Brazil, November 24-29.
89. J. Rest, Y. S. Kim, G. L. Holmes, M. K. Meyer , S. L. Hayes, ANL-09/31, U-Mo Fuels Handbook, RERTR Program, June 2006.
90. M. K. Meyer, J. Gan, J. F. Jue, D.D. Keiser, E. Perez, A. Robinson, D.M. Wachs, N. Woolstenhulme, G.L. Hofman, Y.S. Kim, Nucl. Eng. Technol. 46(2) (2014) 169.
91. S.V. D. Berghe, P. Lemoine , Nucl. Eng. Technol.46(2) (2014) 125.
92. Ho Jin Ryu, Yeon Soo Kim, Nucl. Eng. Technol.46(2) (2014) 159.
93. D. E. Burkes, D. M. Wachs, D. D. Keiser, M. A. Okuniewski, J.F Jue, F. J. Rice, R. Prabhakaran, INL/CON -09-15633.
94. A. Saha, S. B. Deb, and M. K. Saxena, J. Anal. At. Spectrom. 31(2016) 1480.
95. A. C. Bagchi, G.J. Prasad, K.B. Khan , R. P. Singh , J. Material. Sci. Eng. 2(1)(2013) 2.
96. C. Basak , G.J. Prasad , H.S. Kamath , N. Prabhu, J. Alloys. Compd. 480 (2009) 857.

97. Y. Zhang, Xin Wang, G. Zeng, Hui Wang, J. Jia, L. Sheng, P. Zhang, J. Nucl. Mater. 471 (2016) 59.
98. C. B. Basak, J. Nucl. Mater. 416 (2011) 280.
99. Masrukan, Appl. Mechanics and materials 376 (2013) 23.
100. A. Sengupta, B. Rajeswari, R.M. Kadam, and S.V. Godbole, Atom. Spectrosc. 33(2) (2012) 48.
101. L. Heins, A. Roppelt, P. Dewes, IAEA-TECDOC-813, Proceedings of a Technical Committee meeting held in Vienna, 29 November-2 December (1993).
102. A. Abdelghafar Galahom, Ann. Nucl. Energy 94 (2016) 221.
103. J. P. A. Renier, M. L. Grossbeck, ORNL/TM-2001/238 (2001).
104. N. J. Simon, Cryogenic properties of inorganic insulation materials for ITER magnets: A Review, NISTIR 5030.
105. C. Moreno, L. A. Sedano, K. J. McCarthy, E.R. Hodgson, Fusion Engineering and Design 82 (2007) 2647.
106. G. Piatti, P. Fiorini, P. Schiller, High purity aluminium alloys for experimental fusion reactors, Nuclear Engineering and Design/Fusion 1 (1984) 137.
107. Aluminium alloy Selection and Application, Published by The Aluminium Association, Inc., December 1998.
108. P. Rambabu, N. Eswara Prasad, V.V. Kutumbarao, R.J.H. Wanhill, ©Springer Science Business Media Singapore 2017, Aerospace

Materials and Materials Technology, Indian Institute of Metals Series, Chapter 2: Aluminium Alloys for Aerospace Application, DOI: 10.1007/978-981-10-2134_2.

109. M. Gonzalez, E. R. Hodgson, *Fusion Engineering and Design* 84(2009) 829.
110. Enik Tatfir, Imre Varga, Gyula Zfiray, *Mikrochim. Acta* 111 (1993) 45.
111. W. Wien, *Verl. Phys. Ges. Berlin*, 17 (1898) 10.
112. J. J. Thomson, *Rays and Positive Electricity* Longmans Green and Co., London, (1913).
113. F. W. Aston, *Phil. Mag.* 39 (1920) 449.
114. J. De Laeter, M. D. Kurz, *J. Mass Spectrom.* 41 (2006) 847.
115. A. J. Dempster, *Proc. Phil. Soc.*, 75 (1935) 755.
116. A. J. Dempster, *Rev. Sci. Instrum.*, 7 (1936) 46.
117. R.A. Yost, C.G. Enke, *J. Am. Chem. Soc.* 100 (1978) 2274.
118. W. Paul, M. Raether, *Z. Physik*, 140 (1955) 262.
119. W. Paul, H. P. Reinhard, U. von Zahn, *Z. Phys.* 152 (1958) 143.
120. W. Paul, H. Steinwedel, *Z. Naturforsch.*, 8a (1953) 448.
121. A. Goudsmit, *Phys. Rev.*, 74 (1948) 622.
122. R. S. Houk, V. A. Fassel, G. D. Flesch, H. J. Svec, A. L. Gray, C. E. Taylor, *Anal. Chem.*, 52 (1980) 2283.
123. A. Montaser, *Inductively Coupled Plasma Source Mass Spectrometry*, Wiley- VCH Inc., New York (1998).

124. A. L. Gray, *Analyst*, 110 (1985) 551.
125. S. Greenfield, I. J. Jones and C. T. Berry, *Analyst*, 89 (1964) 713.
126. A. L. Gray, A. R. Date, *Analyst*, 108 (1983) 1033.
127. A. R. Date, A. L. Gray, *Analyst*, 106 (1981) 1228.
128. P. Yang , R.M. Barnes, *Spectrochim. Acta*, 45B (1990) 167.
129. S. D. Tanner, *J.Anal. At. Spectrom.* 8 (1993) 891.
130. A.L. Gray, *Spectrochim. Acta*, 40B (1985) 1525.
131. A.L. Gray, *Anal. Atomic Spectrom.* 97A (1986) 58.
132. R. H. Scott, V.A. Fassel, R.N. Kniseley and D.E. Nixon, *Anal. Chem.* 46 (1974) 75.
133. H.B. Fannin, C.J. Seliskar, and D.C. Miller, *Appl.Spectrosc.*, 42 (1987) 621.
134. S. R. Koirtyohann, J. Stephen Jone, C. P. Jester, D. A. Yates, *Spectrochemica Acta B* 36 (1981) 49.
135. A. Canals, V. Hernandis and R.F.Browner, *J.Anal. At. Spectrom.*, 5 (1990) 61.
136. J.W. Olesik, J.A. Kinzer and B.Harkleroad, *Anal Chem.*, 66 (1994) 2022.
137. E. H. Evans, J. J. Giglio, T. M. Castellano, J.A.Caruso. *Inductively coupled and microwave induced plasma sources for mass spectrometry*, RSC Analytical Spectroscopy Monographs. 1995.
138. V.A.Fassel, *Science*, 202 (1978) 183.
139. H. Niu, R.S. Houk, *Spectrochim. Acta*, 51B (1996) 779.

140. R. Campargue, *J. Chem. Phys.* 52 (1970) 1795.
141. J. D. Douglas, J. B. French, *Anal. Chem.* 53 (1981) 37.
142. A. R. Date, A.L.Gray, *Spectrochim. Acta* 38B, (1983) 29.
143. C. E. Melton, *Principles Of Mass Spectrometry And Negative Ions*, Marcel Dekker, New York 1970.
144. J. R. Chapman, *Practical Organic Mass Spectrometry*, 2nd Edn, John Wiley, Chichester, 1993.
145. G. Horlick, S.N. Tan, *Appl. Spectrosc.* 40 (1986) 4.
146. E. H. Evans , J.J. Giglio, *J.Anal. At. Spectrom.* 8 (1983) 1.
147. D. C. Gregorie, *Spectrochim. Acta*, 42B (1987) 895.
148. J. Marshall, J. Franks, *J.Anal. At. Spectrom.*, 6 (1991) 591.
149. P. Allain, I. Jaunault, Y. Mauras, J. Mermet and T.Delaporte, *Anal Chem.* 63 (1991) 1497.
150. H. Kawaguchi, T. Tanaka, T. Nakamura, A. Morishita and A. Mizuike, *Anal. Sci.* 3 (1987) 305.
151. S. H. Tan, G. Horlick, *J. Anal. Atom. Spectrom.* 2 (1987) 745.
152. D. Beauchimin, J. W. McLaren and S. S. Berman, *Spectrochim. Acta* 42B, (1987) 467.
153. J. S. Crain, R. S. Houk and R. G. Smith, *Spectrochim. Acta* 43B, 1355 (1988).
154. G. R. Gillson, D. J. Douglas, F. E. Fulford, K. W. Halligan , S. D. Tanner, *Anal. Chem.* 60 (1988) 1472.

- 155.** Abdel-Fattah Ibrahim Helal, Khalid Ali Kmakhi, 1994, Atomic Physics, King Abdul Aziz University PO Box 1540- Jeddah.
- 156.** Mattson, Barbara. "Scintillators as Gamma-ray Detectors." NASA's Imagine the Universe. 1997.
Goddard Space Flight Center. Last Updated: November 23, 2010.
<http://imagine.gsfc.nasa.gov/docs/science/how_12/gamma_scintillators.html>.
- 157.** K. Debertin , R. G. Helmer, Gamma- and X-Ray Spectrometry with Semiconductor Detectors, North-Holland, 1988.
- 158.** Y. S. Selim, M. I. Abbas, M. A. Fawzy, Radiation Physics and Chemistry, vol. 53(6) (1998) 589.
- 159.** A. Jehouani, R. Ichaoui, M. Boulkheir, Appl. Radia. Isotop. 53(4-5) (2000) 887.
- 160.** J. M. Adams, Appl. Clay Sci. 2 (1987) 309.
- 161.** V. R. Choudhary, V. H. Tillu, V. S. Narkhede, H. B. Borate, R. D. Wakharkar, Catalysis Communications 4 (2003) 449.
- 162.** T.P. Deksnys, R.R. Menezes, E. Fagury-Neto, R.H.G.A. Kiminami, Ceramics International 33 (2005) 67.
- 163.** S. G. Deng, Y.S. Lin, Chemical Engineering Science 10 (1997) 1563.
- 164.** K. A. Kraus and F. Nelson, Proc. Intern. Conf. Peaceful Uses of Atomic Energy, Geneva, 7 (1956) 113.

- 165.** H. Matsumiya, M. Kuromiya, M. Hiraide, ISIJ International, 53 (2013) 81.
- 166.** A. Townshend, E. Jackwerth, Pure&App/. Chem. 61(9) (1989) 1643.
- 167.** V. N. Bulut, H. Demirci, D. Ozdes, A. Gundogdu, O. Bekircan, M. Soylak, C. Duran, Environmental Progress & Sustainable Energy 35(6) (2016) 1709.
- 168.** K.H. Lieser, P. Burba, W. Calmano, W. Dyck, E. Heuss, S. Sondermeyer, Mikrochimica Acta 5-6 (1980) 445.
- 169.** N. Bader, A. A. Benkhayal, B. Zimmermann, Int. J. Chem. Sci.: 12(2) (2014) 519.
- 170.** V. Weimarn, P. P. Chem. Revs. 2 (1925) 217.
- 171.** R. F. Domagla, T.C. Wiencek and H.R. Tresh, Nucl. Tech. 62 (1983)353.
- 172.** A. Bhatnagar, P. Mukhaerjee, S.B. Chafle, S. Sengupta and V.K. Raina, RERTR 2012-34th International Meeting on Reduced Enrichment for Research and Test Reactors (October 14-17, 2012).
- 173.** U.S. Nuclear Regulatory Commission Report: "Safety Evaluation Report Related to the Evaluation of Low-Enriched Uranium Silicide-Aluminum Dispersion Fuel for Use in Non-Power Reactors," NUREG-1313 (July 1988).
- 174.** J. Marín, J. Lisboa, J. Ureta, L. Olivares, H. Contreras and J.C. Chávez, J. Nucl. Mater. 228 (1996) 61.
- 175.** F. Muhammad, A. Majid, Prog. Nucl. Energ. 51 (2009) 141.

176. V.P. Sinha, P.V. Hegde, G.J. Prasad, G.K. Dey and H.S. Kamath, *J. Alloys and Compds.* 506 (2010) 253.
177. India's First Research Reactor Apsara – Fifty years of operation and utilisation, December, 2006.
178. A.L.de Souza, M.E.B. Cotrim and M.A.F. Pires, *Microchem. J.* 106 (2013) 194.
179. A. Saha, S.B. Deb, B.K. Nagar and M.K. Saxena, *Spectrochim. Acta B* 94-95 (2014) 14.
180. R.K. Malhotra and K. Satyanarayana, *Talanta* 50 (1999) 601.
181. P.C. Krueger, M.S. Bloom and J.G. Arnason, *J. Anal. At. Spectrom.* 27 (2012) 1245.
182. D. Dick, A. Wegner, P. Gabrielli, *Anal. Chim. Acta* 621 (2008) 140.
183. S. Tokalioglu, *Food Chem.* 134 (2012) 2504.
184. K. W. Chan, G.H. Tan, R.C.S Wong, *Anal. Lett.* 45 (2012) 1122.
185. T. Ishikawa, E. Nakamura, *Anal. Chem.* 62 (1990) 2612.
186. M. D'Orazio, *Geostandard. Newslett.* 23 (1999) 21.
187. T. Ishika, E. Nakamura, *Proc. Japan Acad.*, 66B (1990) 91.
188. H. Tao, A. Miyazaki, *J. Anal. At. Spectrom.* 10 (1995) 1.
189. P. Konieczka, *Critical Reviews in Analytical Chemistry*, 37 (2007) 173.
190. L. Balcaen, E. Bolea-Fernandez, M. Resano and F. Vanhaecke, *Anal. Chim. Acta*, 809 (2014) 1.
191. V. Yilmaz, Z. Arslan and I. Rose, *Anal. Chim. Acta*, 761 (2013) 18.

- 192.** S. V. D. Berghe, P.Lemoine, Nuclear Engineering and Technology, 46(2) (2014) 125.
- 193.** V. P. Sinha, P. V. Hegde, G . J. Prasad, G. P. Mishra, S. Pal, Trans.Indian Inst. Met.61(2-3) (2008) 115.
- 194.** Y. I. Chang, Nuclear Engineering and Technology, 39(3) (2007) 161.
- 195.** E. Perez, B. Yao, D.D. Keiser Jr., Y-H. Sohn, J. Nucl. Mater. 402 (2010) 8.
- 196.** Y. S. Kim, G. L. Hofman, J. Nucl. Mater.419 (2011) 291.
- 197.** R. Avni, Spectrochimica Acta, 23B (1969) 619.
- 198.** ASTM C1517-16, Standard Test Method for Determination of Metallic Impurities in Uranium Metal or Compounds by DC-Arc Emission Spectroscopy
- 199.** www.iaea.org/inis/collection/NCLCollectionStore/_Public/34/030/34030687.pdf
- 200.** J. R. Kumar, J.S. Kim, J.Y. Lee , H.S. Yoon, Separation & Purification Reviews, 40 (2011) 77.
- 201.** G. Jin-Xin, S. Si-Xiu, D. Dong-li, L. Ming-Xia, P. Hua, M. Zhao- li, J. Radioanal. Nucl. Ch. 267(3) (2006) 675.
- 202.** C. A. Horton, J.C.White, Anal. Chem. 30(11) (1958) 1779.
- 203.** Y. Shigetomi, T. Kojima, H. Kamba, J. Nucl. Sci. Technol 20(2) (1983) 140.

204. I. Haiduc, M. Curtui, I. Haiduc, J. Radioanal. Nucl. Ch. , 99(2) (1986) 257.
205. S. D. Dogmane, R. K. Singh, D. D. Bajpai, J. N. Mathur, J. Radioanal. Nucl. Ch. 253(3) (2002) 477.
206. S. I. Ei-Dessouky, J. Radioanal. Nucl. Ch. 260(3) (2004) 613.
207. R. G. Talla, S. U. Gaikwad, S. D. Pawar, Indian J. Chem. Techn. 17 (2010) 436.
208. S. V. Vartak, V. M. Shinde, Talanta 43 (1996) 1465.
209. A. R. Ghiasv, S. Shadabi, E. Mohagheghzadeh, P. Hashemi, Talanta 66 (2005) 912.
210. A. Rao, A.K Sharma, P. Kumar, M.M.Charyulu, B.S.Tomar, K.L.Ramakumar, Appl. Radiat. Isotopes 89 (2014) 186.
211. http://www.iaea.org/inis/collection/NCLCollectionStore/_Public/20/028/20028872.pdf
212. R. Djogic, V. Cuculic, M. Branica, Croat. Chem. Acta 78(4) (2005) 575.
213. M. O. Sornein, C. Cannes, C. L. Naour, G. Lagarde, E. Simoni, J.C.Berthet, Inorg. Chem. 45 (2006) 10419.
214. P. A. Barnard, I.W. Sun, C. L. Hussey, Inorg. Chem. 29 (1990) 3670.
215. O. A. Vita, C. R. Walker, C. F. Trivisonno, R. W. Sparks, Anal. Chem. 42(4) (1970) 465.
216. F. Tera, J. Korkisch, AnalyticaChimicaActa 25(3) (1961) 222.
217. T. H. Nguyen, M. S. Lee, Hydrometallurgy 136 (2013) 65.

- 218.** P. N. Nomngongo, J.C. Ngila, J. N.Kamau, T. A. M. Msagati, B. Moodley, *Talanta* 110 (2013) 153.
- 219.** F. Monroy-Guzman, *J. Chem. Chem. Eng.* 10 (2016) 90.
- 220.** L. Jauberty, N. Drogat, J. L. Decossas, V. Delpech, V. Gloaguen, V. Sol, *Talanta* 115 (2013) 751.
- 221.** K. A. Krans, G. E. Moore, *J. Am. Chem. Soc.* 75(6) (1953) 1460.
- 222.** R. H. Iyer, Radiochemistry Division Annual Progress Report, IN9300094, BARC/1992/P/002 page 22.
- 223.** Korkisch Johann, *Hand Book of Ion Exchange resin: Their Application to Inorganic analytical Chemistry Vol. 6*, CRC Press Taylor & Francis Group.
- 224.** J.Korkisch, A.Sorio, *Analytica Chemica Acta* 76 (1975) 393.
- 225.** F. J. Alguacil, P. Adeva, M. Alonso, *Gold Bulletin* 38(1) (2005) 9.
- 226.** E. H. Huffman, G. M. Iddings, R. C. Lilly, *J. Am. Chem. Soc.* 73(9) (1951) 4474.
- 227.** J. H. Kanzelmeyer, J.Ryan, H. Freund, *J. Am. Chem. Soc.* 78 (1955) 3020
- 228.** K. Z. Hossain, C. T. Camagong, T. Honjo, *Fresenius' J. Anal. Chem.* 369(6) (2001) 543.
- 229.** J. W. Morgan, D. W. Golightly, A. F. Dorrzape, *Talanta* 38(3) (1991) 259.
- 230.** O. N. Konova, E. V. Duba, N. I. Shnaider, I. A. Pozdnyakov, *Russian J. Appl. Chem.* 90(8) (2017) 1239.
- 231.** M. Pirs, R. J. Magee, *Talanta* 8 (1961) 395.

- 232.** Sung Ho Lee, Jae Hyung Yoo, Jung Hyung Kim, Korean J. Chem. Eng. 21(5) (2004) 1038.
- 233.** A. V. Balnev, V. S. Mityakhina, L. V. Krasnikov, B. Ya. Galkin, V. I. Besnosyunk, Czech J. Phys. 53 (2003) A417.
- 234.** K. Pyzynska, Analyst 120 (1995) 1933.
- 235.** K. Kalinowski, Z. Marczenko, Microchemical J. 39 (1989) 198.
- 236.** K. Wejman-Gibas, M. Pilsniak-Rabiega, E3S Web conferences 8 (2016) 1016.
- 237.** A. A. Larenkov, A. B. Bruskin, G. E. Kodina, ISSN1066-3622. Radiochemistry 56(1) (2014) 57.
- 238.** Y. Inukai, Y. Tanaka, Y. Shirashi, T. Matsuda, N. Mihara, K. Yamada, N. Nambu, O. Itoh, T. Doi, Y. Kaida, S. Yasuda, Analytical Sciences 17 (2001) i1117.
- 239.** J. L. Hagne, E. E. Maczkowske, H. A. Bright, J. Res. Natl. Bur. Stand. 53(6) (1954) 353.
- 240.** S. Misumi, T. Taketatsu, J. Inorg. Nucl. Chem. 20 (1961) 127.
- 241.** J. P. Fariz, T. A. Rettig, Anal. Chem. 34(12) 1962) 1563.
- 242.** J. P. Fariz, J. W. Warton, Anal. Chem. 34(9) (1962) 1077.
- 243.** M. A. Vaugan, G. Horlick, Appl. Spectrosc. 40 (1986) 434.
- 244.** M. M. Kershisnik, R. Kalamegam, K. O. Ash, D. E. Nixon, E. R. Ashwood, Clin. Chem 38(11) (1992) 2197.

- 245.** A. S. Zawadka, P. Konieczka, E. Przyk, J. Namiesnik, *Anal. Lett.* 38 (2005) 353.
- 246.** A. Riyas, P. Mohanakrishanan, *Ann. Nucl. Energy* 35 (2008) 87.
- 247.** R. K. Sinha, *Advanced Nuclear Reactor System- An Indian Perspective*, *Energy procedia*, 7 (2011) 34.
- 248.** Y. Hu, M. and Xu, *Nucl. Power Eng.* , (2008) 53.
- 249.** X. M. Shi, and X. J. Peng, *Nucl. Power Eng.* 4 (2010) 5.
- 250.** International Conference on Fast Reactors and Related Fuel Cycles: March 4-7 (2013) Paris, France.
- 251.** ASTM C753-04 (2009) Standard specification for nuclear grade sinterable uranium dioxide powder
- 252.** A. Taylor, N. Barlow, M. P. Day, S. Hill, M. Patriarca, and M. White, *J. Anal. At. Spectrom.* 32 (2017) 432.
- 253.** S. Carter, A. Fisher, R. Garcia, B. Gibson, S. Lancaster, J. Marshall, I. Whiteside, *J. Anal. At. Spectrom.* 30 (2015) 2249.
- 254.** A. Saha, S. B. Deb, B. K. Nagar, and M. K. Saxena, *Atom. Spectrosc.* 34(4) (2013) 125.
- 255.** V. G. Mishra, S. K. Sali, D. J. Shah, U. K. Thakur, R. M. Sawant, and B.S.Tomar, *Radiochim. Acta* 102(10) (2014) 895.
- 256.** B. S. Mohite, S. H. Burungale, *J. Radioanal. Nucl. Ch.* 241(3) (1999) 589.
- 257.** S. I. El-Dessouky, *J. Radioanal. Nucl. Ch.* 260(3) (2004) 613.

- 258.** Y. Xing-Cun, B. Bo-Rong, and C. Wwi-Guo, *J. Radioanal. Nucl. Ch.* 258(3) (2003) 681.
- 259.** N. V. Deorkar, S. M. Khopkar, *J. Radioanal. Nucl. Ch.* 130(2) (1989) 433.
- 260.** N. V. Deorkar, J. Kulawik, J. Mikulski, *J. Radioanal. Nucl. Ch.* 31 (1976) 9.
- 261.** B. Tamhina, A. Gojmerac, M. J. Herak, *Laboratory of Analytical Chemistry, Faculty of Science, Zagreb, Yugoslavia* 569 (1976).
- 262.** J. A. Daoud, N. A. Rahman, and H.F.Aly, *J. Radioanal. Nucl. Ch.* 221(1-2) (1997) 41.
- 263.** L. Poriel, A. F. Reguillon, S. P. Rostaing, M. lemaire, *Sep. Sci. and Technol.* 41 (2006) 1927.
- 264.** R. Banda, H. Young lee, M. S. Lee, *J. Radioanal. Nucl. Ch.* 295 (2013) 1537.
- 265.** M. Taghizadeh, M. Ghanadi, E. Zolfonoun, *J. Nucl. Mater.* 412 (2011) 334.
- 266.** A. Sadigzadeh, S. Chehrenama, H. Shokri, *J. Theor. Appl. Phys.* 3(3) (2009) 20.
- 267.** L. Y. Wang, H. Y. Lee, and M. S. Lee, *Mater. Trans.* 54 (2013) 1460.
- 268.** S. A. Mohammed, *J. Raf. Sci.* 20(2) (2009) 74.
- 269.** R. Sarkar (Sain), S. Ray, and S. Basu, *J. Chem. Bio. Phy. Sec. A* 4(4) (2014) 3156.
- 270.** T. Sato, *Solvent Extr. Ion Exc.* 1(2) (1983) 251.

- 271.** B. K. Nagar, M. K. Saxena, B. S. Tomar, *Atom. Spectrosc.* 38(5) (2017) 117.
- 272.** S. A. Sheweita, M. A. El-Gabar, and M. Bastawy, *Toxicology* 169 (2001) 83.
- 273.** R. Chiarizia, D. C. Stepinski, P. Thyagarajan, *Sep. Sci. Technol.* 41 (2006) 2075.
- 274.** I. V. Blazheva, Y. S. Fedorov, B. Ya. Zilberman, and L.G.Mashirov, *Radiochemistry* 50(3) (2008) 256.
- 275.** D. Das, V. A. Juvekar, S. B. Roy, and R. Bhattacharya, *J. Radioanal. Nucl. Ch.* 300 (2014) 333.
- 276.** J. M. Fletcher, C. J. Hardy, *Nucl. Sci. Eng.* 16 (1963) 421.
- 277.** E. Hesford, A. C. Mckay, *Trans. Faraday Soc.* 54 (1958) 573.
- 278.** A. S. Al-Ammar, R. K. Gupta, R. M. Barnes, *Spectrochim. Acta Part B* 54 (1999) 1849.
- 279.** T. W. Burgoyne, G. M. Hieftje, R. A. Hites, *Anal. Chem.* 69 (1997) 485.
- 280.** P. Dey, S. Basu, *Int. J. Chem. Tech. Res.* 3(3) (2011) 1349.
- 281.** A. Demirkiran, N. M. Rice, A. R. Wright, *Proceedings of the International Solvent Extraction Conference, ISEC 2002*, page 884.
- 282.** M. Matsumiya, T. Yamada, Y. Kikuchi, S. Kawakami, *Solvent Extr. Ion Exch.* 34(6) (2016) 522.
- 283.** N. M. Rice, M. R. Smith, *J. Chem. Technol. Biotechnol.* 25(5) (1975) 379.
- 284.** J. Hala, P. Stodola, *J. Radioanal. Chem.* 80(1-2) (1983) 31.

285. B. Swain, J. Chem. Technol. Biotechnol. 91 (2016) 2549.
286. R. Banda, S. Ho Sohn, M.S. Lee, Mater. Trans. 54(1) (2013) 61.
287. P. K. Mishra, V. Chakra Vorty, K. C. Dash, S. N. Bhattacharya, J. radioanal. Nucl. Chem. 162 (2) (1992) 289.
288. D. Schrotterova, P. Nekovar, Chem. Pap. 60(6) (2006) 427.
289. O. Sanda, E. A. Taiwo, Hydrometallurgy 127-128 (2012) 168.
290. K. M. Allal, D. Hauchard, M. Stambouli, D. Pareau, G. Durand, Hydrometallurgy 45 (1997) 113.
291. T. Sato, K. Sato, Hydrometallurgy 37 (1995) 253.
292. M. L. P. Reddy, G. P. Preetha, C. V. Meena, T. Prasada rao, C. S. P. Iyer, A. D. Damodaran, J. Radioanal. Nucl. Chem. 211(2) (1996) 305.
293. V. H. Aprahamian, G. P. Demopoulos, Miner. Process. Extr. Metall. Rev. 14 (1995) 143.
294. Jing Yang, Xidan Zhao, Yanzhao Yang, Sep. Sci. Technol. 46 (2011) 1936.
295. J. N. Iyer, P. M. Dhadke, Indian J. Chem. Technol. 10 (2003) 665.
296. P. P. Sun, J. Y. Lee, M. S. Lee, Mater. Trans. 52 (11) (2011) 2071.
297. S. Bano, A. K. Nayak, U. B. Mishra, Y. Balaji Rao, C. Phani Babu, G. Kalyanakrishnan, J. Radioanal. Nucl. Chem. 314 (2017) 151.
298. Hoai Thanh Truong, Man Seung Lee, Seong Ho Son, Metal 7 (2017) 541.
299. Hoai Thanh Truong, Man Seung Lee, Geosystem Engineering 20(4) (2017) 224.

- 300.** M. A. Vaughan, Horlick, *Appl. Spectrosc.* 40(4) (1986) 434.
- 301.** A. L. Gray, J. G. Williams, *J. Anal. Atom. Spectrom.* 2 (1987)599.
- 302.** F. Vanhaecke, C. Vandecasteele, H. Vanhoce, and R.Dams, *Microchim. Acta* 108 (1992) 4.
- 303.** T. S. Lum, K. and S. Y. Leung, *J. Anal. At. Spectrom.* 31 (2016) 1078.
- 304.** N. M. Raut, L. S. Haung, S. K. Aggrawal, and K. C. Lin, *J. Chin. Chem. Soc.* 52 (2005) 589.
- 305.** M. Belter, A. Sajnog, D. Barlkiewtcz, *Talanta* 129 (2014) 606.
- 306.** IAEA-TECDOC-1132: Control assembly materials for water reactors: Experience, performance and perspectives, proceeding of a Technical Committee held in Vienna, 12-15 October (1998).
- 307.** C. Subramanian, A. K. Suri, T. S. R. C. Murthy: *BARC News Letter*, Issue No 313, Mar-Apr 14-22 (2010).
- 308.** Soo-Youl Oh, Choong-Sup Gil, Jonghwa Chang, *J. Korean Chem. Soc.* 33 (1) (2001) 46.
- 309.** ORNL/TM-2001/238 Report: Development of improved burnable poisons for commercial nuclear power reactors.
- 310.** R. Kandan, B. Prabhakara Reddy, G. Panneerselvem, K. Nagarajan, *J. Thermal Anal. Calorim.* 124 (2016) 1349.
- 311.** G. Marinenko, W. F. Koch, S. E. Edgar, *J. Res. Natl. Bur. Stand.* 88(2) (1983)117.

- 312.** J. Slanina, F. Bakker, A. J. P. Groen, W. A. Lingerak, *Fresenius Z. Anal. Chem.* 289 (1978) 102.
- 313.** D. M. Noronha, I. C. Pius, S. Chaudhury, *J. Radioanal Nucl. Chem.* 313 (2017) 523.
- 314.** H. Dogan, N. D. Hilmioğlu, *Carbohydr. Polym.* 75 (2009) 90.
- 315.** N. N. Mirashi, S. Chaudhury, S. K. Aggarwal, *Microchem. J.* 94 (2010) 24.
- 316.** Ho-Sung Yoon, Chul-Joo Kim, Kyeong-Woo Chung, Sung-Don Kim, Jin-Yong Lee, Jyothi Rajesh Kumar: *Hydrometallurgy* 165 (2016) 27.
- 317.** H. T. Truong, T. H. Nguyen, M. S. Lee, *Hydrometallurgy* 171 (2017) 298.
- 318.** X. Hao, L. Lu, B. Liang, C. Li, P. Wu, J. Wang, *Hydrometallurgy* 113-114 (2012) 185.
- 319.** D. K. Sing, M. K. Kotekar, H. Singh, *Desalination* 232 (2008) 49.
- 320.** N. Altunay, R. Gurkan, *Talanta* 159 (2016) 344.
- 321.** M. S. P. Enders, J. P. de Souza, P. Balestrin, P. de Azevedo Mello, F.A. Duarte, E. I. Muller, *Microchem. J.* 124 (2016) 321.
- 322.** B. K. Nagar, A. Saha, S. B. Deb, M.K. Saxena, *At. Spectrosc.* 35(5) (2014) 187.
- 323.** P. S. Asari, C. S. P. Iyer, *Talanta* 30 (6) (1983) 423.
- 324.** F. Hasanpour, M. Fouladgar, M. Taei, E. Mozafari, *J. Appl. Chem.* 11(40) (2016) 63.
- 325.** A. Beltran, F. Caturla, J. Beltran, *J. Inorg. Nucl. Chem.* 43 (1981) 3277.

- 326.** M. Riri, H. Hor, O. Kamal, T. Eljaddi, A. Benjjar, M. Hlaibi, J. Mater. Environ. Sci. 2(3) (2011) 303.
- 327.** L. Zhaogang, L. Mei, H. Yanhong, W. Mitang, S. Zhenxue, J. Rare Earth 26(2) (2008) 158.
- 328.** R. Chi, Z. Xu, Metall. Mater. Trans. B 30 (1999) 789.
- 329.** J. H. Yoe, L. R. Armstrong, Anal. Chem. 19(2) (1947) 100.
- 330.** V. Srilalitha, A. R. G. Prasad, K. R. Kumar, V. Seshagiri, FACTA UNIVERSITATIS series Physics, Chemistry and Technology 8 (2010) 15.
- 331.** B. V. N. Reddy, V. Saleem, T. S. Reddy, Der. Pharma. Chemica. 7(3) (2015) 16.
- 332.** P. K. Tarafder, S. Durani, R. Saran, G. V. Ramanaiah, Talanta, 41(8) (1994) 1345.
- 333.** Xianfeng Du, Youlong Xu, Li Qin, Xiangfei Lu, Qiong Liu, Yang BaiAm. J. Analyt. Chem. 5 (2014) 149.
- 334.** F. A. Al-Sanabani, A. A. Madfa, N. H. Al-Qudaimi, A review article, Am. J. Mater. Res. 1(1) (2014) 26.
- 335.** M. V. Silva, D. Stainer, H. A. Al-Qureshi, O. R. K. Montedo, D. Hotza, J. Ceram. Vol. 2014, Article ID 618154, 6 pages, <http://dx.doi.org/10.1155/2014/618154>
- 336.** G. Liao, Keying He, Liusheng Li, M. Jiang, J. Mineral and Material Characterization and Engineering 3(2) (2004) 81.

- 337.** K. Davis, Material Review: Alumina (Al₂O₃), School of Doctoral Studies (European Union) Journal (2010) 109.
- 338.** M. R. Buchmeiser, J. Chromatogr. A 918 (2001) 233.
- 339.** G. T. Furukawa, T. B. Douglas, R. E. McCoskey, D. C. Ginnings, J. Res. Natl. Bur. Stand. 57(2) (1956) 67.
- 340.** R. F. Geller, P. J. Yavorsky, J. Res. Natl. Bur. Stand. 34 (1945) 395.
- 341.** N. Tangboriboon, N. Uttanawanit, M. Longtone, P. Wongpinthong, A. Sirivat, R. Kunanuruksapong, Mater. 3 (2010) 656 . ; doi: 10.3390/ma301056
- 342.** M. K. Park, H. N. Kim, S. Su Baek, E. S. Kang, Y. K. Baek, Do Kyung Kim, Solid State Phenomena, 124-126 (2007) 743. doi: 10.4028/www.scientific.net/SSP.124-126.743
- 343.** J. W. Kaczmar, K. Granat, A. Kurzawa, E. Grodzka, Archives of Foundry Engineering 14(2) (2014) 85. ISSN (1897-3310)
- 344.** F. Habasi, Bull. Hist. Chem. 17/18 (1995) 15.
- 345.** OLAREMU, Int. J. Eng. Technol. Manag. Appl. Sci. 3(7) (2015) 103. www.ijetmas.com ISSN 2349-4476
- 346.** S. Ali Hosseini, A. Niaei, D.s Salari, J. Phys. Chem. 1 (2011) 23.
- 347.** N. J. Simon, Cryogenic properties of inorganic insulation materials for ITER magnets: A Review, NISTIR 5030
- 348.** Peggy Y. Hou, J. Am. Ceram. Soc. 86(4) (2003) 660.

- 349.** T. Higuchi, K. Shiiyama, Y. Izumi, M. M. R. Howlader, M. Kutsuwada, C. Kinoshita, J. Nucl. Mater. 307-311 (2002) 1250.
- 350.** Jung Ho Yoo, Jong Chul Nam, Sunggi Baik, J. Am. Ceram. Soc. 82 (8) (1999) 2233.
- 351.** J. P. Buban, K. Matsunaga, J. Chen, N. Shibata, W. Y. Ching, T. Yamamoto, Y. Ikuhara, Science, 311 (2006) 212.
- 352.** Indian Minerals Yearbook 2013 (Part II: Metals & Alloy), 52nd Edition Aluminium & alumina, Government of India, Ministry of Mines, Indian Bureau of Mines, www.ibm.gov.in
- 353.** DOE-HDBK-1017/2-93 REACTOR USE OF ALUMINUM
- 354.** IAEA-TECDOC-1637, Corrosion of Research Reactor Aluminium Clad Spent Fuel in Water, International Atomic Energy Agency Vienna, 2009, <http://www.iaea.org/books>
- 355.** F. Thummler, H. E. Lilienthal, S. Nazare, Powder Metall. 12(23), (1969) 1.
- 356.** Personal Care Products Council. 1-23-2013. Concentration of use by FDA Product Category: Alumina and Sodium Aluminate. 3 pages.
- 357.** Personal Care Products Council. 5-2-2013. Concentration of Use by FDA Product Category: Aluminum Hydroxide, March 2013 Survey. 3 pages.
- 358.** Personal Care Products Council. Vaccines, Blood & Biologics: Common Ingredients in U.S. Licensed Vaccines. <http://www.fda.gov/BiologicsBloodVaccines/SafetyAvailability/VaccineSafety/ucm187810.htm>.

- 359.** American Society for Testing and Materials (ASTM). Standard specification for high-purity dense aluminum oxide for medical application. West Conshohocken, PA, ASTM International. 2012. www.astm.org. Report No. DOI: 10.1520/F0603- 12.
- 360.** A. V. J. Lombardi, K. R. Berend, B. E. Seng, I. C. Clarke, J. B. Adams. Clin. Orthop. Relat. Res. 468(2) (2010) 367.
- 361.** U.S. Department of Health and Human Services, Public Health Services. Toxicological profile for aluminum. Atlanta, GA, Agency for Toxic Substances and Disease Registry. 2008. <http://www.atsdr.cdc.gov/toxprofiles/tp22.pdf>.
- 362.** F. DE Corte, A. Simonits, J. Radioanal. Nucl. Chem. 133 (1989) 43.
- 363.** C. E. Caicedo-Martinez, E. V. Koroleva, G. E. Tompson, P. Skeldon, K. Shimizu, G. Hoellrigl, C. Campbell, E. McAlpine, Corros. Sci. 44 (2002) 2611.
- 364.** M. A. Guitar, E. Ramos-Moore, F. Mucklich, J. Alloys Compd. 594 (2014) 165.
- 365.** J. M. Ducere, M. Djafari Rouhani, C. Rossi, A. Esteve, Compt. Mater. Sci. 126 (2017) 272.
- 366.** J. Auchet, P. Terzieff, J. Alloys Compd. 261 (1997) 295.
- 367.** N. D. Kerness, T. Z. Hossain, S. C. Mc Guire, Appl. Radat. Isot. 48(1) (1997) 5.

- 368.** A. D. Shinde, R. Acharya, A. V. R. Reddy, *J. Radioanal. Nucl. Chem.*, 299 (2014) 1287.
- 369.** S. Shibata, S. Tanaka, T. Suzuki, H. Umezawa, J. G. Lo, S.J.Yeh, *Inter. J. Appl. Radiat. Isotopes* 30 (1979) 563.
- 370.** J. C. P. de Mattos, L. F. Rodrigues, E. M. de Mores Flores, V. Krivan, *Spectrochimica Acta Part B* 66 (2011) 637.
- 371.** Li Hong-kun, Liu Ming, Chen Zhi-jiang, Li Run-hua, *Tran. Nonferrous. Met. Soc. China* 18 (2008) 222.
- 372.** Cheng Yonga, *Procedia. Eng.* 24 (2011) 447.
- 373.** K. Nakane, Y. Uwamino, H. Morikawa, A. Tsuge, T. Ishizuka, *Analytica Chimica Acta* 369 (1998) 79.
- 374.** J. D. Lellie, S. J. Hall, G. I. Crawford, D. B. C. B. Syme, J. McKeown, *J. Phy. A: Math., Nucl. Gen.*, 7(14) (1974) 1758.
- 375.** J. Lee , Y. Kim, *Mater. Trans.* 52(110) (2011) 2067.
- 376.** H. Matusiewicz, *Microchim. Acta* 111 (1993) 71.
- 377.** E. Tatar, I. Varga, G. Zaray, *Microchim. Acta* 111 (1193) 45.
- 378.** K. H. Gayer, L. C. Thompson, O. T. Zajicek, *J. Chem.* 36 (1958) 1268.